



NAVAL POSTGRADUATE SCHOOL

MONTEREY, CALIFORNIA

THESIS

**THE RELATIONSHIP BETWEEN SEA BREEZE
FORCING AND HF RADAR-DERIVED SURFACE
CURRENTS IN MONTEREY BAY**

by

Emre Tukenmez

June 2014

Thesis Advisor:
Second Reader:

Jeffrey D. Paduan
Jamie MacMahan

Approved for public release; distribution is unlimited

THIS PAGE INTENTIONALLY LEFT BLANK

REPORT DOCUMENTATION PAGE			<i>Form Approved OMB No. 0704-0188</i>	
Public reporting burden for this collection of information is estimated to average 1 hour per response, including the time for reviewing instruction, searching existing data sources, gathering and maintaining the data needed, and completing and reviewing the collection of information. Send comments regarding this burden estimate or any other aspect of this collection of information, including suggestions for reducing this burden, to Washington headquarters Services, Directorate for Information Operations and Reports, 1215 Jefferson Davis Highway, Suite 1204, Arlington, VA 22202-4302, and to the Office of Management and Budget, Paperwork Reduction Project (0704-0188) Washington, DC 20503.				
1. AGENCY USE ONLY (Leave blank)		2. REPORT DATE June 2014	3. REPORT TYPE AND DATES COVERED Master's Thesis	
4. TITLE AND SUBTITLE THE RELATIONSHIP BETWEEN SEA BREEZE FORCING AND HF RADAR-DERIVED SURFACE CURRENTS IN MONTEREY BAY			5. FUNDING NUMBERS	
6. AUTHOR(S) Emre TUKENMEZ				
7. PERFORMING ORGANIZATION NAME(S) AND ADDRESS(ES) Naval Postgraduate School Monterey, CA 93943-5000			8. PERFORMING ORGANIZATION REPORT NUMBER	
9. SPONSORING /MONITORING AGENCY NAME(S) AND ADDRESS(ES) N/A			10. SPONSORING/MONITORING AGENCY REPORT NUMBER	
11. SUPPLEMENTARY NOTES The views expressed in this thesis are those of the author and do not reflect the official policy or position of the Department of Defense or the U.S. Government. IRB Protocol number ____ N/A ____.				
12a. DISTRIBUTION / AVAILABILITY STATEMENT Approved for public release; distribution is unlimited			12b. DISTRIBUTION CODE	
13. ABSTRACT (maximum 200 words) <p>Despite the importance of sea breeze, only Hendrickson and MacMahan's research has been done to determine sea breeze effects in Monterey Bay; other than that not much research has been done. In this thesis, CODAR SeaSonde radars are used to map the surface current in Monterey Bay. Temperature, wind speed and wind direction are analyzed for five locations to establish the algorithm for determining the sea breeze days in Monterey Bay. Harmonic analysis is used to understand the relationship between sea breeze and high frequency (HF) radar-derived surface currents. To explain the cause of the peaks and lows in the amplitude of the sea breeze as shown by the harmonic analysis, coastal jet influences, boundary layer height changes, temperature gradient variations and cloudiness are investigated. Current patterns clearly respond to changing sea breeze strength with the strongest amplitudes corresponding to days with fully developed coastal jets. No coastal jet, lower amplitude sea breeze days, however, appear to have a more classical response in terms of wind direction changes. It is understood that rapid decrease of the amplitude of sea breeze in harmonic analysis is the day with sea breeze including obvious wind shifting, and rapid increase is the day when strong synoptic effect is seen obviously over the region.</p>				
14. SUBJECT TERMS Sea Breeze, Coastal jet, HF Radar derived surface currents, Harmonic analysis			15. NUMBER OF PAGES 95	
			16. PRICE CODE	
17. SECURITY CLASSIFICATION OF REPORT Unclassified	18. SECURITY CLASSIFICATION OF THIS PAGE Unclassified	19. SECURITY CLASSIFICATION OF ABSTRACT Unclassified	20. LIMITATION OF ABSTRACT UU	

THIS PAGE INTENTIONALLY LEFT BLANK

Approved for public release; distribution is unlimited

**THE RELATIONSHIP BETWEEN SEA BREEZE FORCING AND HF RADAR-
DERIVED SURFACE CURRENTS IN MONTEREY BAY**

Emre Tukenmez
Lieutenant Junior Grade, Turkish Navy
B.S., Turkish Navy Academy, 2009

Submitted in partial fulfillment of the
requirements for the degree of

MASTER OF SCIENCE IN PHYSICAL OCEANOGRAPHY

from the

**NAVAL POSTGRADUATE SCHOOL
June 2014**

Author: Emre Tukenmez

Approved by: Jeffrey D. Paduan
Thesis Advisor

Jamie MacMahan
Second Reader

Peter Chu
Chair, Department of Oceanography

THIS PAGE INTENTIONALLY LEFT BLANK

ABSTRACT

Despite the importance of sea breeze, only Hendrickson and MacMahan's research has been done to determine sea breeze effects in Monterey Bay; other than that not much research has been done. In this thesis, CODAR SeaSonde radars are used to map the surface current in Monterey Bay. Temperature, wind speed and wind direction are analyzed for five locations to establish the algorithm for determining the sea breeze days in Monterey Bay. Harmonic analysis is used to understand the relationship between sea breeze and high frequency (HF) radar-derived surface currents. To explain the cause of the peaks and lows in the amplitude of the sea breeze as shown by the harmonic analysis, coastal jet influences, boundary layer height changes, temperature gradient variations and cloudiness are investigated. Current patterns clearly respond to changing sea breeze strength with the strongest amplitudes corresponding to days with fully developed coastal jets. No coastal jet, lower amplitude sea breeze days, however, appear to have a more classical response in terms of wind direction changes. It is understood that rapid decrease of the amplitude of sea breeze in harmonic analysis is the day with sea breeze including obvious wind shifting, and rapid increase is the day when strong synoptic effect is seen obviously over the region.

THIS PAGE INTENTIONALLY LEFT BLANK

TABLE OF CONTENTS

I.	INTRODUCTION.....	1
II.	BACKGROUND	3
	A. HF RADAR.....	3
	B. SEA BREEZE.....	7
	C. COASTAL JETS.....	11
III.	DATA	13
IV.	ANALYSIS OF DATA AND RESULTS.....	19
	A. ESTABLISHING CRITERIA TO DETERMINE SEA BREEZE IN MONTEREY BAY.....	29
	B. ROTARY SPECTRA.....	36
	C. ROTARY COEFFICIENT	37
	D. POWER SPECTRA ANALYSIS	38
	E. COMPLEX CORRELATION.....	39
	F. HARMONIC ANALYSIS	40
	1. Analysis of July 2009	42
	a. Analysis of Coastal Jets Influence	43
	b. Comparison of Days with/without Coastal Jet.....	51
	2. Analysis of August 2009.....	54
	3. Analysis of September 2009	59
	G. SEA BREEZE STRENGTH	63
V.	CONCLUSION AND RECOMMENDATIONS FOR FUTURE RESEARCH...67	
	LIST OF REFERENCES	71
	INITIAL DISTRIBUTION LIST	75

THIS PAGE INTENTIONALLY LEFT BLANK

LIST OF FIGURES

Figure 1.	Backscatter spectrum showing Bragg peaks due to waves advancing toward and away from the receiver (from Paduan and Graber 1997).....	4
Figure 2.	Electromagnetic spectrum showing the HF band relative to other bands (from Paduan and Graber 1997).	6
Figure 3.	Representation of some remote sensing methods exploiting signals backscattered from the sea surface (from Shearman 1981).	6
Figure 4.	Representation of Sea Breeze (from Nuss 2003).	8
Figure 5.	Locations of CODAR HF Antennas along the California Coast (triangles) and the individual radial current observations points (dots) for a sample hour in January 2014, from California Coastal Ocean Currents Monitoring Program at http://cencalcurrents.org	14
Figure 6.	The Plot of all CODAR HF Grid Radar Points in the Region.	15
Figure 7.	The Data Availability of Each Grid Point in July 2009.	15
Figure 8.	Radial Coverage of HF Radar from 2008–2012.	16
Figure 9.	Locations of M0, M1, M2 Ocean Buoys, Wind Profiler (ORD) and Salinas (SNS) Observations Sites, and the NOAA Buoy 46042 (N42B, not used) location (from Google Earth).	17
Figure 10.	The Area of Focus used in CFSR Model to Examine Coastal Jets (from Google Earth).	18
Figure 11.	July–September Average Hourly Plot of Air Temperature and Wind Speed for Salinas, Fort Ord and M0 Buoy.	20
Figure 12.	Temperature Difference between 2 p.m. and 11 a.m. for Salinas in 2009.	22
Figure 13.	Summer and Winter Average Hourly Plot of Air Temperature and Wind Speed for Salinas.	22
Figure 14.	Wind Speed Differences Plot for M0 Buoy, July–September 2009.	24
Figure 15.	Wind Speed Differences Plot for M1 Buoy, July–September 2009.	24
Figure 16.	Wind Speed Differences Plot for M2 Buoy, July–September 2009.	25
Figure 17.	Wind Speed Differences Plot for Fort Ord, July–September 2009.	25
Figure 18.	Wind Speed Differences Plot for Salinas, July–September 2009.	26
Figure 19.	Mean Wind Speed and Direction Plot for M0 Buoy, July–September 2009.	26
Figure 20.	Mean Wind Speed and Direction Plot for M1 Buoy, July–September 2009.	27
Figure 21.	Mean Wind Speed and Direction Plot for M2 Buoy, July–September 2009.	27
Figure 22.	Mean Wind Speed and Direction Plot for Fort Ord, July–September 2009.	28
Figure 23.	Mean Wind Speed and Direction Plot for Salinas, July–September 2009.	28
Figure 24.	Sea Breeze Algorithm Chart.	30
Figure 25.	Sea Breeze Days Determined Manually and by Algorithm Conditions.	32
Figure 26.	Wind Profiler Site Plot for Surface Meteorology Data, from Naval Postgraduate School at http://met.nps.edu/~lind/nps/archive/ARCHIVE.HTM	33
Figure 27.	Wind Profiler Site Plot for Mixing Length Heights, from Naval Postgraduate School at http://met.nps.edu/~lind/nps/archive/ARCHIVE.HTM	34

Figure 28.	Rotary Spectra for the Wind (July–September 2009) at M0 Buoy Location.	36
Figure 29.	Rotary Spectra for the HF-radar derived Current (July–September 2009) at M0 Buoy Location.	37
Figure 30.	Rotary Coefficient for Wind in M0 Buoy Location (July–September 2009).	37
Figure 31.	Rotary Coefficient for Current in M0 Buoy Location (July–September 2009).	38
Figure 32.	Power Spectra for Wind and Current at M0 Buoy Location (July–September 2009).	39
Figure 33.	Harmonic Analysis of ADCP 6m depth Current and HF Radar-derived Surface Current.	41
Figure 34.	Harmonic Analysis of Buoy Wind and HF Radar-derived Surface Current at M0 Buoy Location (July 2009).	43
Figure 35.	July 8, 2009 Sea Level Pressure and Horizontal Isotachs (obtained using GARP CFSR Model).	44
Figure 36.	July 8, 2009 Vertical Cross Section of Isotachs (obtained using GARP CFSR Model).	45
Figure 37.	July 8, 2009 Vertical Cross Section of Potential Temperature (obtained using GARP CFSR Model).	45
Figure 38.	July 16, 2009 Sea Level Pressure and Horizontal Isotachs (obtained using GARP CFSR Model).	46
Figure 39.	July 16, 2009 Vertical Cross Section of Isotachs (obtained using GARP CFSR Model).	47
Figure 40.	July 16, 2009 Vertical Cross Section of Potential Temperature (obtained using GARP CFSR Model).	47
Figure 41.	Average Velocity Map of Surface Current on July 8, 2009.	49
Figure 42.	Surface Current Map at 7 p.m. on July 8, 2009.	49
Figure 43.	Average Velocity Map of Surface Currents on July 16, 2009.	50
Figure 44.	Surface Current Map at 7 p.m. on July 16, 2009.	50
Figure 45.	Air Temperature at 2 p.m. at the Los Banos and M2 Buoy Locations and the Temperature Differences between these two Locations in July 2009.	53
Figure 46.	Positions of Los Banos and M2 Buoy (from Google Earth).	53
Figure 47.	Harmonic Analysis of Buoy Wind and HF Radar-derived Surface Current at M0 Buoy Location (August 2009).	55
Figure 48.	Wind Profiler Site Plot for Surface Meteorology Data (from http://met.nps.edu/~lind/nps/archive/ARCHIVE.HTM).	55
Figure 49.	Wind Profiler Site Plot for Surface Meteorology Data (from http://met.nps.edu/~lind/nps/archive/ARCHIVE.HTM).	56
Figure 50.	August 10, 2009 Sea Level Pressure and Horizontal Isotachs (obtained using GARP CFSR Model).	56
Figure 51.	August 13, 2009 Sea Level Pressure and Horizontal Isotachs (obtained using GARP CFSR Model).	57
Figure 52.	Average Velocity Map of Surface Current on August 10, 2009.	57
Figure 53.	Surface Current Map at 5 p.m. on August 10, 2009.	58

Figure 54.	Average Velocity Map of Surface Current on August 13, 2009.....	58
Figure 55.	Surface Current Map at 5 p.m. on August 13, 2009.	59
Figure 56.	Harmonic Analysis of Buoy Wind and HF Radar-derived Surface Current at M0 Buoy Location (September 2009).	60
Figure 57.	Wind Profiler Site Plot for Surface Meteorology Data (from http://met.nps.edu/~lind/nps/archive/ARCHIVE.HTM).	60
Figure 58.	Wind Profiler Site Plot for Surface Meteorology Data (from http://met.nps.edu/~lind/nps/archive/ARCHIVE.HTM).	61
Figure 59.	Synoptic Winds on September 9, 2009, along the California Coast (obtained from GARP, CFSR model).....	61
Figure 60.	Average Velocity Map of Surface Current on September 9, 2009.	62
Figure 61.	Surface Current Map at 4 p.m. on September 9, 2009.....	62
Figure 62.	Cloud Coverage and Amplitudes of Surface Currents Map (from ge.ssec.wisc.edu/modis-today).....	65
Figure 63.	Sea Breeze Analysis for Specific Days.....	69

THIS PAGE INTENTIONALLY LEFT BLANK

LIST OF TABLES

Table 1.	CODAR Stations, from California Coastal Ocean Currents Monitoring Program at http://cencalcurrents.org	13
Table 2.	Mean Wind Speed/Direction between July and September 2009.....	23
Table 3.	Conditional Probability Matrix of Sea Breeze Conditions.	35
Table 4.	Table of Complex Correlation for M0, M1 and M2 Buoy Locations between July and September in 2009.....	40
Table 5.	Comparison of Days with/without Coastal Jet with Respect to Select Parameters.....	52
Table 6.	Sea Breeze Strength with Respect to Standard Factors.	64

THIS PAGE INTENTIONALLY LEFT BLANK

LIST OF ACRONYMS AND ABBREVIATIONS

ADCP	acoustic Doppler current profiler
CFSR	Climate Forecast System Reanalysis
CODAR	Coastal Ocean Dynamics Application Radar
cw	clockwise
ccw	counter clockwise
GARP	GEMPAK Analysis and Rendering Program
GEMPAK	General Meteorology Package
HF	high frequency
MBARI	Monterey Bay Aquarium Research Institute
MBL	marine boundary layer
NDBC	National Data Buoy Center
NPS	Naval Postgraduate School
PBL	planetary boundary layer
PST	Pacific Standard Time
SAR	search and rescue
UTC	Coordinated Universal Time

THIS PAGE INTENTIONALLY LEFT BLANK

ACKNOWLEDGMENTS

I received unbelievable support from the Oceanography and Meteorology Department. First of all, I would like to express my gratitude and appreciation to Professor Jeffrey Paduan and Oceanographer Mike Cook, who guided and helped me and answered all my questions patiently. Also, I would like to thank Professor Jamie MacMahan who was so kind and added so much to my understanding of time series. Professor Wendell Nuss answered my meteorological questions every time. This project could not have been done without their help and wisdom.

All HF radar data and wind profiler data were provided by Mr. Mike Cook and Mr. Richard Lind, to whom I owe great appreciation. I would like to thank Mr. Mike Cook again for making me an expert in Matlab. He also assisted me by creating key figures that I needed for analysis. I appreciate Mr. Bob Creasey's endless help, since he showed me how to get the figures in GARP, which helped me to understand the coastal jet influence on the California coast.

I wish to express my thankfulness to my family and my section, who have supported me.

THIS PAGE INTENTIONALLY LEFT BLANK

I. INTRODUCTION

The surface of ocean is extremely important. It is where people interact with the ocean, and it is where air and sea interactions impact the movement of surface ocean currents. There are many factors that affect the speed and direction of current, such as density of water, synoptic events, depth of the ocean and winds. Sea breeze is also an important phenomenon in coastal regions. Behavior of the wind near the coast has been studied on many occasions, but not much research has been done to relate the sea breeze offshore with the response of the ocean surface currents until today. Understanding the diurnal current fluctuations driven by the wind over the period of one day is harder than understanding the effect for a longer time period. Nonetheless, circulation patterns created by sea breeze forcing and its local variations have many effects on the near surface current structure and that structure has influence over the coupled atmosphere's response, as well as our ability to navigate in the coastal waters or to effectively implement oil spill mitigation or search and rescue efforts.

This thesis focuses on explaining and showing the relationship between sea breeze forcing and high frequency (HF) radar-derived currents. Our main interest is a change during a period of one day or a few days (short period of time). To get the relationship between the sea breeze and the current during the 24-hour period, hourly data are used for both currents and winds. The surface ocean current is examined by using data from Coastal Ocean Dynamics Application Radar (CODAR), Monterey Bay Aquarium Research Institute (MBARI), and a 915 MHz wind profiler along the Monterey Bay coast. The Climate Forecast System Reanalysis Model is used to examine the coastal jet influence in Monterey Bay. Three months of 2009 HF radar data are compared with concurrent MBARI (M0, M1 and M2), acoustic Doppler current profiler (ADCP) and 915 MHz wind profiler data. It can be difficult to compare two time series of vectors, so the wind and current data are compared with respect to not only time but also frequency. Complex correlation, power spectrum, harmonic analysis and rotary spectra methods for understanding the HF-derived currents and sea breeze relationship are used. The

Monterey Bay Region contains a lot of surface observations from both HF radar and meteorological buoys, which were an advantage for this study.

The most challenging problem we had to deal with in this study is that, as previous studies show, there is no direct or clear relationship between sea breeze and its parameters (topography, cloud, synoptic scale winds, etc.). Another challenge is Monterey Bay itself, since it is a complex region to study. Taking on this challenge provides the possibility to establish more fundamental links between diurnal wind and current responses in a complex coastal area. Such linkages may be useful when applied to other regions, such as the Aegean and Black Sea coasts of Turkey, which is a major motivation for this work.

II. BACKGROUND

In this study, first the general characteristics of the sea breeze and factors that influence the sea breeze are reviewed and analyzed to understand sea breeze forcing and to choose sea breeze days in the Monterey Bay region. After some specific sea breeze days are chosen we try to examine the correlation between sea breeze forcing and surface currents in Monterey Bay. To begin, background information on sea breeze forcing, HF radar-derived currents and HF radar itself is provided.

A. HF RADAR

The surface of the coastal ocean is very important for humankind because so many essential activities go on there, such as transportation and fishing (Paduan and Washburn 2013). Wind, sea breeze, tides, pressure differences and buoyancy forcing can all drive the surface of ocean. Hence, mapping the surface currents in real time over a large area is very important to understand air-sea interaction, coastal circulation and related processes (Paduan and Washburn 2013). For example, the large-scale flow of the California Current System has a strong influence on local circulation, fishing and upwelling along the coast of California. HF radar is good at mapping the surface currents in real time and mapping surface currents hourly from shore to more than 200 km (Paduan and Washburn 2013). If data are available in real time, then all transport processes can be tracked and predicted quickly. Having accurate data in real time can be critical and valuable; for example, it can enable improved search and rescue (SAR) operations (Paduan and Washburn 2013). Compilation of surface current mapping data over time can be used to support ecological connectivity studies thus extending the utility of HF radar observations into the biological sciences. Much of the use of these types of measurements follows from Paduan and Rosenfeld (1996) who also worked in Monterey Bay and were able to confirm that the use of reflected high-frequency electromagnetic waves is an effective observation technique.

HF radars have been used for mapping currents for more than 45 years (Harlan et al. 2010). Especially during the last 15 years the many advantages of HF radar have been recognized. HF radar ocean surface observations begin with Crombie (1955). He discovered that HF radar wavelength signals come back from ocean surface waves. After Crombie, Barrick (1968, 1972) derived the Bragg scatter. Backscattered echoes from ocean waves travel from or to the radar, and the wavelength of the ocean wave backscattering the radar signal is one half the radar's wavelength (Neal 1992). This process is called Bragg scattering (Barrick 1977). Two dominant peaks in the frequency spectrum are obtained when spectral analysis of the returning signals is examined (Neal 1992). Figure 1 shows the Doppler technique for HF radar current determination (Paduan and Graber 1997). As we see in Figure 1, the spectrum has two significant peaks because of Bragg waves moving on and off the receiver (Paduan and Graber 1997).

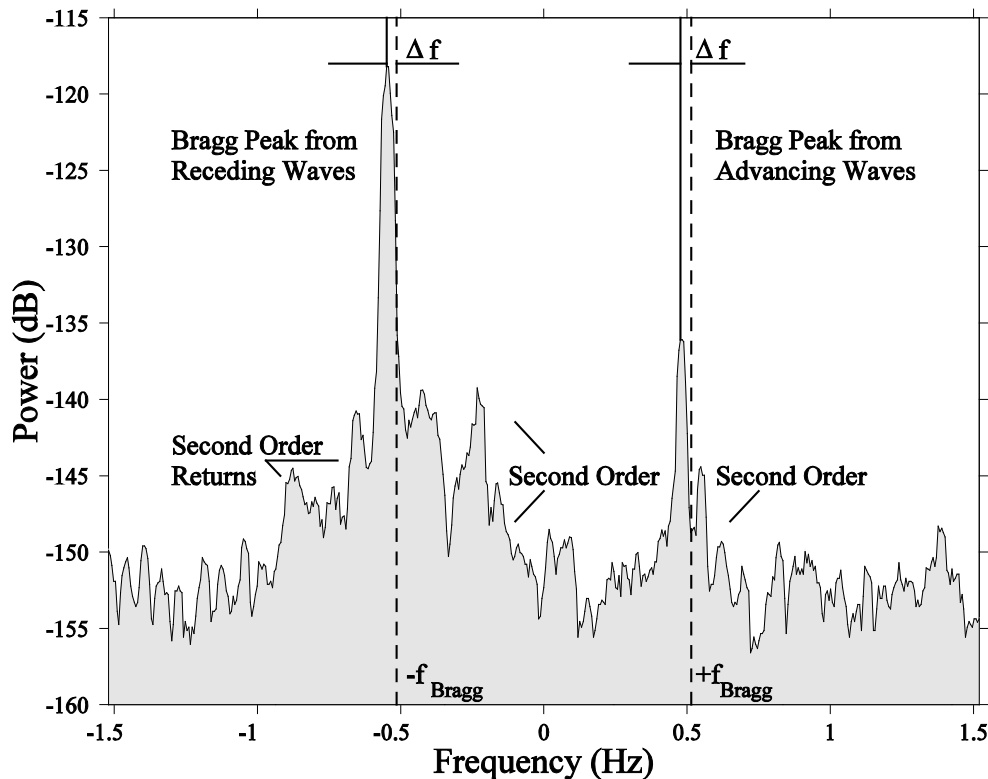


Figure 1. Backscatter spectrum showing Bragg peaks due to waves advancing toward and away from the receiver (from Paduan and Graber 1997).

In 1970, the Coastal Ocean Dynamics Application Radar Company was organized to develop an antenna system for coastal ocean surface current mapping (Harlan et al. 2010). CODAR systems help oceanographers to get data easily and cover a large area with frequent observations at low cost. To understand complex air sea interactions along the coast, CODAR systems are used because HF radar-derived current information provides real-time data with a broad range (Neal 1992). CODAR is a popular research tool and continues to gain credibility for high resolution measurement (Delgado 1999).

Important conditions for HF radar current mapping include good conductivity of surface water, salinity rate and the existence of surface gravity waves of enough length and height (Harlan et al. 2010). Conductivity is connected to salinity, so when salinity decreases, the strength of the sea echo and range of measurement reduces directly. Long (2006) proved that in brackish or freshwater areas ranges are significantly decreased due to the reduced electrical conductivity of the water (Harlan et al. 2010).

The ocean surface is not flat; it has slopes, crests and troughs which scatter/reflect signals in every direction (Harlan et al. 2010). However, we know from Bragg scattering that in this structure the waves whose wavelength is half the radar wavelength can create a resonant backscatter (Harlan et al. 2010). Scattered energy is delayed due to traveling time since it is transmitted away from the radar and it is received back (Harlan et al. 2010). The transmit frequency of radar is important because it helps us to figure out the length of the ocean waves and backscattered radar wavelength (Harlan et al. 2010). It is known that high frequencies have a shorter range because attenuation and frequency are inversely proportional. The HF electromagnetic spectrum has frequencies from 3 to 30 MHz (wavelengths 10 to 100m) as shown in Figure 2.

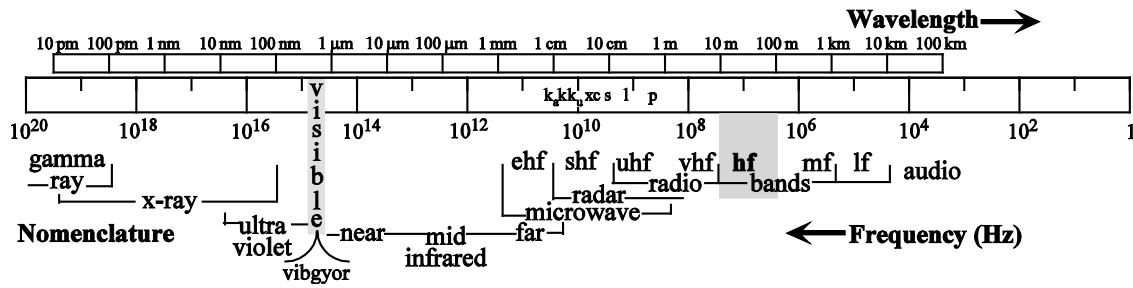


Figure 2. Electromagnetic spectrum showing the HF band relative to other bands (from Paduan and Graber 1997).

Two or more sites' radial currents should be gathered and combined to get vector surface current estimates, because one radar station can measure only the part of the flow along the radial beam spreading from site (Paduan and Graber 1997). That result is shown in Figure 3. Generally speaking it is mandatory to have an angle <150 and >30 between two radials to analyze the current vector. If not, we will have a baseline problem, which means both measure the same component of velocity (Paduan and Graber 1997).

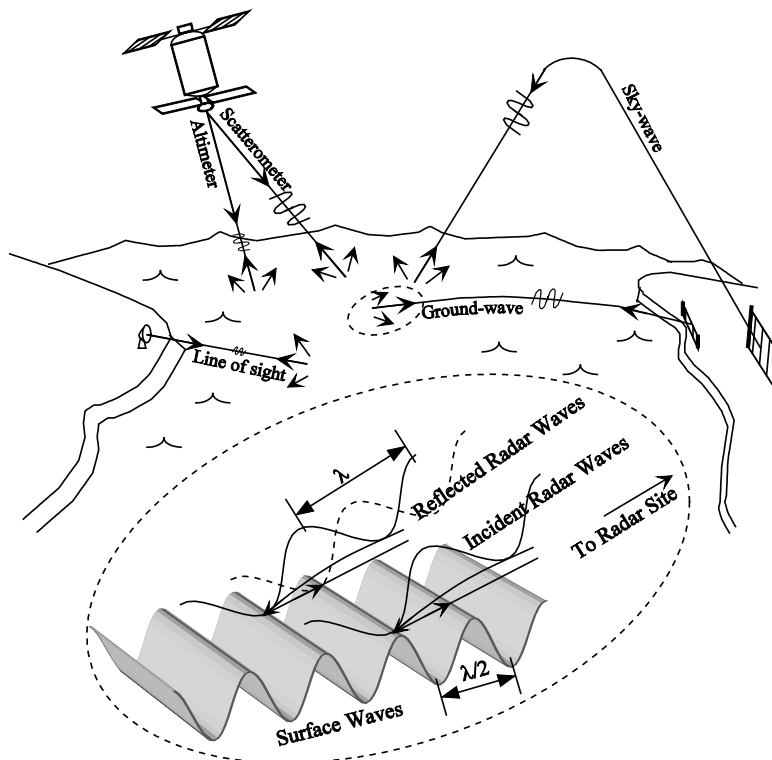


Figure 3. Representation of some remote sensing methods exploiting signals backscattered from the sea surface (from Shearman 1981).

HF radars have many advantages with respect to other methods for sea surface current mapping for a variety of reasons. These reasons are pointed out in a paper by Harlan et al. (2010) as:

First the targets required to produce coherent echo using HF are surface gravity waves. Second vertically polarized HF waves can propagate over conductive seawater via coupling to the mean spherical sea surface, producing range out to 200 km. Third Doppler sea echo at HF, under most wave conditions, has a well-defined signal from wave-current interactions that is easily distinguishable from wave-wave processes. This allows for robust extraction of current velocities.

These factors make HF radar unique for coastal mapping.

The biggest advantage of HF radar data is the coverage and resolution, which would not be possible with other platforms. An area of hundreds of square kilometers can be measured with a resolution of a few kilometers. This enables us to give a sufficiently detailed report about the sea breeze evolutions, flows close to topography and wind structures for a large area. That is not possible with data obtained from single mooring or from ships.

B. SEA BREEZE

Sea breeze is a popular and familiar subject for people who live close to the west coast of Turkey and coasts all over the world. Sea breeze affects the shoreline. Sea breeze circulation seems easy to detect, but measuring and understanding the components and dynamics of circulation is challenging due to lack of data over water. In addition, topography makes accurate measurement of sea breeze circulation much more complex (Duvall 2004).

Land surface type (absorption coefficient), latitude, cloud (these relate to ground absorption of solar energy), season, depth of planetary boundary layer (which relate to amount of temperature change) are the factors that may affect the daily heating cycle (Nuss 2003). These factors are important because they have some impacts on the surface energy balance on daily heat circulation (Nuss 2003).

Coastal thermal gradient is the main forcing mechanism for the sea breeze circulation (Jeffrey 1996). In summer, long periods of sunshine make the land warmer than the ocean; also we know that the land surface absorbs solar radiation much more readily than the water because the radiative properties of water and land are very different (Nuss 2003, Jeffrey 1996). Because of this absorption, a temperature rise occurs over the land area. In turn, this developed coastal temperature gradient causes a coastal pressure gradient (Jeffrey 1996). The effect of the temperature gradient on the pressure gradient force is obvious in coastal areas. As Nuss (2003) points out:

Temperature gradient is distributed vertically through much of the boundary layer and consequently produces gradient that is coincident with thermal gradient. The warm air over the land area tends to lower the surface pressure relative to the unchanged or cooler boundary layer air over the water. In horizontal equation of motion, the pressure gradient form is the dominant factor. The other terms are the coriolis and the friction.

Because of having high pressure over the water and low pressure over the land, a pressure gradient force is created resulting in the onshore flow. This onshore flow is called a sea breeze. This process is illustrated in Figure 4 (Jeffrey 1996).

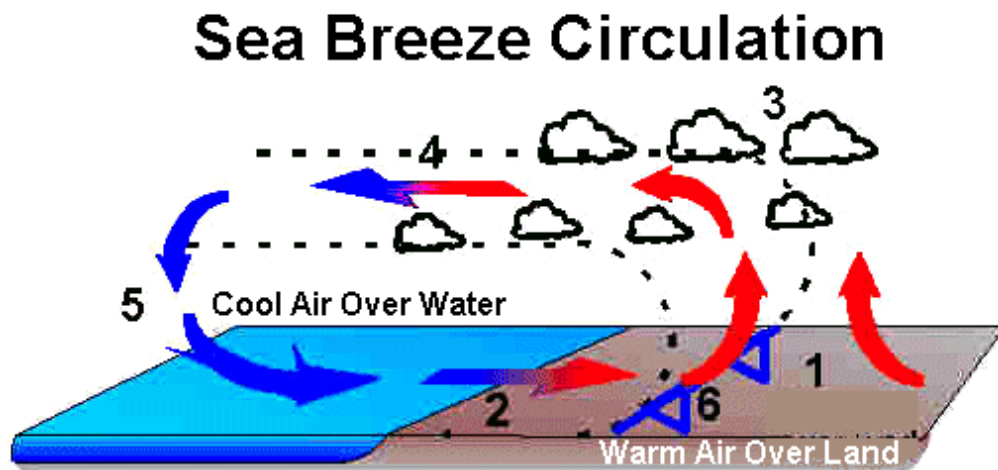


Figure 4. Representation of Sea Breeze (from Nuss 2003).

At night the warmer land surface has outgoing long wave radiation which cools the land surface inversely to the day time (Nuss 2003). Even though this cooling is not particularly strong with respect to daytime sea breeze, it is enough to reverse the thermal gradient in the coastal region at night—but not all the time and not everywhere (Foster 1996).

There is a relationship between thermal gradient and sea breeze. If thermal gradient increases, sea breeze forcing increases (Holton 1979). However, the length scale and depth of the circulation produce inverse effects (Holton 1979). For example, large horizontal scales create weaker winds than shorter ones. Also thermal gradients occur over a limiting or narrow area (Nuss 2003). The strength of these thermal gradients is affected by the depth of the planetary boundary layer (PBL). For instance a shallow boundary layer experiences much more warming than a deep one, which is good for sea breeze circulation (Nuss 1992).

Basic structure of the sea breeze and its evolution are determined by the direction of the flow. Flow directions include onshore, offshore, flow parallel to the coast with land on the left and flow parallel to the coast with land on the right. Nuss (2003) describes the flow and time scale of a sea breeze: “The 11 a.m. local time shows the beginning of sea breeze with a well-developed thermal gradient over the land and the initial sea breeze is barely noticeable in the offshore background flow at 11 a.m. local. The 5 p.m. local circulation shows stronger onshore winds.” Some experiences show that thermal gradient and horizontal length scale are the biggest factors that affect the sea breeze forcing; for example, the winds may change from 0–26 m/s for the temperature change from 0–15 °C (Nuss 2003).

Clouds, which limit heating in the day time and cooling at nights, are another factor impacting sea breeze circulation. It can be said clouds reduce and block the heating cycle (Nuss 2003). As a result, strong sea breezes occur on sunny days not cloudy ones (Nuss 2003). In her thesis (2004), Duvall pointed out that “cloud-free days generate the strongest heating which provides the potential for strong sea breeze circulation.”

Mountainous coastlines and the geometry of the shoreline also have an influence on the development of the sea breeze circulation (Nuss 2003). For instance, concave coastlines such as those along a bay create a sea breeze that is divergent/diffluent, but convex coastlines such as those surrounding a peninsula create a sea breeze that is convergent on the coast (Nuss 2003). Darby et al. (2002) showed that the complex terrain surrounding the Monterey Bay causes the sea breeze to be more complicated. In addition, the mountainous coastline in Monterey causes an earlier sea breeze onset in comparison to flat areas such as the Texas gulf coast (Jeffrey 1996). This difference in onset can be attributed to coastlines with a slope warming up faster than flat ones (Nuss 2003). A rugged coastline can contribute to other unusual effects. Normally the sea breeze blows perpendicular to the shore, but the sea breeze in Salinas (located on the Monterey Bay) is nearly parallel to the coastline because the valley in Salinas is directed at an angle to the coastline. This causes the sea breeze to rotate along the valley direction because of channeling effects, which has been pointed out in many previous studies (Nuss 2003).

Another factor affecting transport of sea breeze along the coast is the Coriolis force. If the air parcel stays in the circulation for a long period of time, then Coriolis force may have an effect on sea breeze circulation. Coriolis force needs time to perform its influence, because it does not happen suddenly (Jeffrey 1996). Anthes (1978) determined that Coriolis effects did not become significant until six hours after the heating cycle began; also he found the Coriolis force is important in transport along the coast.

If the atmosphere is stable (warm air over the cold air) then sea breeze circulation will be negatively affected because vertical movement will be limited. Wexler (1946) pointed out that “vertical instability is the most favorable time for sea breeze.” Also Estoque’s (1962) model showed that the intensity of the circulation is decreased with stable thermal stratification. If the boundary layer is unstable then we will have the strong sea breeze winds. A study by Haurwitz (1967) showed that maximum sea breeze intensity does not happen when $T(\text{land}) - T(\text{ocean})$ reduces to ‘0’; rather, it happens when the ocean is cooler than the land (Jeffrey 1996). This is because a positive temperature difference is needed to beat the frictional force (Jeffrey 1996).

Generally sea breeze flow covers the region within 20 km of the coast in Monterey Bay. An increase in wind speed, a decrease in temperature, a rise in humidity and a change in the direction of the wind are the indicators of the beginning time of the sea breeze (Duvall 2004). In late afternoon the sea breeze decreases and ends after sunset.

C. COASTAL JETS

To understand and explain this study, we need to offer a brief description of the coastal jet. Firstly, we should know that the coastal jet is not diurnal like sea breeze (Steven 1997). Coastal jets generally occur in the warm seasons, that is, summer time in the Northern Hemisphere and winter time in the Southern Hemisphere when temperature gradients are greater (Zemba and Friehe 1987, Burk and Thomson 1996). Thermal structure is a critical factor to determine the existence of the coastal jets (Nuss 2003).

When the air gets colder it becomes denser and moves to the ground, and inversely, warm air becomes less dense and moves upwards (Beardsley et al. 1987). This temperature gradient drives the pressure gradients. When we get closer to the shore the pressure gradient becomes larger (Nuss 2003). The pressure gradient decreases not only toward land but also toward sea; however, it reaches its maximum value at the coast (Nuss 2003). In this pressure field, the difference in winds is seen due to the cross-coast pressure gradient in the shore, even though there is a difference in friction between land and ocean (Nuss 2003).

Because of the cooler temperature over the ocean and warmer temperature over land, the inversion layer slopes down to the coast. Similarly, the marine boundary layer (MBL) slopes downward to the ground, and the low-level temperature gradient reaches its maximum value at this location. This results in baroclinic structure and acceleration of the wind near the coast (Nuss 2003, Cross 2003). As mentioned previously, temperature gradient leads to pressure gradient, and finally, as the wind increases near the coast the coastal jet is formed. The jet is strongest near the bottom of the MBL. According to hydraulic theory, higher wind speed occurs in thinner layers (Winant et al. 1988). The hydraulic theory also indicates that the height of the flow decreases when the wind speed

increases (Samelson 1992). In this theory MBL is assumed to be like a pipe or channel (Winant et al. 1988).

Along the California coast, the ocean surface temperature stays cooler than land because of coastal upwelling and cold ocean currents. Coastal upwelling cools the MBL, which causes an increase in temperature gradient perpendicularly to the coast. This thermal gradient leads to a stronger pressure gradient and lastly creates stronger winds. Finally, the coastal jet is developed. If there are mountains along the coast, then these mountains force the winds to blow parallel to the shoreline, as it occurs on the California coast (Cross 2003).

III. DATA

Many instruments, such as aircraft, lidar, radiosondes and wind profilers, have been used over the years to measure the horizontal and vertical movement of sea breeze. Surface currents maps obtained in this study are derived from CODAR-type HF radar by using SeaSonde units. HF sensor stations are based on the shore. The importance of installing HF radar systems close to the coast is to allow maximum range and benefit from the surrounding wet and sandy soils (Paduan and Graber 1997). The CODAR data consist of total current and radial current vector files. The CODAR data set contains the location, U and V velocity components. Four CODAR stations are used to get data for the Monterey Bay area; these stations are shown with their location and name in Table 1. The positions of these CODAR HF radar antennas are shown in Figure 5. Time series are created for each CODAR grid point from the collection of total current vector files. The missing data are different for each grid point. Because of gaps in the data, linear interpolation is used to fill the gaps. To determine the sea breeze circulation and know the vertical movement of air, the wind profiler and MBARI buoy data are used.

CODAR Station	Position
Moss Landing	36.80N 121.78W
Santa Cruz	36.94N 122.06W
Naval Postgraduate School	36.60N 121.87W
Point Sur	36.30N 121.90W

Table 1. CODAR Stations, from California Coastal Ocean Currents Monitoring Program at <http://cencalcurrents.org>.

To see the difference between surface and deep currents ADCP data are used in addition to CODAR HF radar data set. The 6 Meter depth (first bin) ADCP data are used for analysis because these data come from the closest bin to the surface. ADCP data are gathered from three MBARI buoys (M0 M1 M2 ADCP data). ADCP and wind

measurements concurrent with the CODAR data set are compared with nearby CODAR grid points (mean values of the six grid points near to the buoy locations), as shown in Figure 6, and also the availability of the data for each grid point, as shown in Figure 7. If the percentage coverage for a grid point is less than 70%, to ensure accurate results from the analysis, the data for that grid point are not used.

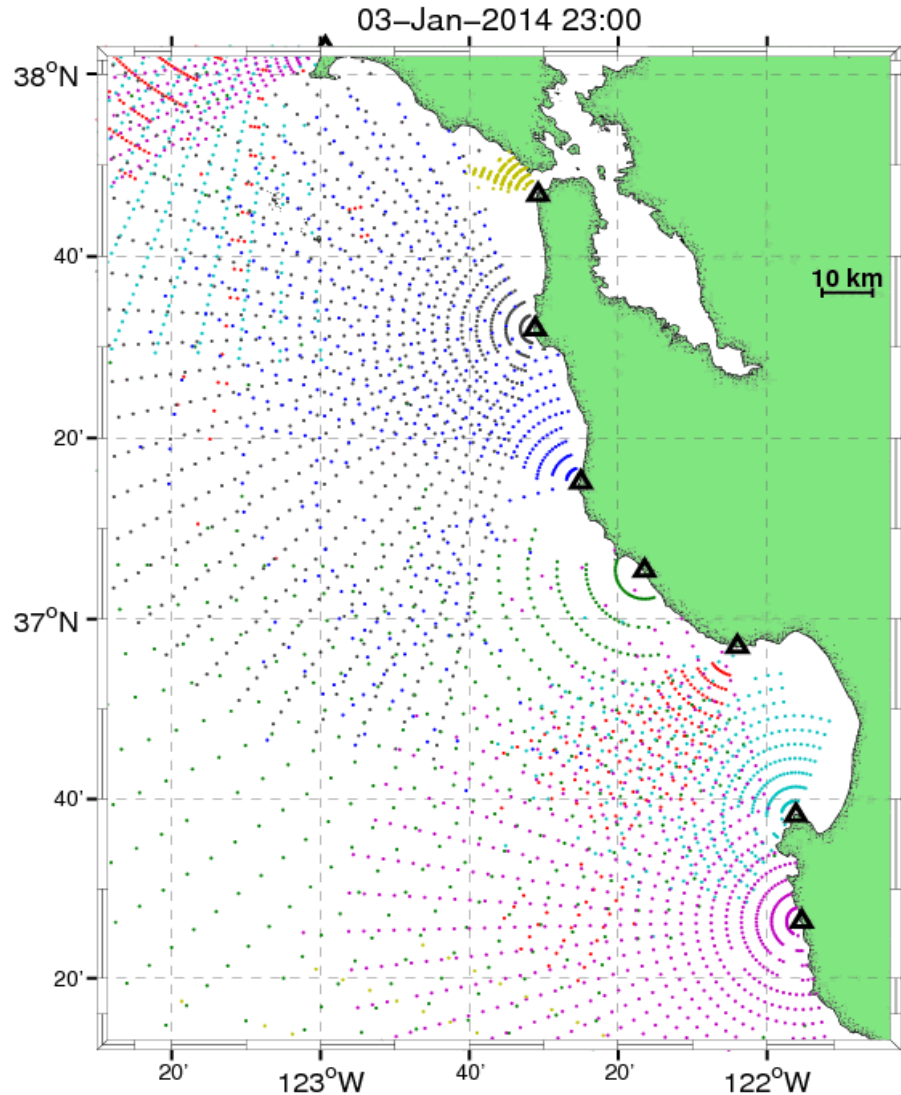


Figure 5. Locations of CODAR HF Antennas along the California Coast (triangles) and the individual radial current observations points (dots) for a sample hour in January 2014, from California Coastal Ocean Currents Monitoring Program at <http://cencalcurrents.org>.

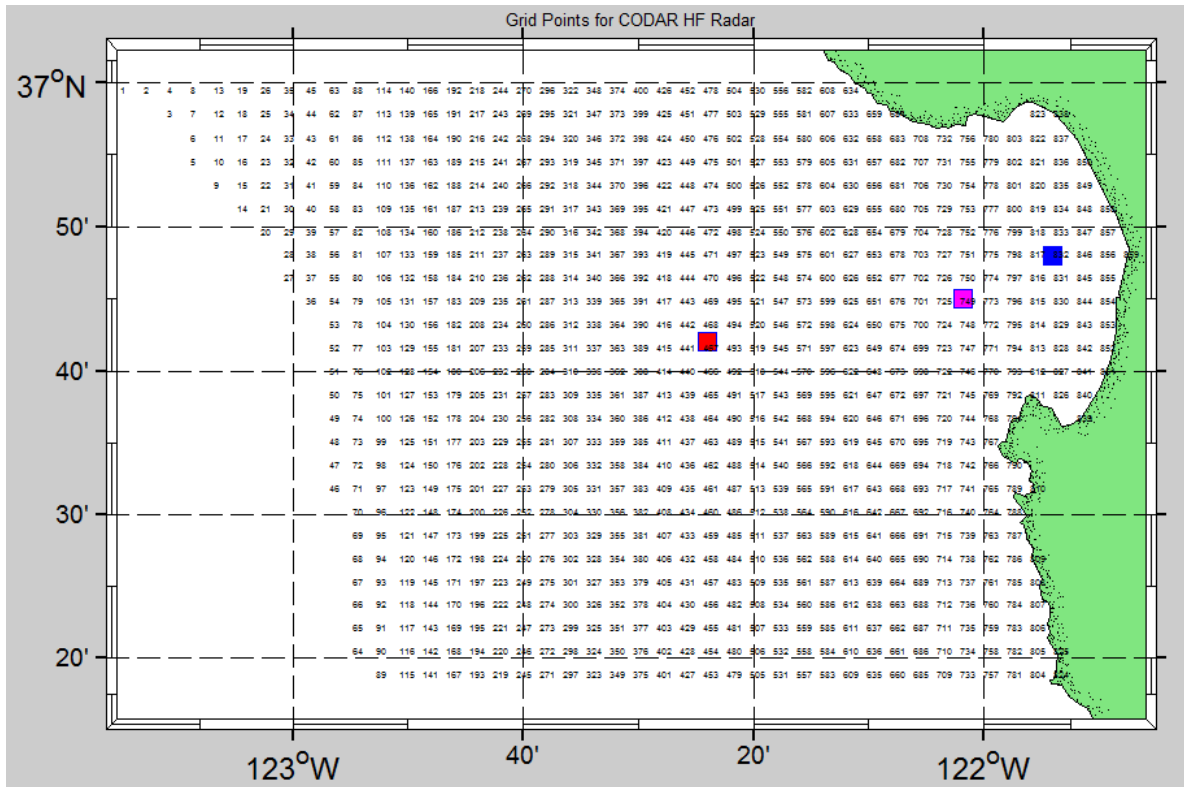


Figure 6. The Plot of all CODAR HF Grid Radar Points in the Region.

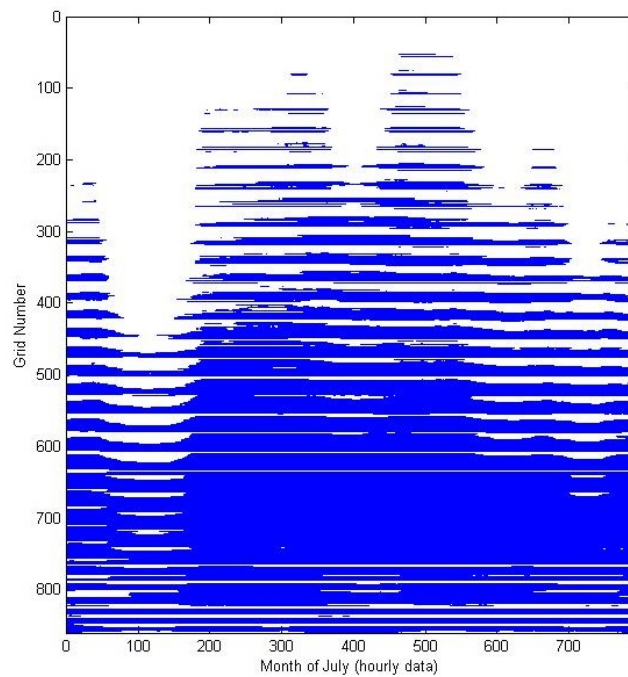


Figure 7. The Data Availability of Each Grid Point in July 2009.

All data analyzed were gathered from July 1, 2009, to September 31, 2009. The year of 2009 was chosen because of having the best available data set with minimum gaps for HF radar data, as shown in Figure 8. Data from the same time scale were retrieved from wind profiler and MBARI buoys. The 915 MHz wind profiler that provided wind data in this study is located in Marina, as shown in Figure 9. The distances of M0 and M1 buoys to the coast are ~10 km and ~18 km.

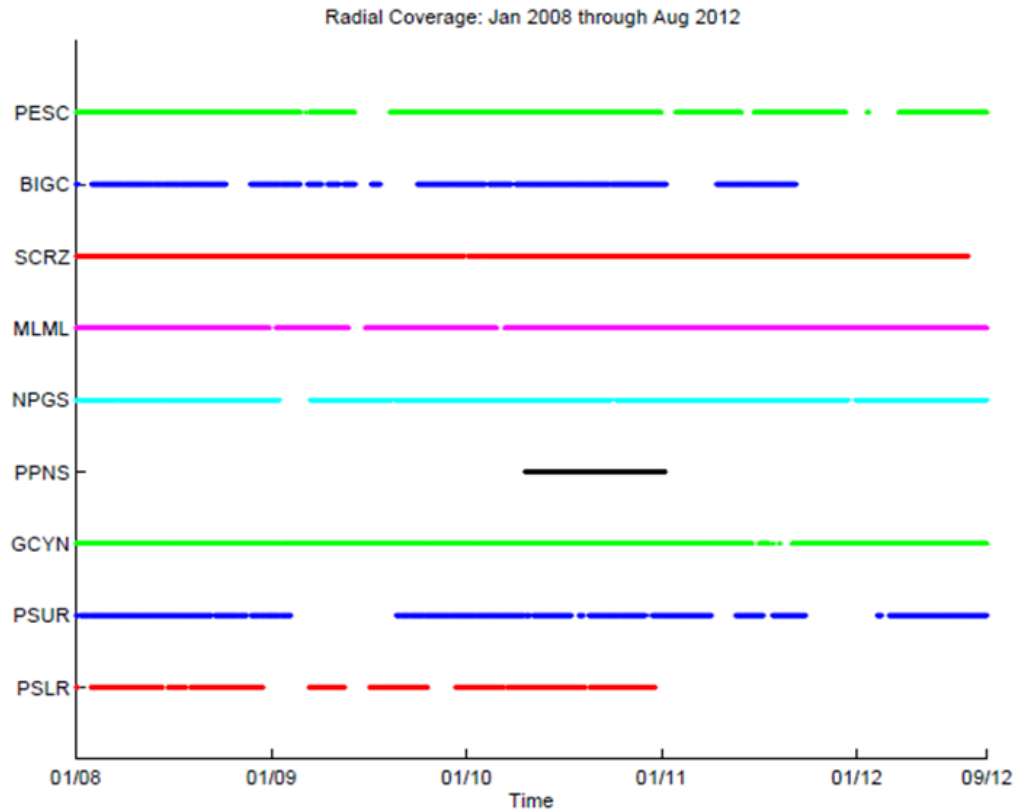


Figure 8. Radial Coverage of HF Radar from 2008–2012.

In order to make comparison among the data sets, all data must be formatted in the same way. Thus, all of the wind/current time series:

- Are interpolated for gaps under three hours, and
- Use hourly data, which are arranged for yearly, seasonal, monthly and daily influences.

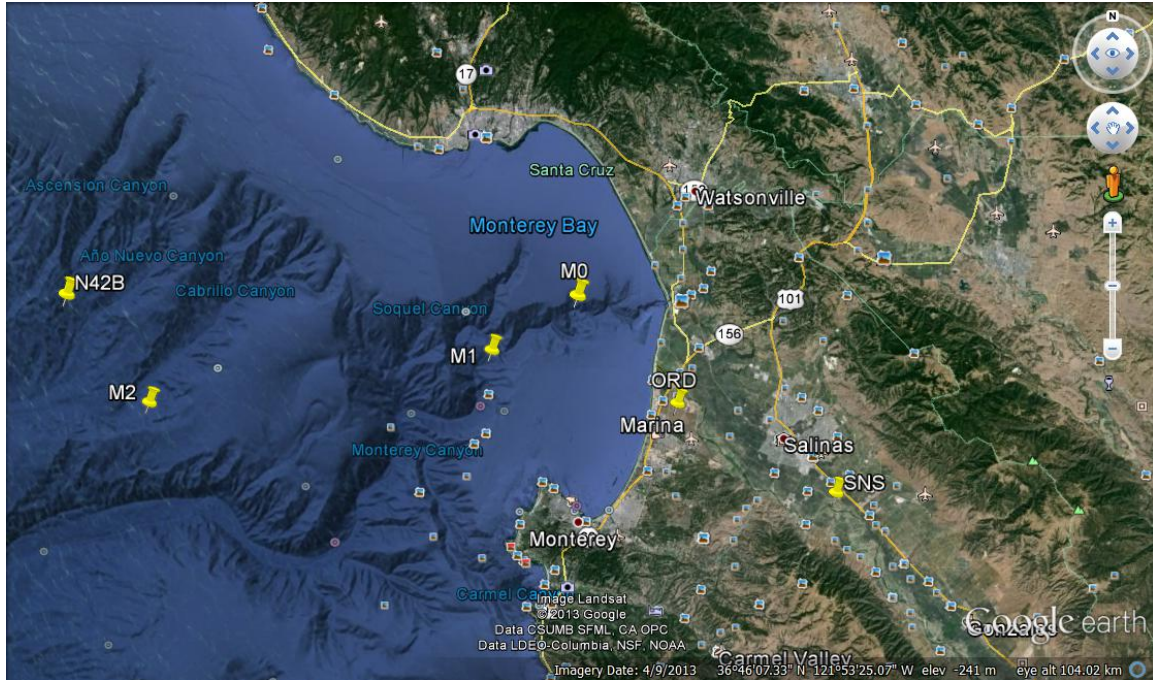


Figure 9. Locations of M0, M1, M2 Ocean Buoys, Wind Profiler (ORD) and Salinas (SNS) Observations Sites, and the NOAA Buoy 46042 (N42B, not used) location (from Google Earth).

Figure 10 shows the area we focused on to analyze the coastal jets for the California coast. The Climate Forecast System Reanalysis Model (CFSR) is used. This model is contained in the General Meteorology Package (GEMPAK) Analysis and Rendering Program (GARP). The resolution of the CFSR model is 0.5 degree latitude-longitude. We used it at 37N latitude and covered 30 grid points of longitude at this latitude in the model data. The CFSR model has 0.5 degree grid resolution (30 nm in the latitudinal direction), so at 37N we obtained $30\text{nm} \cdot \cos(37\text{deg}) \approx 24\text{nm}$ resolution in the longitudinal direction of our cross section. Synoptic scale data used in this study is six-hour data. Synoptic data are used to pick up sea breeze days when we apply the conditions to determine sea breeze days.

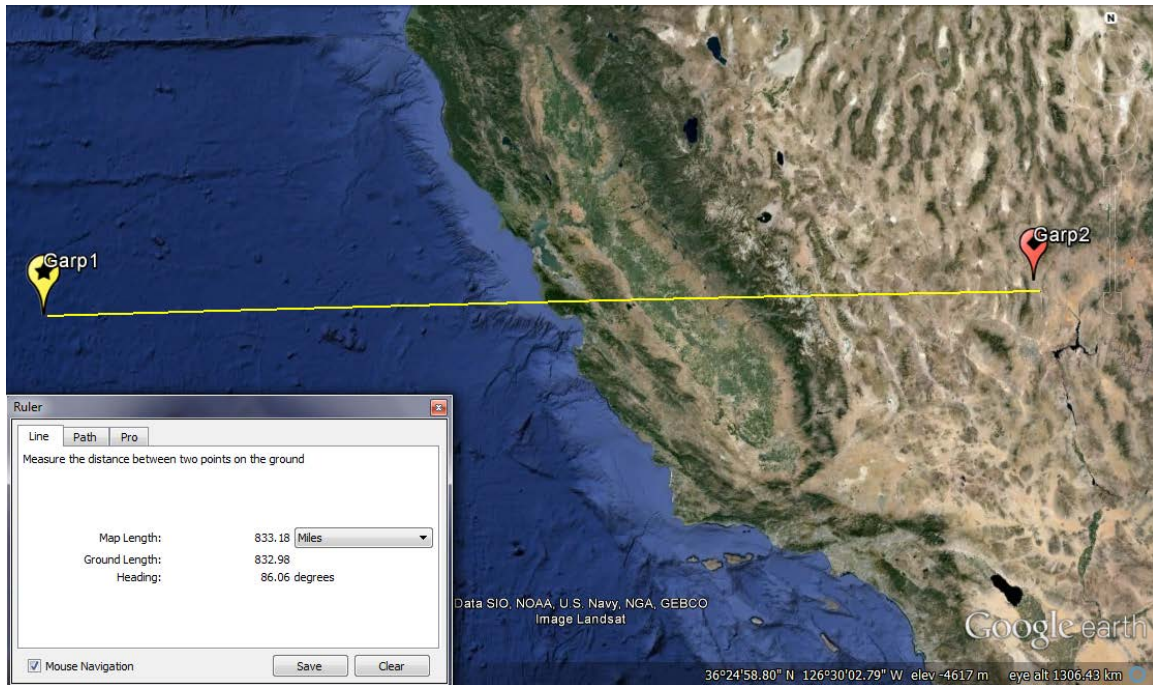


Figure 10. The Area of Focus used in CFSR Model to Examine Coastal Jets (from Google Earth).

IV. ANALYSIS OF DATA AND RESULTS

It is easy to define sea breeze as we showed in Chapter II, but it is hard to forecast. We know that sea-land breezes are common in summer time. Despite improvements in technology and gathering data of winds, people are far from predicting and analyzing the dynamics and effects of sea breezes over currents and waves.

To determine sea breeze days, many parameters such as temperature change, topography, time of year, wind speed and wind direction should be taken into consideration besides synoptic scale effect. The sea breeze occurs daily in Monterey throughout the summer, but the synoptic conditions have some unusual effects on the direction of sea breeze and land breeze in Monterey Bay, so it is not easy to predict. This synoptic effect might change from region to region. Due to synoptic conditions, the wind direction change cannot be accepted as the critical criterion in Monterey Bay, even though it is a very important phenomenon for determining sea breeze days. For example, synoptic wind direction is generally onshore, as is the sea breeze in Monterey Bay. At night time, land breeze occurs, but land breeze is weaker than sea breeze. Most of the time, this wind direction change at night cannot be seen in Monterey Bay due to strong synoptic winds and weak land breeze. In Hendrickson and MacMahan's study (2009) they pointed out that "[d]uring sea breeze cross-shore exchange of material seems to occur onshore near the surface but it is not reversed during land breeze." What we expect to see on a typical sea breeze day is shifting offshore; however, due to background onshore wind that does not occur in Monterey Bay. So, we cannot see the reversal of cross-shore exchange of materials (Hendrickson and MacMahan 2009). Borne et al. (1998) used wind direction change criteria to pick up sea breeze days, but his criteria are not applicable in Monterey Bay. Because of the reasons mentioned here, in this study the reversal of wind direction criterion is not a filter.

Temperature difference between land and sea surface has an effect on sea breeze as well. The effects of synoptic winds should be analyzed to get the relationship between wind speed and temperature differences to depict sea breeze days. Temperature difference is the most important factor which causes sea breeze, but it is more complex to

determine sea breeze days. If we look at the average values for individual days, it is not easy to identify sea breeze days for this region. It is hard to see the direct relationship between the temperature change and sea breeze through this analysis. However, when we examine the hourly average air temperature (see plot in Figure 11), we realize that there are some certain results to point out about temperature change between 2 p.m. and 11 a.m. at each location in our study.

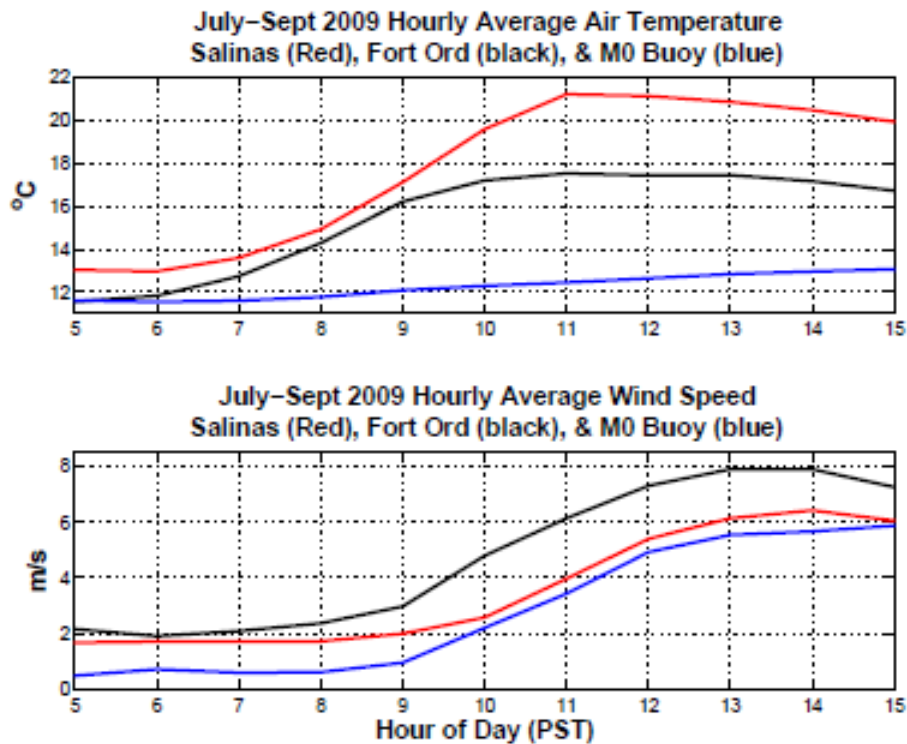


Figure 11. July–September Average Hourly Plot of Air Temperature and Wind Speed for Salinas, Fort Ord and M0 Buoy.

As we see in Figure 11, the temperature is reaching its highest value at 11 a.m. in Salinas, which is what we expect to see. Because of cold air rising from the ocean to the land, on sea breeze days there should be a decrease in temperature over land. We cannot see this drop in Fort Ord because it is close to ocean. Salinas is an inland region; that is why we see a dramatic drop in temperature there. Not surprisingly, for the M0 buoy location in the ocean we cannot see much change in temperature. Meanwhile, though,

there is an increase in wind speed in all locations until 2 p.m., when the wind speed reaches its highest value. With respect to Figure 11, we can say that the increase in wind speed at Fort Ord is much greater than it is at Salinas and the M0 buoy location.

The time scale for sea breeze cycle is 24 hours. The start of every sea breeze is after sunup, generally at 11 a.m. (Foster 1996). Morning times are accepted as the time that sea breeze effect is weak and cannot be seen. In this study 2 p.m. is accepted as the time sea breeze reaches its maximum value on land, as indicated in Foster's dissertation (1996) and shown in Figure 11, which plots the average hourly wind speed for July to September in Salinas and at Fort Ord. The end of the sea breeze is determined when the wind speed reduces to 50% of its value, as indicated by Foster.

Before choosing the specific time period to study for the thesis, we wanted to see how temperature behaves throughout the year of 2009. When we look at Figure 12, it is easy to notice that summer time is the time when afternoon temperature is lower than it is in the morning time. That means most probably we have sea breeze on these days. That is why we focus on the summer time in this study. Hendrickson and MacMahan (2009) studied all seasons. What they determined is that sea breeze has the strongest effect on generating waves in the summer season. Moreover, they pointed out that in winter sea breeze is the weakest. These results are consistent with our study.

In addition to changes over the course of a day, seasonal changes are also important. As Figure 13 illustrates, not only is the change in temperature between morning and afternoon in summer greater than it is in the winter, but so is the change in wind speed. With respect to Figure 13, it is also obvious that sea breeze forcing dominates Monterey Bay's surface winds in summer time. Table 2 shows the values of mean wind speed, mean wind direction and mean wind speed difference between morning (6 a.m.) and afternoon (2 p.m.). It is obvious to see in Table 2 that wind speed difference is greater at the M0 location due to sea breeze, and the values increase as we move towards the coast.

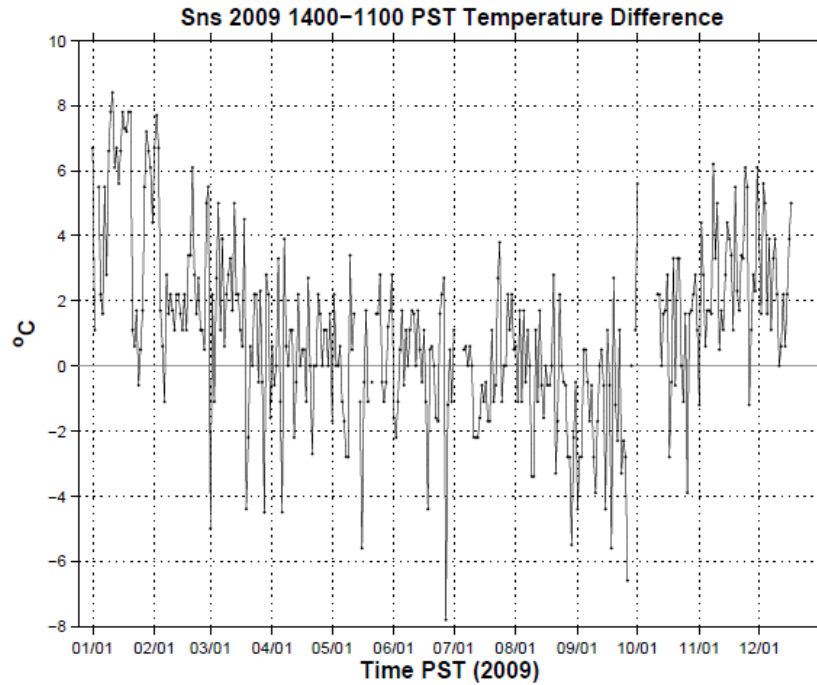


Figure 12. Temperature Difference between 2 p.m. and 11 a.m. for Salinas in 2009.

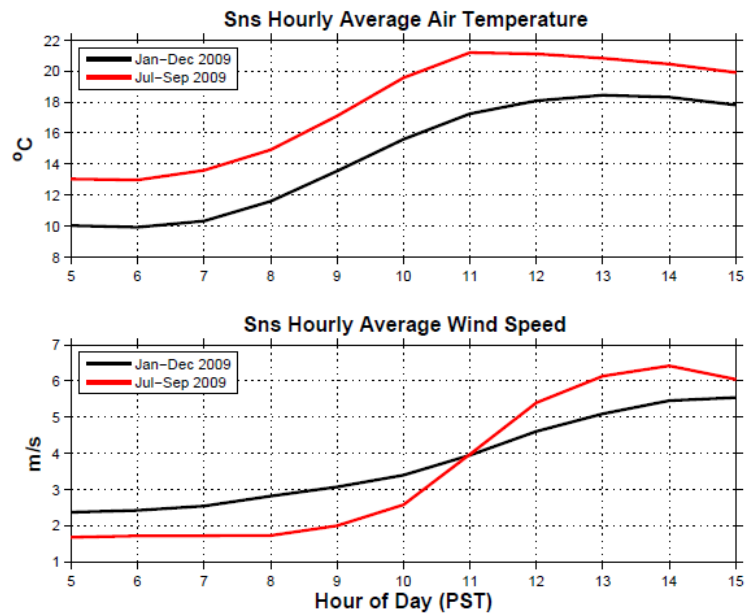


Figure 13. Summer and Winter Average Hourly Plot of Air Temperature and Wind Speed for Salinas.

Based on the reasons outlined in the previous paragraphs, we chose to analyze sea breezes in Monterey Bay during the period of July to September 2009. In the following sections, we detail our methodology for collecting data during that period and analysis of that data.

When we used wind data from the buoys or wind profiler we considered it carefully, because wind is a vector value with its magnitude and direction. The easiest way to understand the behavior of wind is to focus on the power spectra/rotary spectra to get the frequency distribution. Alternatively, getting the wind direction or wind speed components allows us to see how wind is behaving hourly, daily or monthly. Mean values may not describe everything, but this information does tell us the general behavior of the winds for the time scale we selected.

The plots of M0, M1, M2, Fort Ord and Salinas wind speed differences are shown in Figures 14, 15, 16, 17 and 18, respectively. Wind speed differences figures are one of the main ways to see the sea breeze effect. To give us a good understanding of the wind behavior in Monterey Bay we used wind profiler data, which is shown in Figures 19, 20, 21, 22 and 23. In particular, mean wind direction plots show that the wind is blowing on shore and the average value is between 270 and 300.

	M0 BUOY	M1 BUOY	M2 BUOY	FORT ORD	SALINAS
	JUL-SEP	JUL-SEP	JUL-SEP	JUL-SEP	JUL-SEP
<i>Mean WSpd Vector Diff 2 p.m.-6 a.m.</i>	<u>4.92 m/s</u>	<u>3.21m/s</u>	<u>0.917m/s</u>	<u>5.99m/s</u>	<u>4.71m/s</u>
<i>Mean Wind Speed</i>	<u>2.55 m/s</u>	<u>4.72m/s</u>	<u>5.06m/s</u>	<u>4.36m/s</u>	<u>3.45m/s</u>
<i>Mean Wind Direction</i>	<u>277°</u>	<u>299°</u>	<u>307°</u>	<u>260°</u>	<u>282°</u>

Table 2. Mean Wind Speed/Direction between July and September 2009.

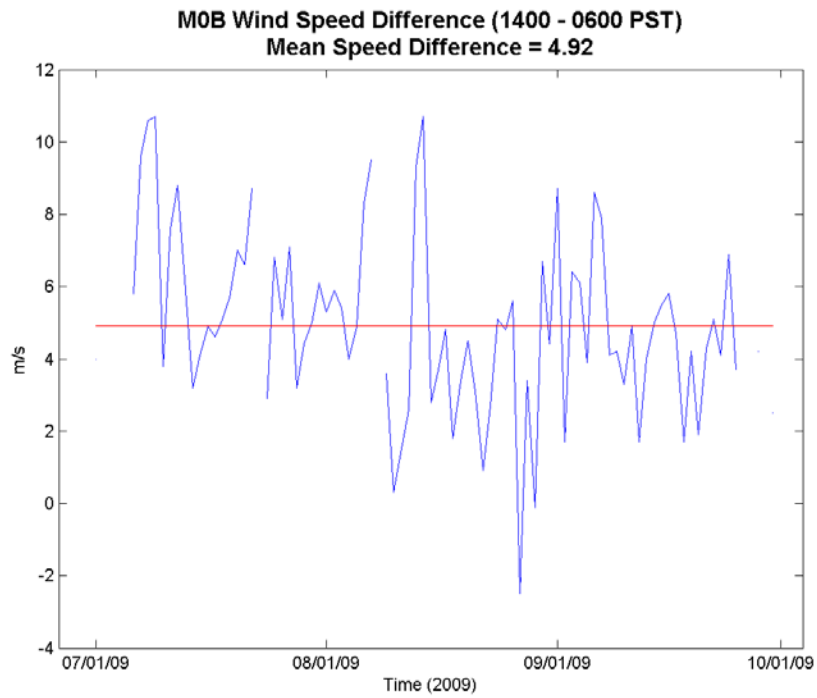


Figure 14. Wind Speed Differences Plot for M0 Buoy, July–September 2009.

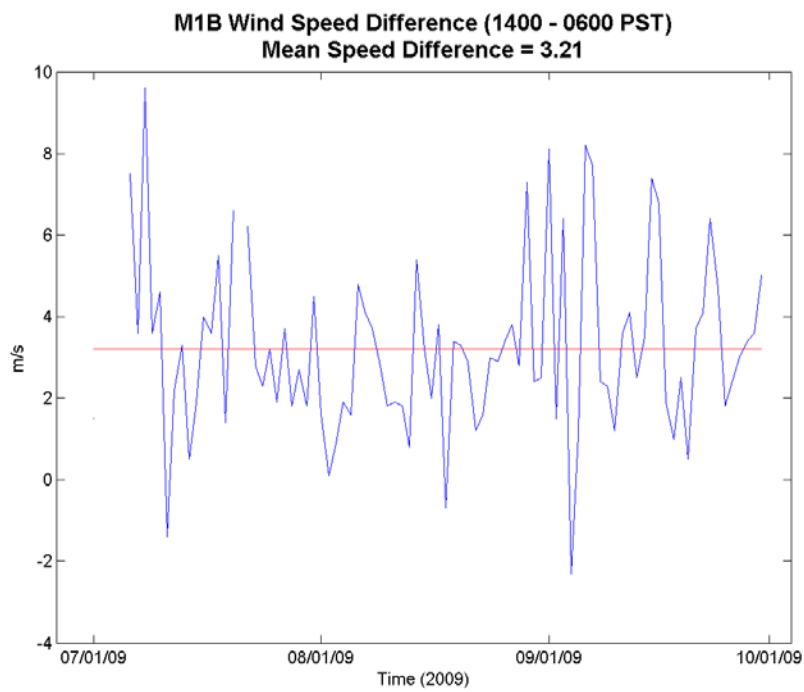


Figure 15. Wind Speed Differences Plot for M1 Buoy, July–September 2009.

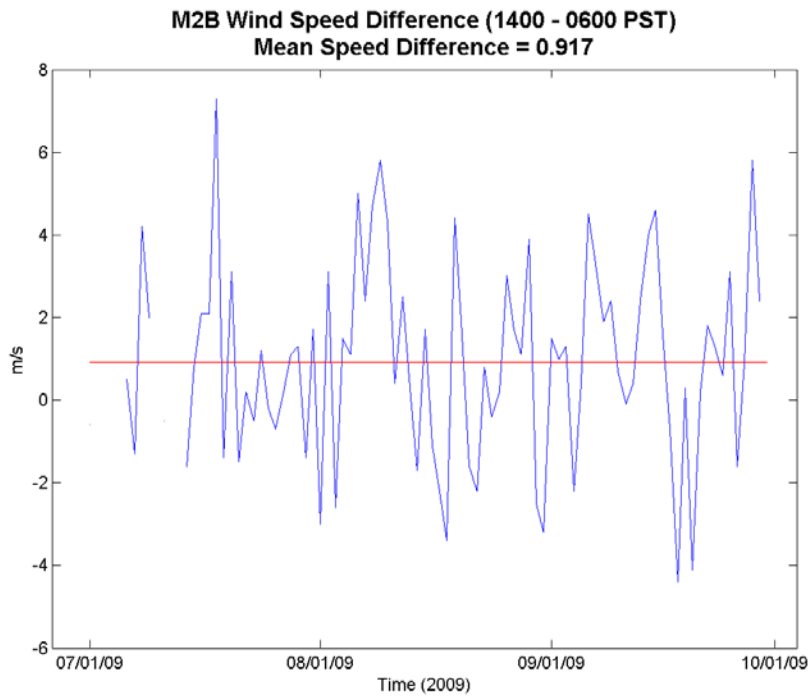


Figure 16. Wind Speed Differences Plot for M2 Buoy, July–September 2009.

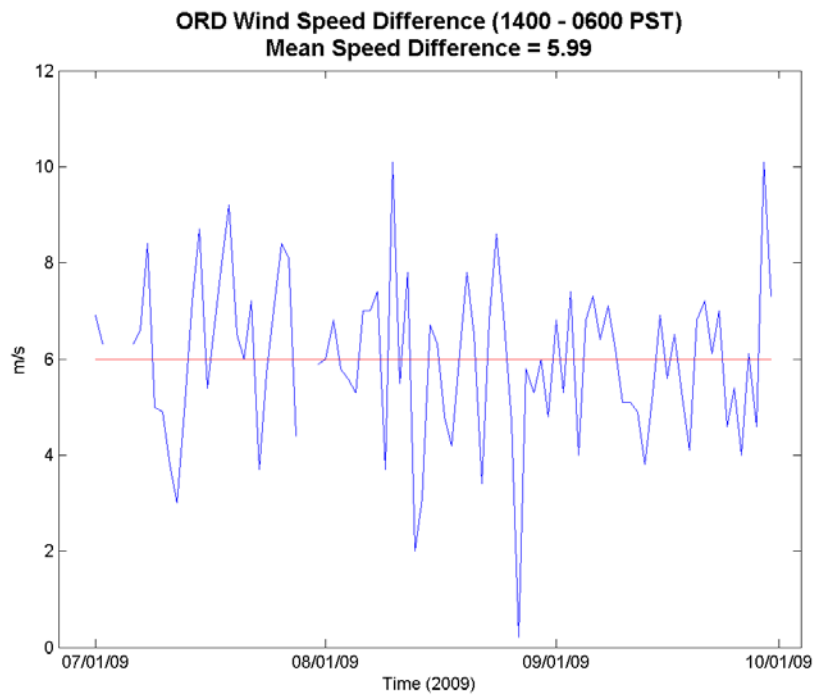


Figure 17. Wind Speed Differences Plot for Fort Ord, July–September 2009.

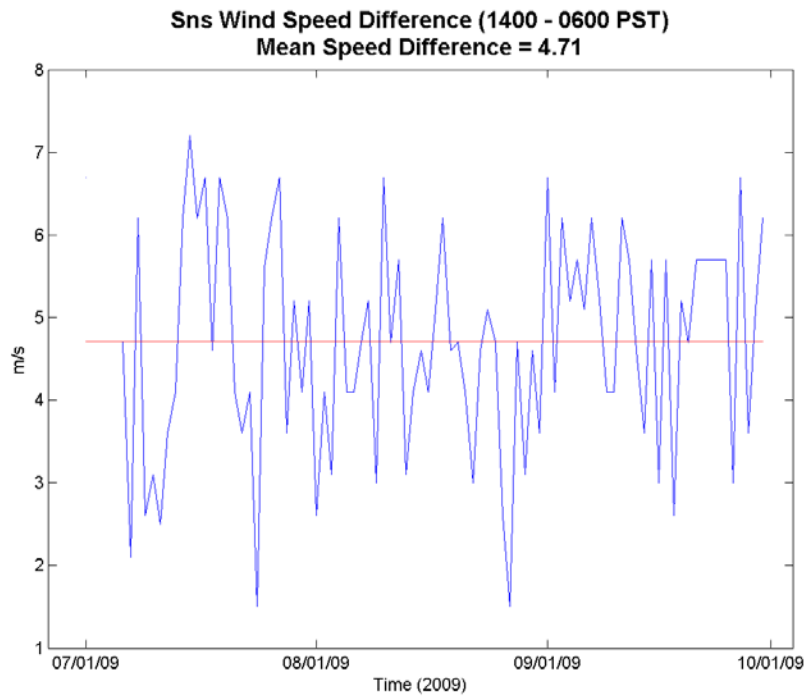


Figure 18. Wind Speed Differences Plot for Salinas, July–September 2009.

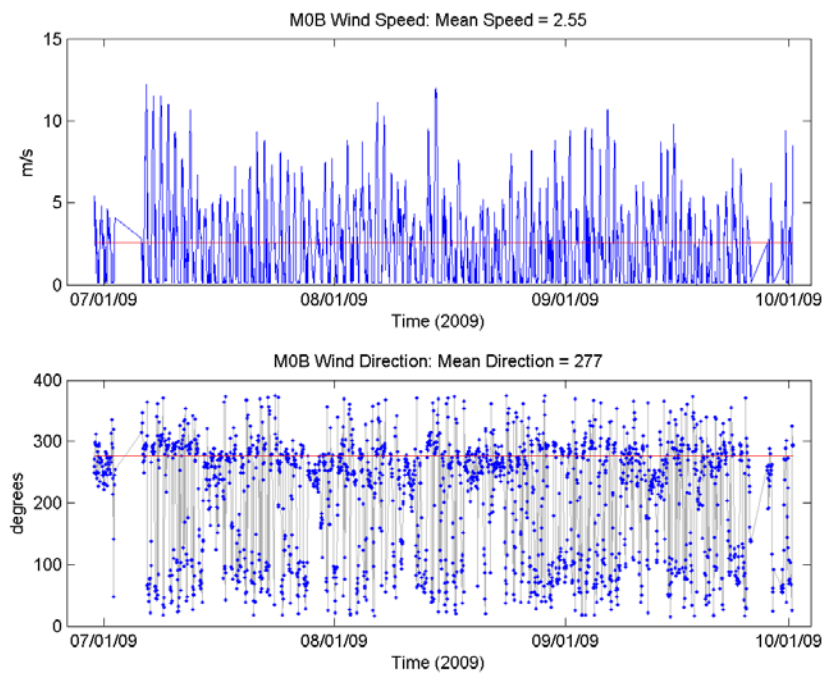


Figure 19. Mean Wind Speed and Direction Plot for M0 Buoy, July–September 2009.

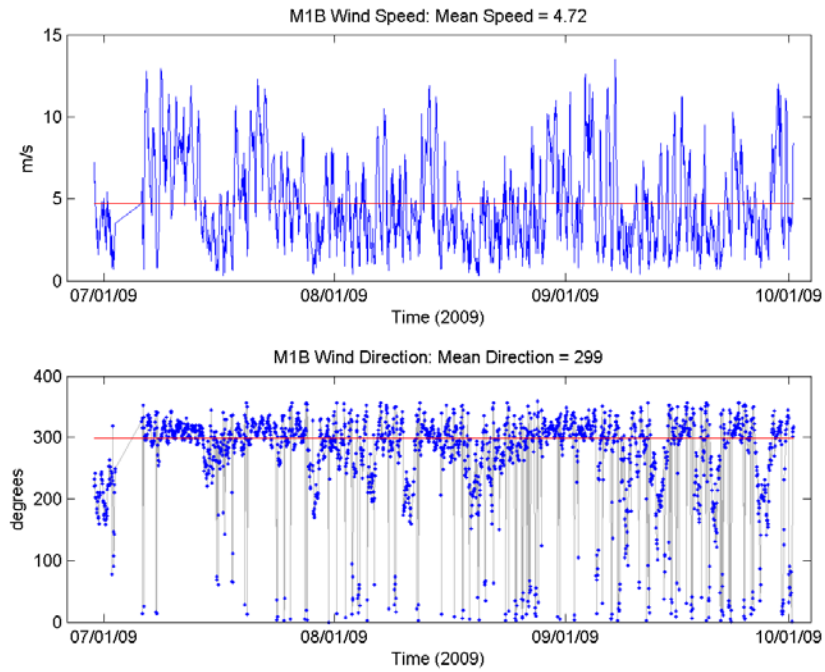


Figure 20. Mean Wind Speed and Direction Plot for M1 Buoy, July–September 2009.

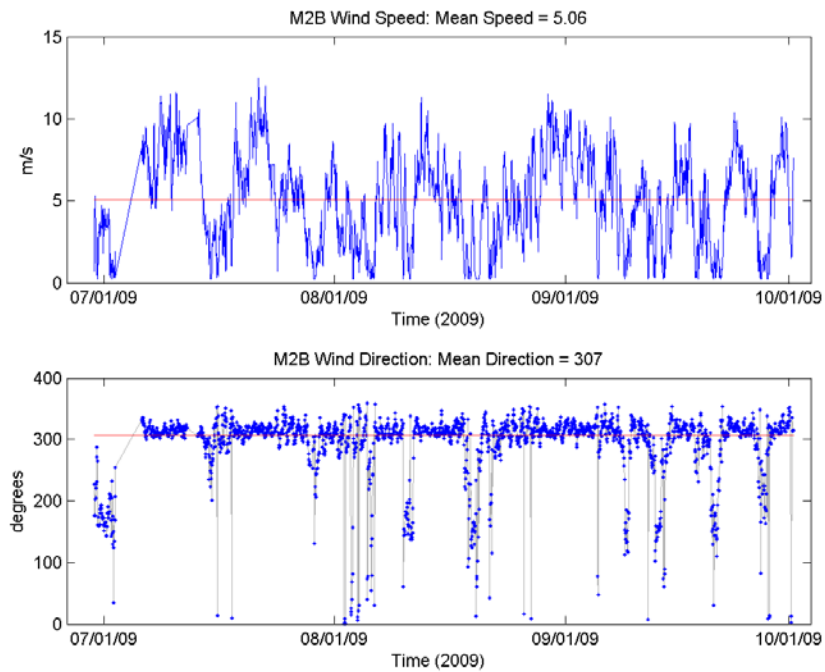


Figure 21. Mean Wind Speed and Direction Plot for M2 Buoy, July–September 2009.

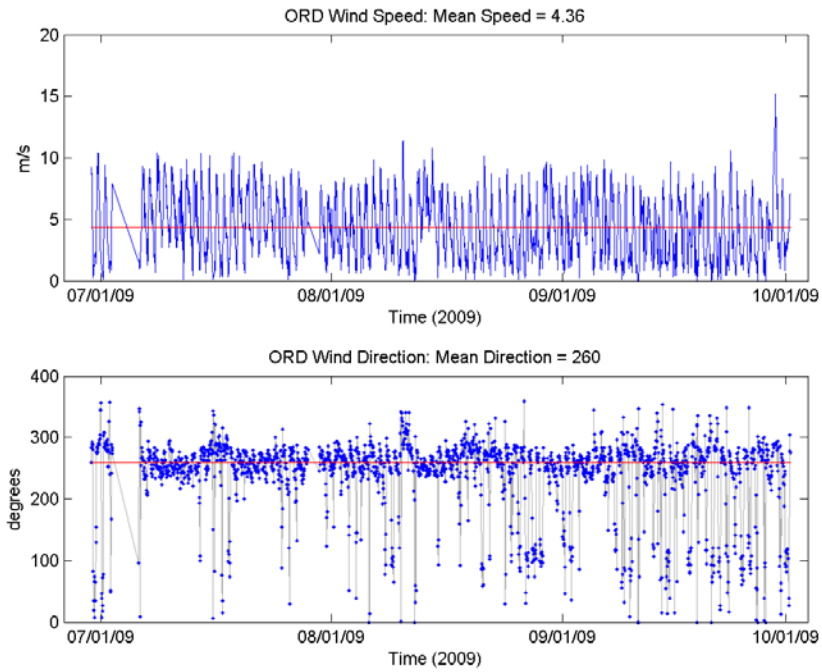


Figure 22. Mean Wind Speed and Direction Plot for Fort Ord, July–September 2009.

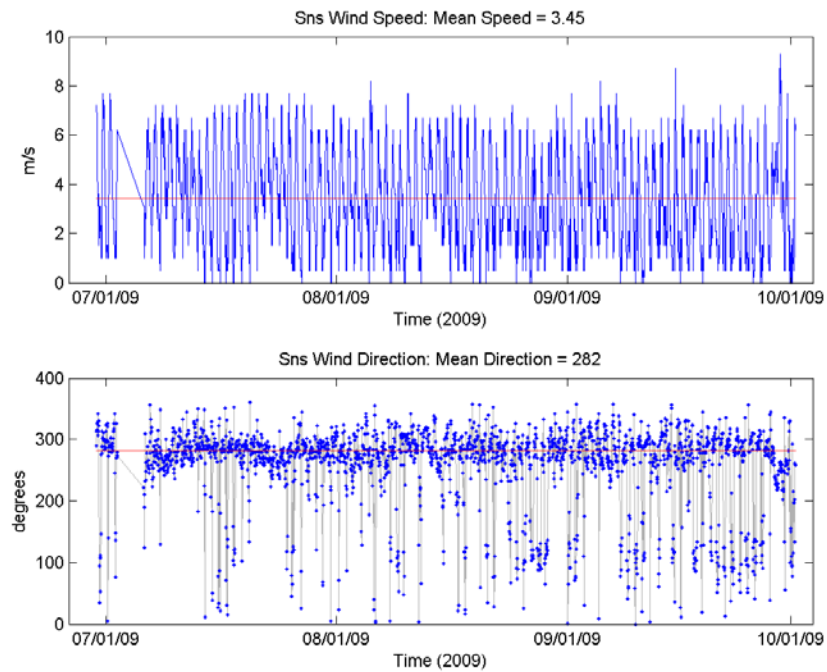


Figure 23. Mean Wind Speed and Direction Plot for Salinas, July–September 2009.

A. ESTABLISHING CRITERIA TO DETERMINE SEA BREEZE IN MONTEREY BAY

Accurate forecast of sea breeze is not possible today; we know that we are still far from that. By using empirical knowledge, however, we can set up some conditions to determine sea breeze days. Even though sea breeze is a complicated event, our method for analyzing it is simple and easy to understand. Also we believe that, with minor changes, this method can be used to study sea breeze in other regions. Our approach is based on temperature, wind speed change over the surface water/land, synoptic scale winds and wind direction data over the surface water/land.

To accept a day as a sea breeze day, six conditions, shown in Figure 24, should be investigated. Some conditions are related to synoptic scale since if synoptic winds at 700hPa are strong, then winds block vertical movement of winds. So we add synoptic scale conditions to get rid of the dominating effect of synoptic winds as stated in Borne et al. (1998). Temperature difference, wind direction difference and wind speed differences will help us to obtain some objective results.

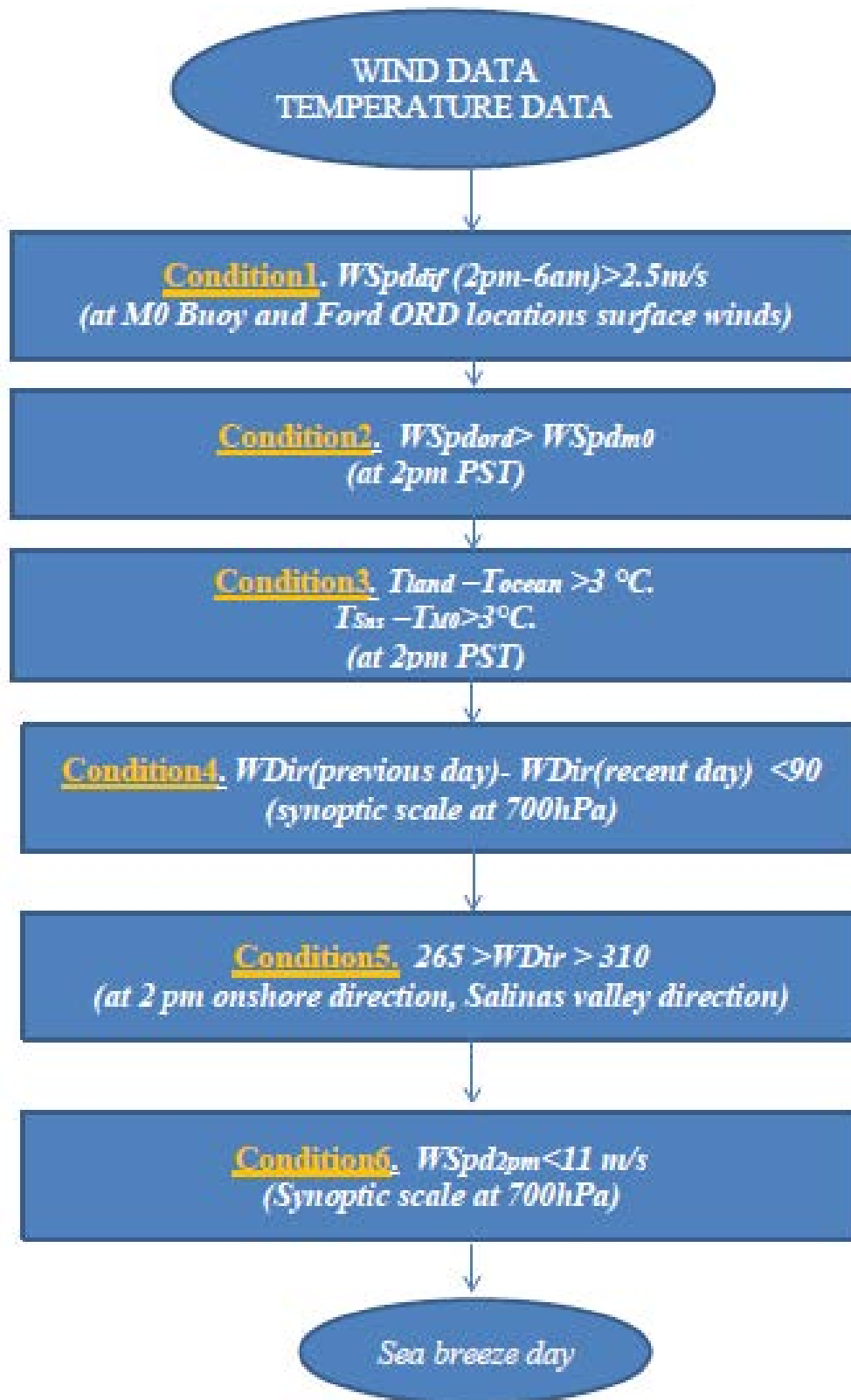


Figure 24. Sea Breeze Algorithm Chart.

Six filters are created as an algorithm for Monterey Bay to determine sea breeze days. This algorithm is applicable only for Monterey Bay since sea breeze characteristics depend on many criteria as mentioned in Chapter II and change from region to region. These conditions are explained as follows:

- **Condition 1** – As Foster (1996) stated, “if wind speed increases by more than 2.5 m/s in an onshore direction between morning and afternoon (in both M0 buoy location and Fort Ord) during day is classified as sea breeze days.”
- **Condition 2** – Wind speed at 2 p.m. at Fort Ord is greater than the wind speed at 2 p.m. at the M0 buoy location. We expect to see much stronger wind speed at Fort Ord with respect to the M0 buoy location at 2 p.m. (as determined with help from Prof. Wendell Nuss).
- **Condition 3** – The temperature difference between Salinas and the M0 buoy location at 2 p.m. should be greater than 3 degrees Celsius (Borne et al. 1998). Watts (1955) pointed out that a sea breeze can develop at small temperature differences, such as 2 degrees Celsius. In addition, a decrease in temperature should be seen when the sea breeze begins. Because of that, we expect the sea breeze to bring cold air from the ocean to the land.
- **Condition 4** – To see the effects of synoptic scale, we need to observe how the wind direction changes. To ensure that synoptic scale has no effect, Borne et al. (1998) pointed out that wind direction change over two days (the present and previous day) should be less than 90 degrees at 700hPa.
- **Condition 5** – The general direction of the sea breeze in Monterey Bay area is from between 265 and 310 degrees. Sea breeze blows in an onshore direction during daylight and is classified as a southwesterly sea breeze day.
- **Condition 6** – As Bourne et al. (1998) used the criterion which states “synoptic wind speed at 700hPa (3000m height hPa=mb) should be less than 11 m/s not to see dominating synoptic winds effect in the area;” we also used this to eliminate synoptic scale effects.

To determine sea breeze days for the period studied, we used the algorithm conditions as well as our own experience and knowledge. In Figure 25 “manual” represents the sea breeze days that were chosen by analyzing individual wind profiler images using our experience and knowledge about sea breeze. The other conditions were determined by separately applying the filters created by the six algorithms above. By comparing our results in Figure 25, it is easy to determine sea breeze days (shown in

black) or those that were not sea breeze days (shown in gray). Lastly, the white color is for the days when there are no data.

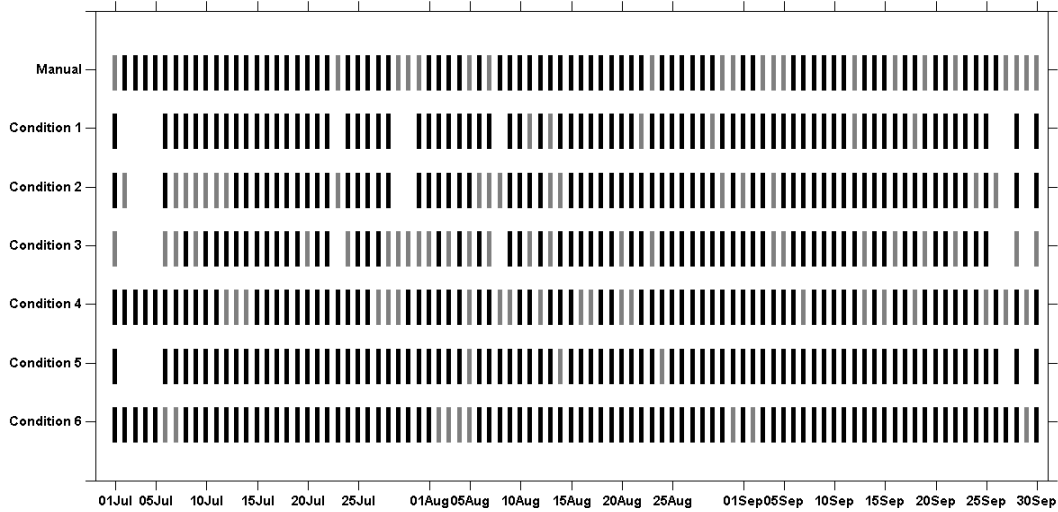
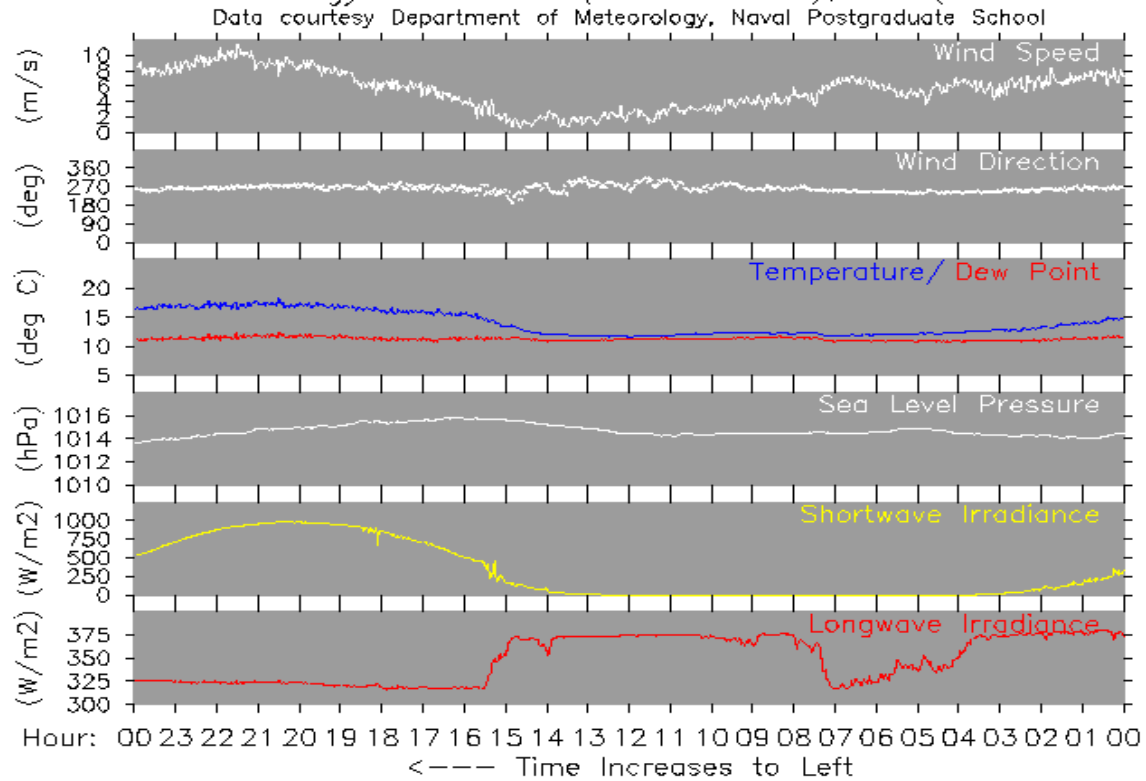


Figure 25. Sea Breeze Days Determined Manually and by Algorithm Conditions.

The manual processing involves inspection of daily output from the Fort Ord wind profiler. Figure 26 and Figure 27 provide examples of those output formats. Gradual wind speed decrease at the surface followed by rapid increase, as shown in Figure 26, is one form of evidence for a sea breeze day. The upward propagation of the wind front, as shown in Figure 27, is another indication of a sea breeze day. In interpreting data from the wind profiler, we should be careful because time is increasing to the left, and it is UTC (Coordinated Universal Time). Looking again at the example in Figure 26, from July 8, 2009 it is easily identified as a typical sea breeze day in Monterey Bay. The increase in wind speed can be easily seen in the afternoon in Figure 26. Also because it is not a rainy day, solar irradiance and temperature values are increasing during the day time. Wind direction is not shifting at night. Figure 27 helps us to understand the vertical movement of wind in the air. It is important to check vertical movement since sea breeze is a cycle as mentioned in Chapter II. In Figure 27 the wind speed is significantly increasing at the surface. Time is increasing to the left again, but here it is PST (Pacific Standard Time).

Surface Meteorology: Fort Ord (Profiler Site), CA (elev. 51 m)



Data from 08-JUL-2009 00:00 through 08-JUL-2009 23:58 UTC
 Image generated by Department of Meteorology, Naval Postgraduate School

Figure 26. Wind Profiler Site Plot for Surface Meteorology Data, from Naval Postgraduate School at <http://met.nps.edu/~lind/nps/archive/ARCHIVE.HTM>.

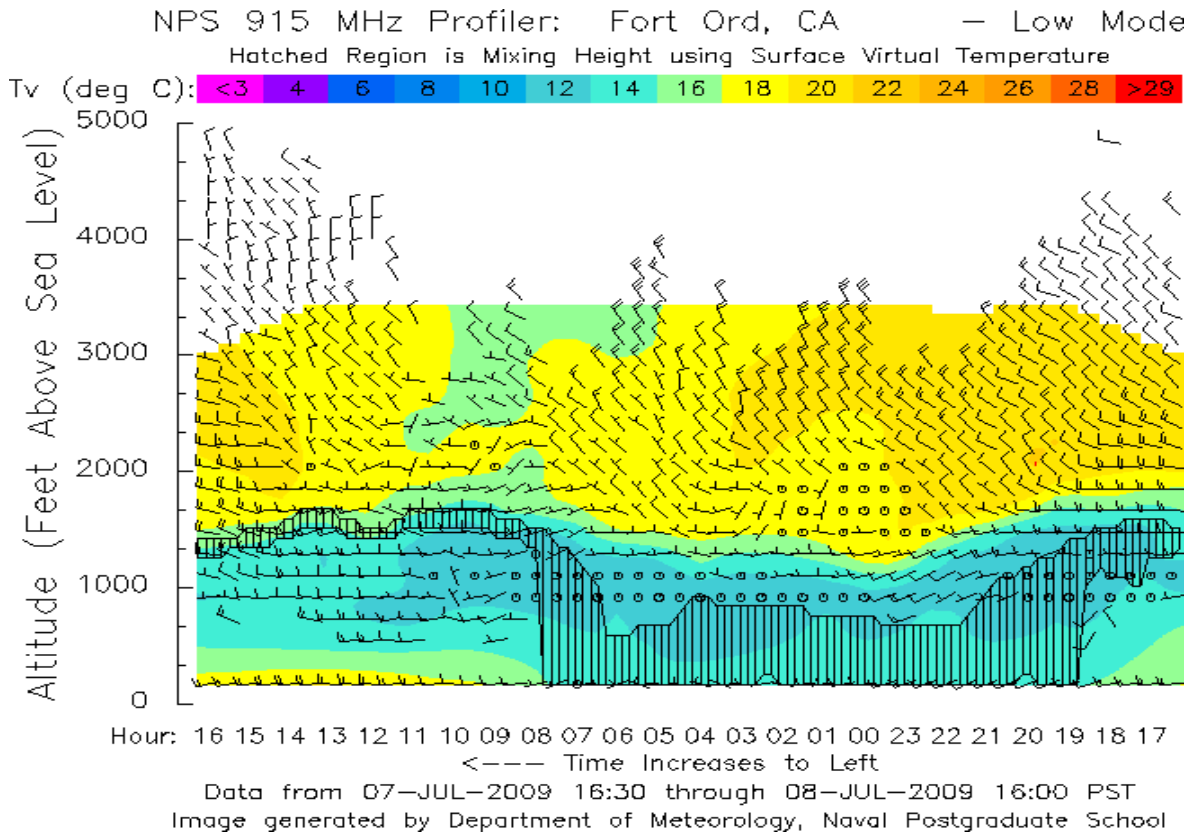


Figure 27. Wind Profiler Site Plot for Mixing Length Heights, from Naval Postgraduate School at <http://met.nps.edu/~lind/nps/archive/ARCHIVE.HTM>.

Table 3 represents the conditional probability table for each condition separately. It seems like most of the days in Monterey Bay are sea breeze days. July 8, 2009 is believed to be a sea breeze day and was picked up as a sea breeze day with all the conditions except Condition 2. Coastal jets, which will be explained in the following pages, cause an increase in wind speed over the ocean that might be the reason for this disagreement. So we can say that Condition 2 is not a good criterion to pick up sea breeze days for Monterey Bay on coastal jets days, or we should have different conditions for coastal jet days to determine sea breeze days.

In most cases for sea breeze, people expect to see the wind shifting at night; however, this does not happen most of the time in Monterey Bay due to dominating synoptic scale winds and coastal jets. So we did not apply this condition to determine sea breeze days. Instead of wind shifting, Condition 5 is used to make sure the wind is blowing onshore in the afternoon when the sea breeze reaches its maximum wind speed.

<u>Condition 1</u>	<u>Observed (manual)</u>	<u>Not observed</u>	<u>Total</u>
Predicted	60	15	75
Not predicted	10	7	17
Total	70	22	92
<u>Condition 2</u>	<u>Observed (manual)</u>	<u>Not observed</u>	<u>Total</u>
Predicted	54	13	67
Not predicted	16	9	25
Total	70	22	92
<u>Condition 3</u>	<u>Observed (manual)</u>	<u>Not observed</u>	<u>Total</u>
Predicted	53	4	57
Not predicted	17	18	35
Total	70	22	92
<u>Condition 4</u>	<u>Observed (manual)</u>	<u>Not observed</u>	<u>Total</u>
Predicted	53	18	71
Not predicted	17	4	21
Total	70	22	92
<u>Condition 5</u>	<u>Observed (manual)</u>	<u>Not observed</u>	<u>Total</u>
Predicted	64	19	83
Not predicted	6	3	9
Total	70	22	92
<u>Condition 6</u>	<u>Observed (manual)</u>	<u>Not observed</u>	<u>Total</u>
Predicted	64	19	83
Not predicted	6	3	9
Total	70	22	92

Table 3. Conditional Probability Matrix of Sea Breeze Conditions.

B. ROTARY SPECTRA

In this study, rotary spectra are used to divide current or wind data into counterclockwise and clockwise components. That subdivision helps us to compare these signals in a rotation sense. The figures that are obtained by using rotary spectra for winds and currents at the M0 buoy location are presented in Figure 28 and Figure 29.

It is clear to see that there are two peaks for wind rotary spectra. One represents the diurnal peak and the other one represents the semidiurnal peak. Diurnal and semidiurnal peaks are similar for both clockwise (cw) and counterclockwise (ccw) rotation components of the wind. The ccw component has nearly the same energy as the cw component at diurnal frequency, but the ccw component has a little more energy than the cw component at semidiurnal frequency.

For current, it is obvious that there are two peaks as well. But the energy of the semidiurnal and diurnal components of the current is close, as shown in Figure 29. We cannot see that much difference between them in Figure 29. At diurnal frequency the cw rotation component has much more energy than the ccw component; however, at semidiurnal frequency they have the same energy.

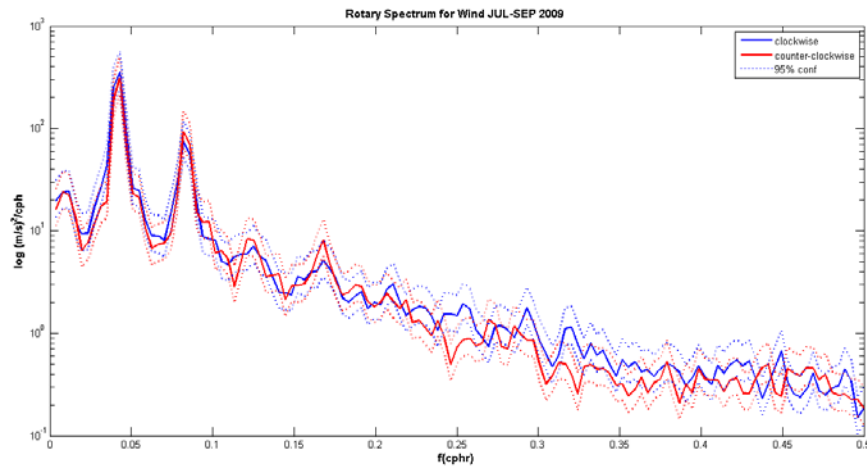


Figure 28. Rotary Spectra for the Wind (July–September 2009) at M0 Buoy Location.

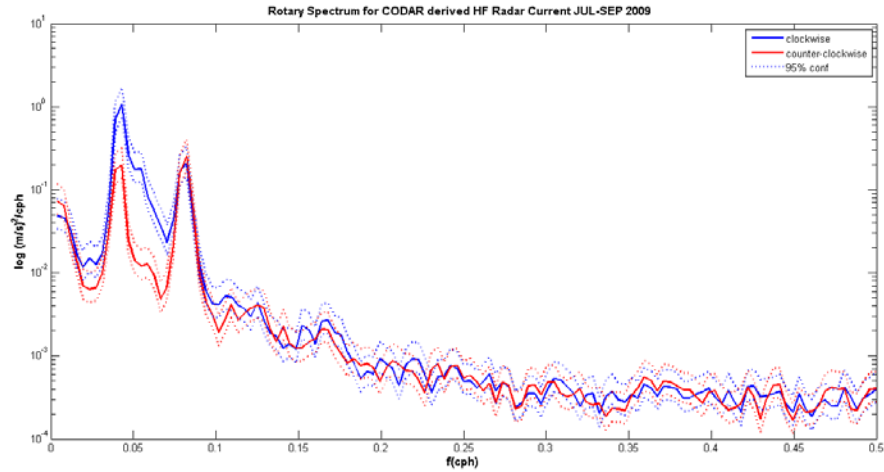


Figure 29. Rotary Spectra for the HF-radar derived Current (July–September 2009) at M0 Buoy Location.

C. ROTARY COEFFICIENT

Rotary coefficient is applied to see if the current is much more rotational than the winds or not (Gonella 1972). If the rotary coefficient is “1” that means this signal is a rotating signal. If it is “0” that means it is a non-rotational signal. Figure 30 and Figure 31 show that the current is rotating much more than winds at under ten hours, and after ten hours its rotary coefficient varies between -0.25 and 0.25, which are close to “0.”

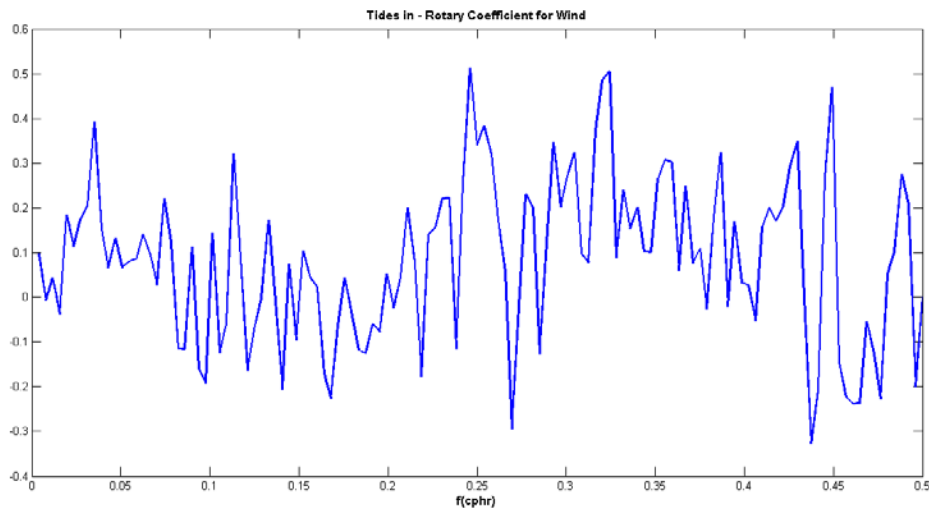


Figure 30. Rotary Coefficient for Wind in M0 Buoy Location (July–September 2009).

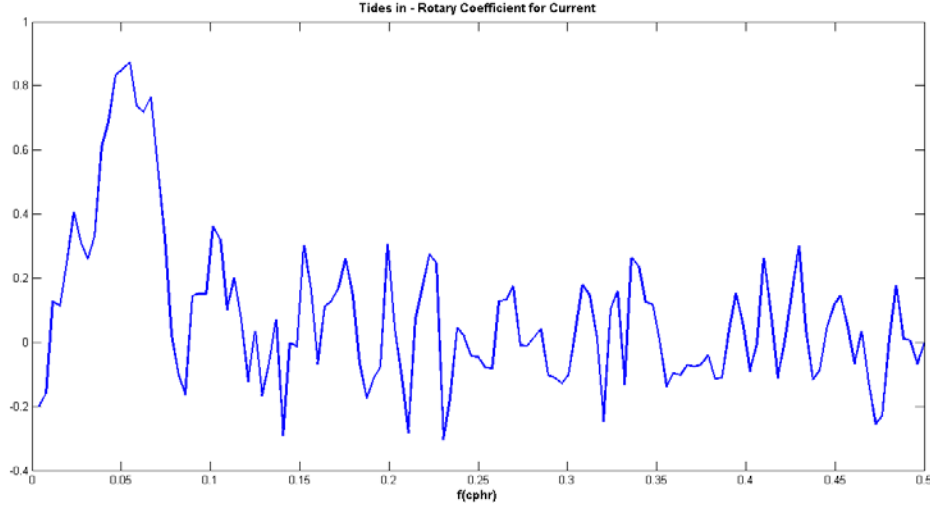


Figure 31. Rotary Coefficient for Current in M0 Buoy Location (July–September 2009).

D. POWER SPECTRA ANALYSIS

The power spectra describe how the energy of time series is distributed with frequency (http://en.wikipedia.org/wiki/Spectral_density). There are two peaks, as shown in Figure 32, which are diurnal and semidiurnal for both current and winds. Currents nearly have the same energy for both the diurnal and semidiurnal cycles. However, currents have less energy than winds. Also winds have greater peaks for the diurnal cycle as compared to sea breeze effect since sea breeze is diurnal and dominates. But we cannot see that much difference for currents. For currents diurnal and semidiurnal peaks are almost the same due to strong tidal influence over the currents at semidiurnal time.

Hendrickson and MacMahan (2009) pointed out that 50% of the total energy is the diurnal variability in Monterey Bay, which is consistent with our results. For semidiurnal peaks in wind power spectra analysis Militello and Kraus (2001) have a clear explanation. At first we could not define it, but by using the results of Militello and Kraus (2001) we have explained it well enough. According to Militello and Kraus (2001) the reason for diurnal oscillation is sea breeze, as we defined it previously; however, the reason for semidiurnal variability is the combination of nonlinear interactions, time-shifting sea breeze and a quasi-steady wind.

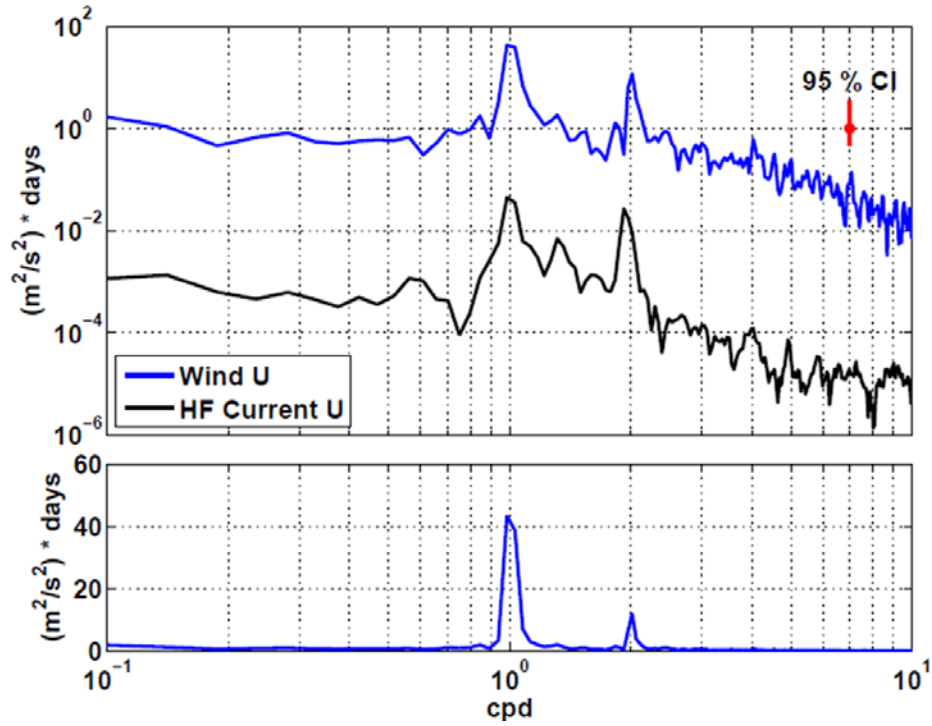


Figure 32. Power Spectra for Wind and Current at M0 Buoy Location (July–September 2009).

E. COMPLEX CORRELATION

Complex correlation is used to understand the relationship between wind and current. In complex correlation, the phase angle helps us to see the angle between two time series and magnitude, which shifts between 0 and 1. It shows how well wind and current are correlated (Kundu 1975, Delgado 2009). Table 4 shows the results for M0, M1 and M2 buoy locations in July, August and September 2009. It is clear to see that the correlation value of the July M0 buoy location is the highest one, with a value of 0.60. The reason is probably because of strong winds in Monterey Bay at that time. In August there is also strong correlation between wind and current. Then the angles for M0 buoy are less than Ekman's 45 degree.

	M0			M1			M2		
	JUL	AUG	SEP	JUL	AUG	SEP	JUL	AUG	SEP
Theta Angle	-31.82	-28.92	-23.92	-57.03	-56.22	-42.34	-60.56	-63.19	-53.21
Correlation between Wind & Current	0.605	0.532	0.447	0.56	0.58	0.55	0.38	0.34	0.47

Table 4. Table of Complex Correlation for M0, M1 and M2 Buoy Locations between July and September in 2009.

Due to its having the highest correlation value and being the closest location to the coast, we focus on the M0 buoy to come up with results about the relationship between sea breeze and surface currents. For the angles “-” means the current is rotated clockwise, which is what we expect in the Northern Hemisphere (Delgado 2009). The reason for the small angles between wind and current at the M0 buoy location is probably that the steady state has not yet been reached (Durst 1924).

F. HARMONIC ANALYSIS

Before getting started analyzing the data, we would like to give a definition of harmonic analysis from *Data Analysis Methods in Physical Oceanography* (Emery and Thomson 2004). Harmonic analysis uses the least squares method to solve the constituents, and the user chooses the frequencies to be worked on. In the least squares method, we are minimizing the squared difference between the original data and the fit to that time series (K1, M2) to estimate the amplitudes and phases of the various components. The goal of the least squares analysis is to minimize the variance of the residual time series. As stated by Emery and Thomson (2004), “Harmonic analysis was designed for the analysis of tidal change but applies equally to analysis at the annual and semi-annual periods or any other well-defined cyclic oscillation. The hierarchy of harmonic tidal constituents is dominated by diurnal and semidiurnal motions, followed by fortnightly, monthly, semiannual and yearly variability.”

The reason for using harmonic analysis in this thesis is to obtain the amplitude of the sea breeze signal over time for both wind and current. Also, the method's tolerance of missing data gaps of up to 50% argues for the use of this method, particularly in the case of the gapping HF radar data. This is how we applied it: K1 component is chosen as the fit to match with the real data. K1's time period is 23.98 hours, which is a daily cycle like the sea breeze cycle. For window size, 72 hours is used.

Harmonic analysis of July 2009 wind and CODAR-Type HF Radar-derived current data show that there is a strong correlation between wind and current at the M0 buoy location. To see the sea breeze effect clearly, we focused on the closest buoy to the coast location, which is the M0 buoy. When we examine the ADCP data as shown in Figure 33, we come up with the result that there is no significant relationship between amplitude of the diurnal surface currents and those at 6 meter depth. When we calculate the cross correlation between ADCP 6 meter depth current and HF radar-derived surface currents we get -0.0319 for the correlation coefficient, which is almost "0" and means that surface and deep currents are not correlated. Vesecky et al. (1997) point out that at deeper depth, tide or upwelling currents dominate rather than surface currents.

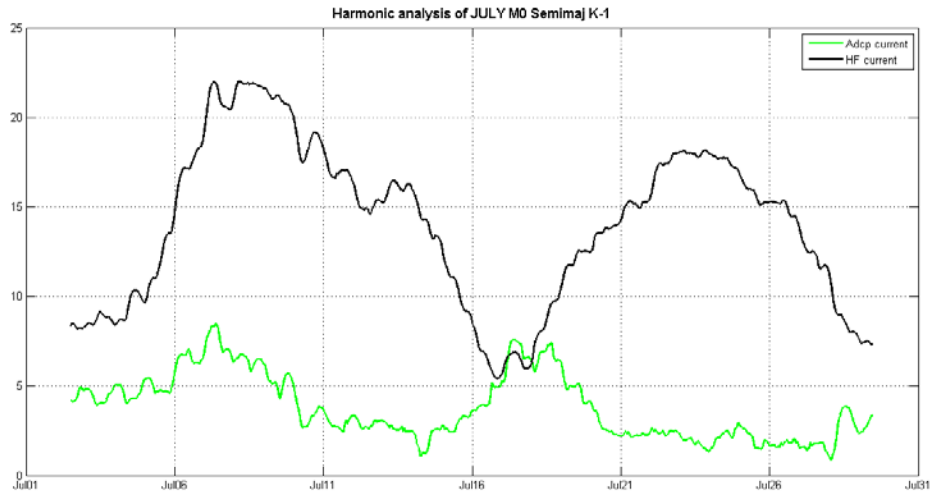


Figure 33. Harmonic Analysis of ADCP 6m depth Current and HF Radar-derived Surface Current.

1. Analysis of July 2009

Wind and surface current are following the same pattern as seen in Figure 34 in the month of July. When we look carefully, highs and lows in Figure 34 also point out that surface currents and winds are strongly correlated. To see quantitatively the correlation between surface winds and currents, we used the cross correlation method again. We got 0.896 for the correlation coefficient, which means surface winds and currents are highly correlated.

To see the sea breeze effect we applied the wind speed difference between morning (6 a.m.) and afternoon (2 p.m.) of each day to get meaningful results. However, this was not enough information to determine sea breeze days. Also, we still could not explain why there are peaks for July 7, 8, 9 and 10, 2009, and lows for July 15, 16, 17 and 18, 2009. To understand the dominating forcing for these specific days, as will be mentioned in the following pages, we examined the satellite images, available data, amplitude of currents, vertical cross section of potential temperature, sea level pressure and vertical cross section of isotachs for these days. At first, we believed the reason for these peaks is the strong sea breeze, and for lows, vice versa. But when we go into more detail, we noticed that the reason for these highs and lows is coastal jet.

If the percentage coverage for the grid point was less than 70%, the data for that grid point were not used in this study. The available data for these all days were checked for current and wind data.

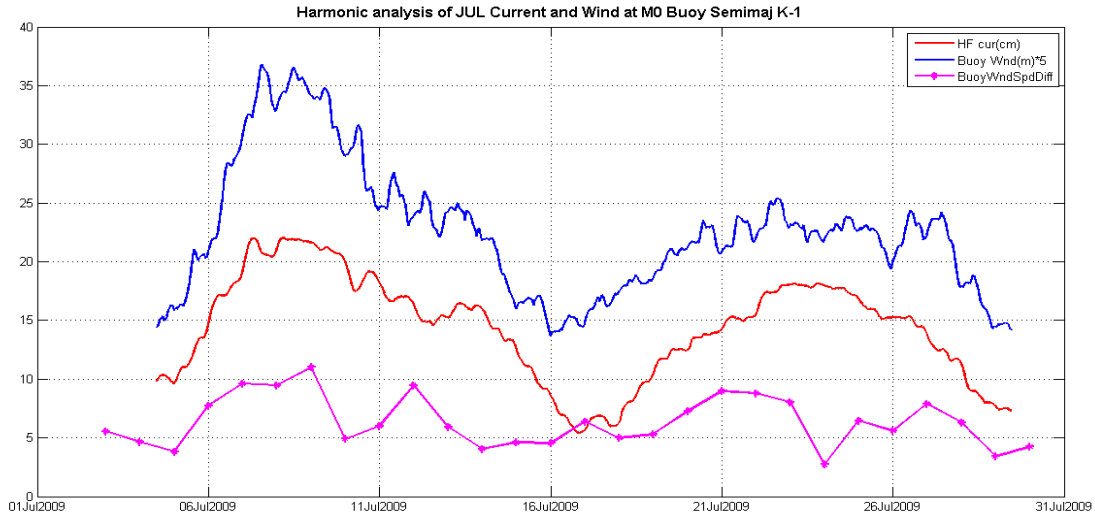


Figure 34. Harmonic Analysis of Buoy Wind and HF Radar-derived Surface Current at M0 Buoy Location (July 2009).

a. Analysis of Coastal Jets Influence

In fact the sea breeze event is not that strong by itself, but if the coastal jet is formed then the sea breeze effect will be stronger at the coast. To see the coastal jet effect we focus on two specific days. One of them is picked up from the days when there is a peak in the amplitude of the sea breeze; the other day is picked up from the days when we have a low value of that amplitude in Figure 35. July 8 and 16 of 2009 are chosen to work with to explain the difference between these days and dominating forces for these days.

First of all we get started analyzing the day of July 8, 2009. In Figure 35 the sea level pressure and horizontal isotachs over California coast are shown for that day. It is obvious that the pressure gradient reaches its maximum value at the coast and decreases both landward and seaward. Figure 36 shows the vertical cross section of isotachs, where wind speed is reaching its highest value near the coast. As seen in Figure 36 the size of the jet is about 20–60 km wide. It is clear to see that coastal jet is reaching its maximum speed near the bottom of the MBL inversion. However, over the land the jet speed is decreasing due to friction on land. Also, mountains along the California coast force the jet to blow along the California coast, as mentioned in Chapter II. Figure 37 presents the vertical cross section of potential temperature. It is clear to see that the MBL is cool and

stable in Figure 37. With the downward sloping boundary layer, the inversion layer is ‘squeezing’ the coastal air vertically; then that makes the winds blow faster horizontally. As the MBL is covered by the inversion layer, the inversion slopes downward to the east swallowing the MBL with decreasing distance to the shore. We have warmer air over the land, cooler air over ocean. Also we should say that the front is significant; it can be easily seen over the mountain.

All the information related to pressure gradient, potential temperature and MBL points out that the coastal jet is dominating the region on this day. We examined the other days when there are peaks in harmonic analysis Figure 34. In all those days strong synoptic winds or coastal jets were formed, and it is the main factor that dominates the California coastline.

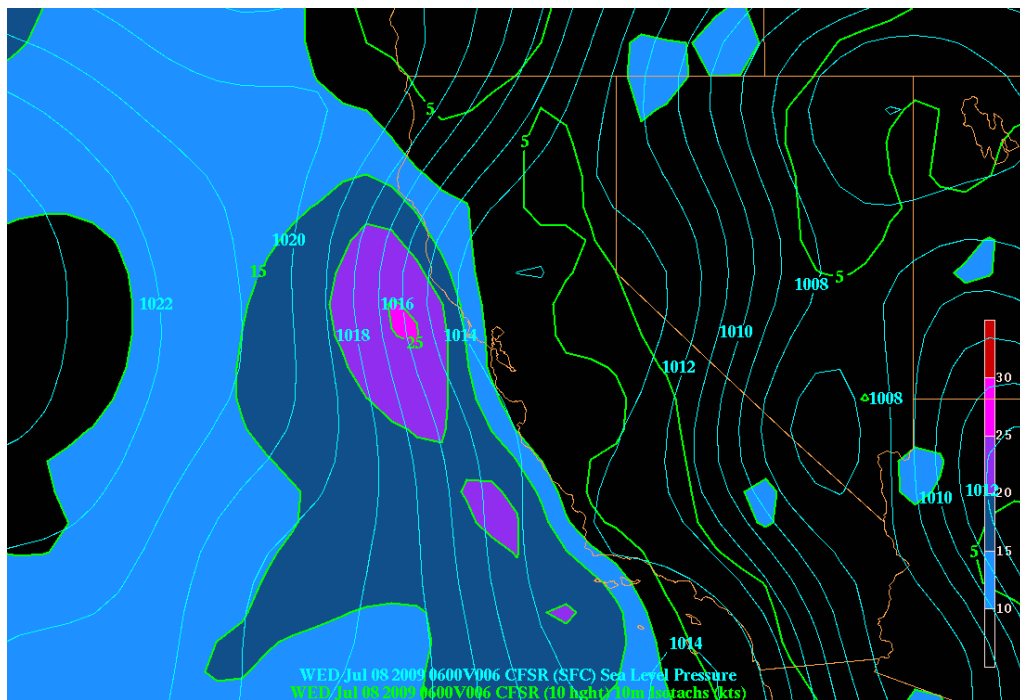


Figure 35. July 8, 2009 Sea Level Pressure and Horizontal Isotachs (obtained using GARP CFSR Model).

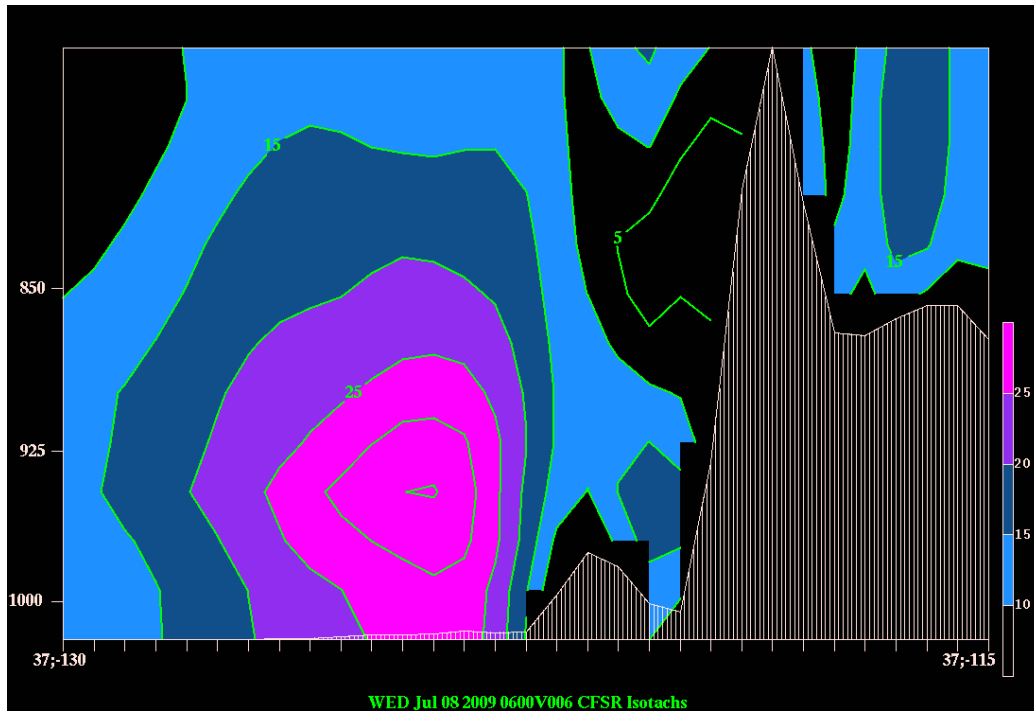


Figure 36. July 8, 2009 Vertical Cross Section of Isotachs (obtained using GARP CFSR Model).

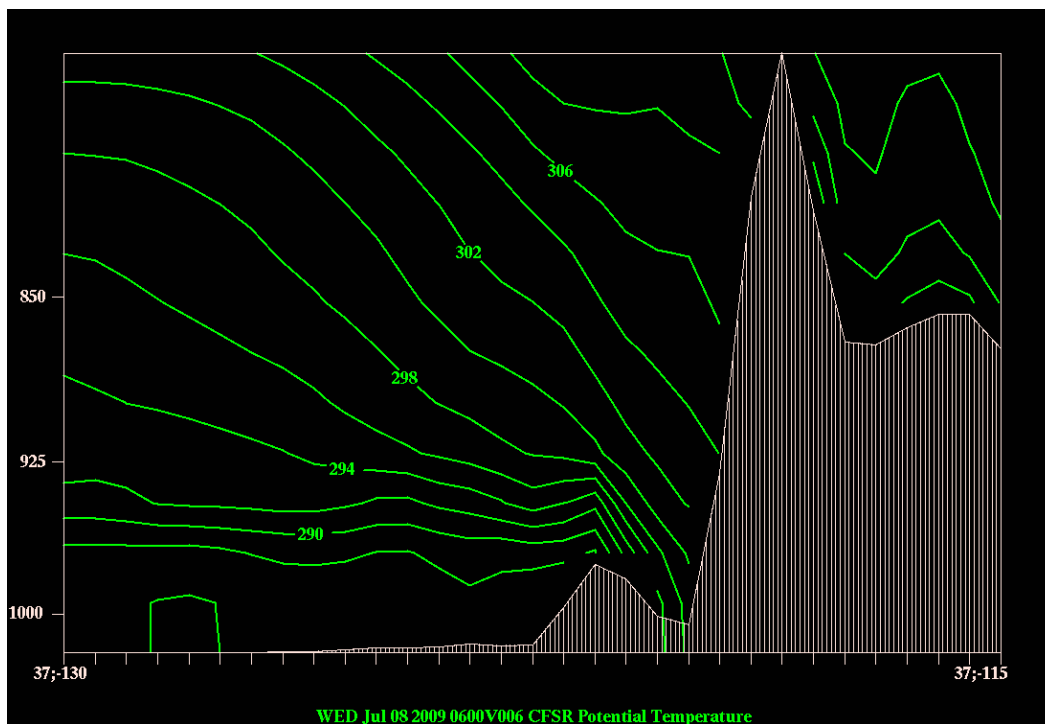


Figure 37. July 8, 2009 Vertical Cross Section of Potential Temperature (obtained using GARP CFSR Model).

Secondly we analyzed the day of July 16, 2009. In Figure 38 the sea level pressure and horizontal isotachs are shown for that day. It is obvious that pressure gradients are not as tight as they were on July 8, and it is not changing as much as it had on July 8. Figure 39 shows the vertical cross section of isotachs, where again wind speed is very weak with respect to July 8. Moreover, the front is not significant here. Figure 40 presents the vertical cross section of potential temperature. It is clear to see that the MBL is warm and unstable in Figure 40.

We have cool and stable air on July 8, 2009 and synoptic winds dominate the region. On July 16, 2009 there is warm and unstable air. Synoptic scale winds are not as consistent and strong as they were on July 8. It is known that sea breeze is much stronger in warm and unstable weather conditions since it does not block vertical movement of the winds. So examining the day of July 16 will give us a better understanding of sea breeze and its influence alone.

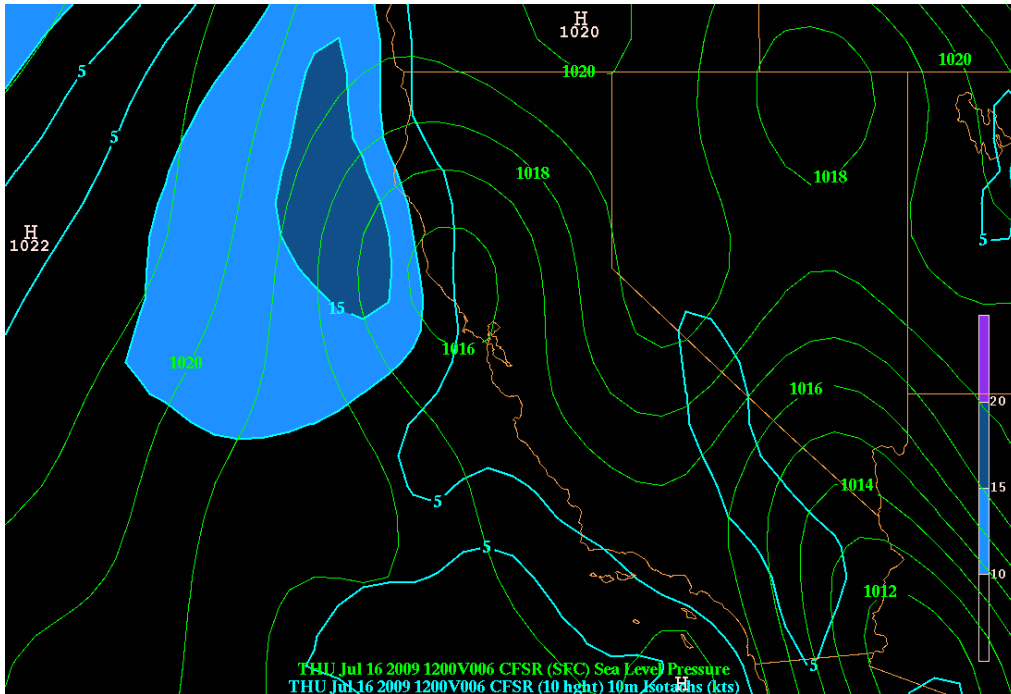


Figure 38. July 16, 2009 Sea Level Pressure and Horizontal Isotachs (obtained using GARP CFSR Model).

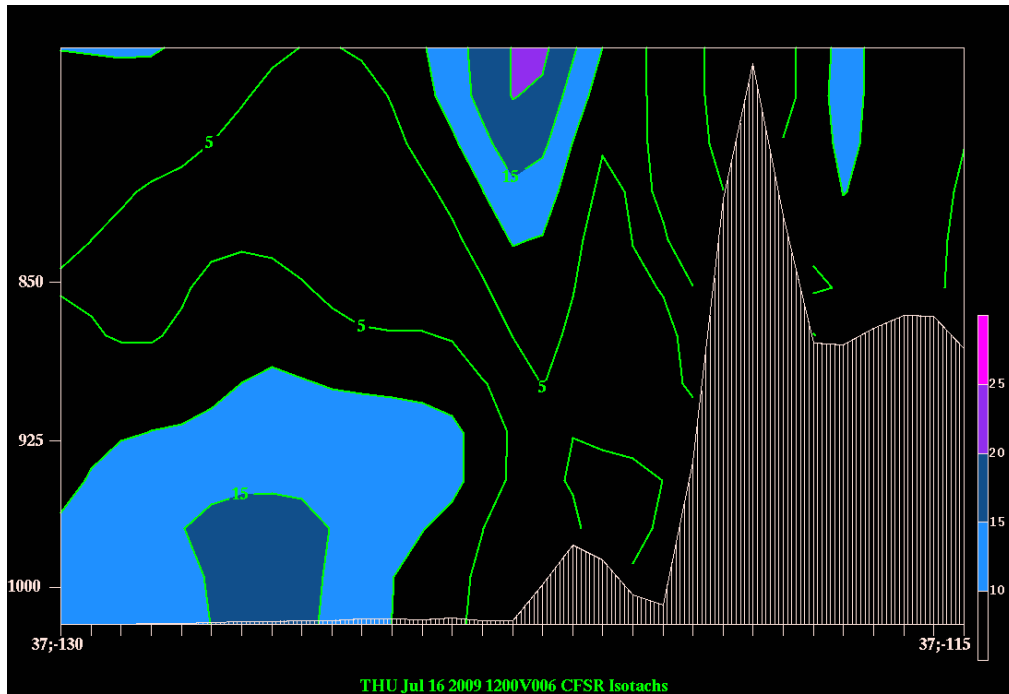


Figure 39. July 16, 2009 Vertical Cross Section of Isotachs (obtained using GARP CFSR Model).

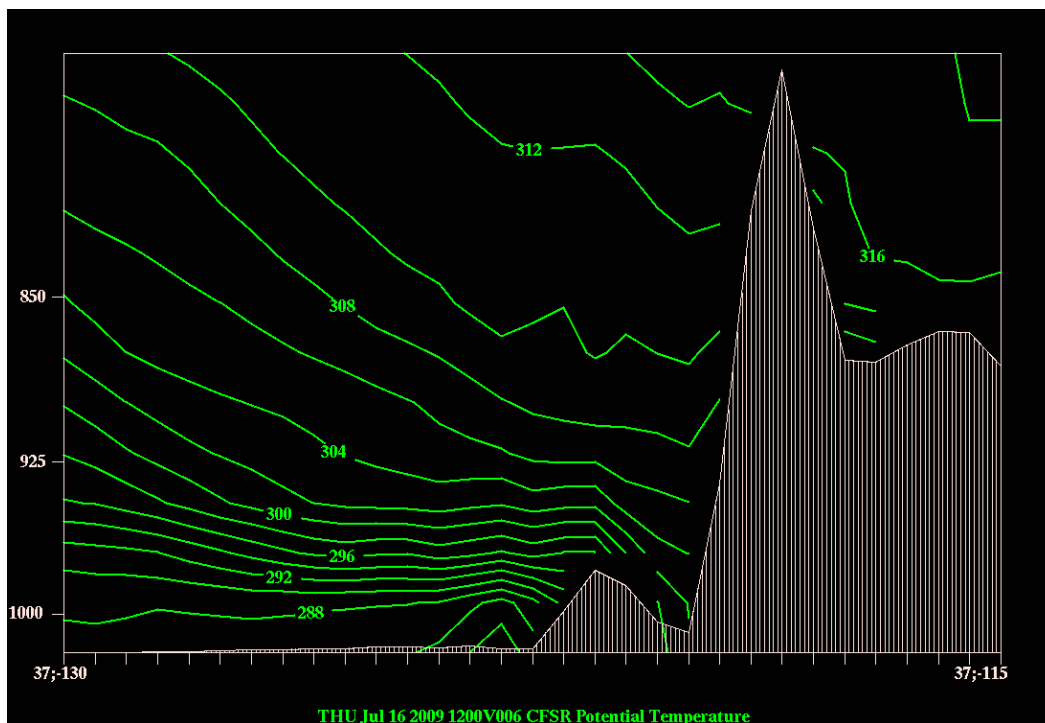


Figure 40. July 16, 2009 Vertical Cross Section of Potential Temperature (obtained using GARP CFSR Model).

After understanding the reasons for peaks and lows in the winds, we tried a different perspective to understand the behavior of the currents on July 8 and 16 of 2009 with respect to sea breeze. Afternoon is the time when the sea breeze effect is maximal, as is known. So we chose the time of 7 p.m. to make sure we could see the sea breeze effect over current, knowing that current response to the wind does not happen suddenly. Hendrickson and MacMahan (2009) point out that “[s]ea breeze affects the diurnal wave height and increases local waves a few hours after the winds get their highest values.” That is why we do not focus on 2 p.m. to see breeze effects over currents. Also, in July, the average time for sunset is around 8 p.m., for August 7:40 p.m. and for September 6:40 p.m. Days are longer than in winter time.

As it is seen in Figure 41 the average movement of currents on July 8, 2009 is parallel to the coast due to strong coastal jet effect. There is sea breeze on this day, and in Figure 42, the influence of the sea breeze can be seen to cause the surface currents to change direction toward the shore. The sea breeze alters the direction of surface currents to the coast.

Current movement varies a lot in Figure 43, which represents the average of currents on the day of July 16, 2009. There is no strong synoptic scale influence over the region. Surface currents at 7 p.m. along the coast, as shown in Figure 44, move on shore clearly due to sea breeze effect. However, the amplitudes of surface currents on July 8 are greater than the amplitudes of July 16. I should also point out, as we see in these figures, HF radar provides us unbelievable plots to map the surface currents for a large area and does a great job to illustrate the movement and behavior of the currents.

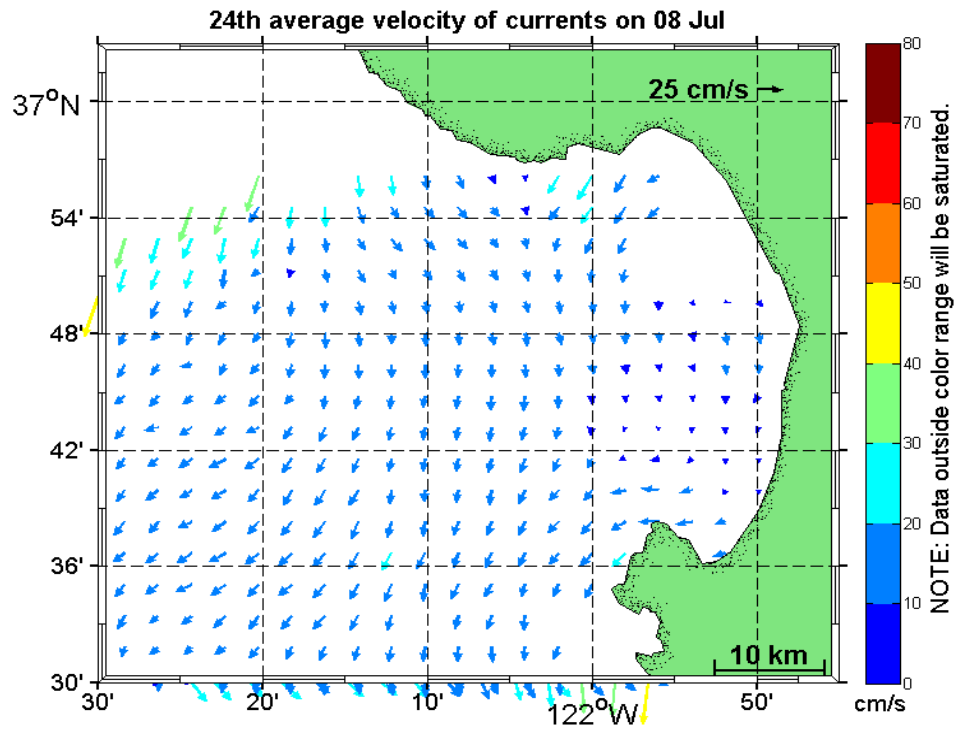


Figure 41. Average Velocity Map of Surface Current on July 8, 2009.

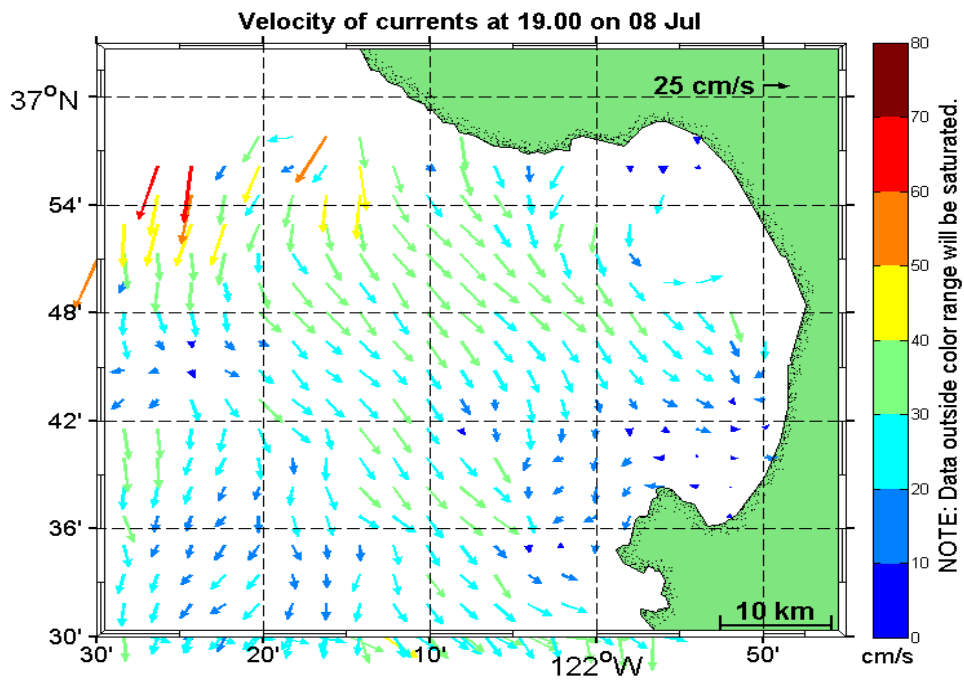


Figure 42. Surface Current Map at 7 p.m. on July 8, 2009.

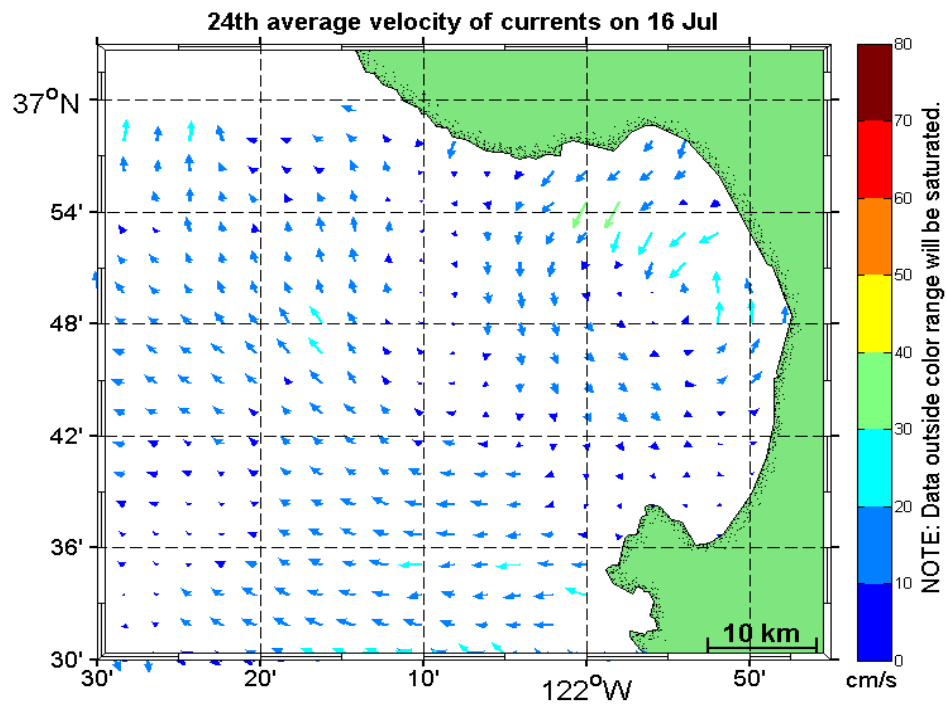


Figure 43. Average Velocity Map of Surface Currents on July 16, 2009.

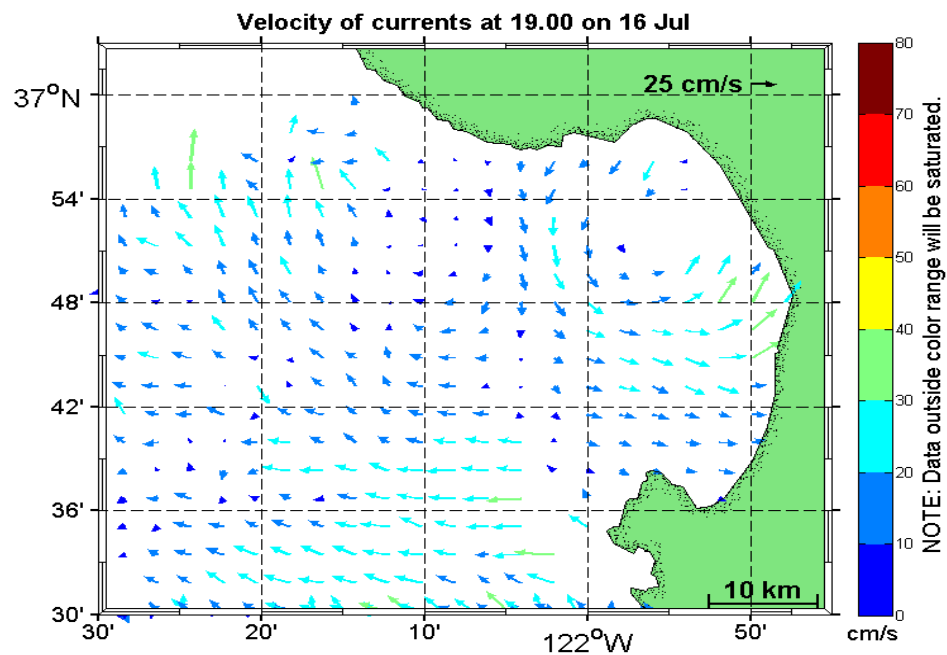


Figure 44. Surface Current Map at 7 p.m. on July 16, 2009.

b. Comparison of Days with/without Coastal Jet

To compare the days with and without coastal jet we created Table 5. Table 5 helps our understanding of the differences between those days better.

08-09-10 July: These days have a deep inversion layer, cool surface temperature, deeper MBL and cloud-free atmosphere. These results are the indications of weak sea breeze but deep MBL with coastal jet or synoptic winds that can create a strong influence if they move together and support each other. However, it is known that the inversion layer blocks heating, mixing and looping and weakens sea breeze. That does not mean we are not going to have sea breeze. We will still have sea breeze on those days, but it will be weak on such days. As seen in Figure 42, the coastal jet is obviously increasing the amplitude of currents, and the sea breeze is forcing the coastal jet winds to change their direction to the shore.

16-17-18 July: These days are cloudy with a shallow inversion layer, no significant inversion layer and warm surface temperature, and shallow MBL. All these results show that we have a day with sea breeze. There are weak synoptic winds on these days as well. Clouds are over the ocean and blocking radiation of sunlight to the ocean. There is a relationship between cloud and sea breeze, but these factors do not have to be correlated since we can see very strong sea breeze on cloudy days, as Duvall (2004) illustrated in an example situation in her thesis. Also clouds are only over the ocean on these days, not over the land. An unstable layer helps the sea breeze structure to create a cycle in the atmosphere (Ahrens 1991). On July 16 we come up with the result that sea breeze does not affect the amplitude of currents much, but it does change the direction of the surface current significantly as is seen on no coastal jet days.

In Figure 45 we see how the temperature changes in July 2009. Figure 46 helps us to see how far inland Los Banos is located. When we examine how the temperature is changing in July 2009, we notice that the temperature and temperature difference in the day time is increasing as we move away from the coast. Actually that is what we expect to see. The temperature difference of Los Banos and M2 buoy locations and coastal jets days show that they are inversely proportional since the inversion layer occurs on coastal

jet days and blocks heating. On July 8, 9 and 10 we can see the temperature is decreasing due to having an inversion layer, which is the indication of coastal jet along the California coast. However, on the days when we cannot see the coastal jet, the temperature difference is increasing in the region between Los Banos and Monterey Bay due to having no significant inversion layer. Thus, neither heating nor looping is blocked.

	08-09-10 JULY	16-17-18 JULY
CLOUD	08—No cloud 09—Partly cloudy 10—Partly cloudy	08—Cloudy 09—Cloudy 10—Partly cloudy
MBL	08—1800 feet 09—1300 feet 10—1300 feet	16—950 feet 17—900 feet 18—850 feet
STABILITY	08—Cool & stable 09—Cool & stable 10—Cool & stable	16—Warm & unstable 17—Warm & unstable 18—Warm & unstable
INVERSION LAYER	08—Significant inversion layer 09—Significant inversion layer 10—Significant inversion layer	16—No inversion layer significantly 17—No inversion layer significantly 18—No inversion layer significantly
WINDS AT 700hPa	08- ~10m/s at 18.00GMT (from SW) 09- ~7m/s at 18.00GMT (from SW) 10- ~10m/s at 18.00GMT (from SW)	08- ~5m/s at 18.00GMT (from SW) 09- ~5m/s at 18.00GMT (from SW) 10- ~5m/s at 18.00GMT (from SW)

Table 5. Comparison of Days with/without Coastal Jet with Respect to Select Parameters.

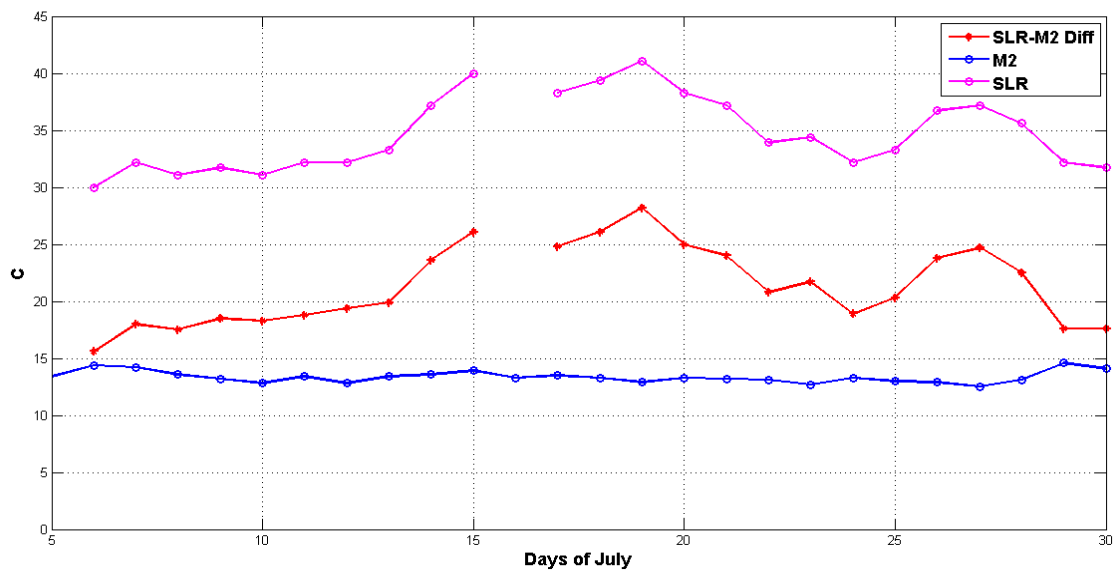


Figure 45. Air Temperature at 2 p.m. at the Los Banos and M2 Buoy Locations and the Temperature Differences between these two Locations in July 2009.

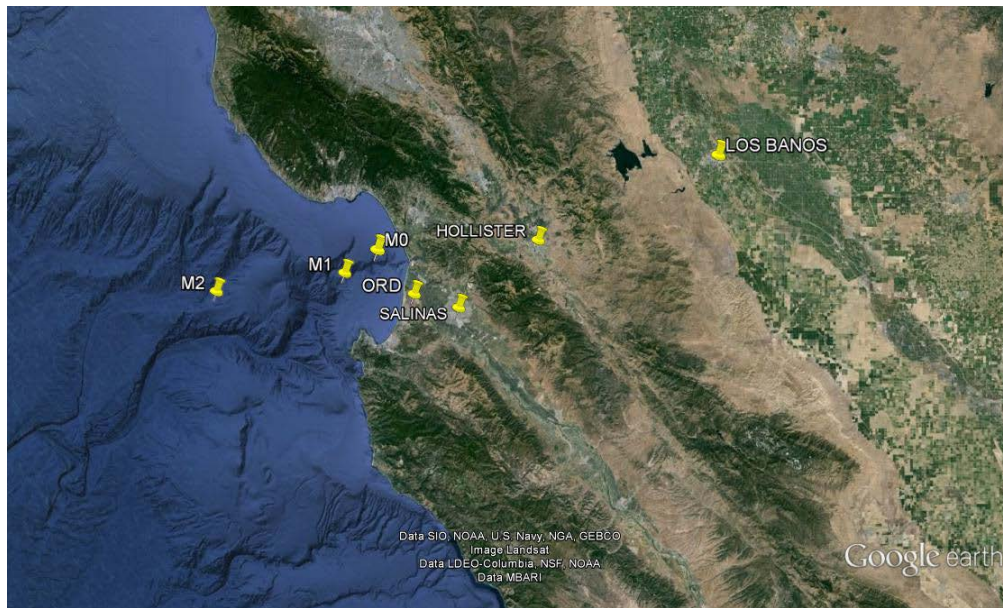


Figure 46. Positions of Los Banos and M2 Buoy (from Google Earth).

2. Analysis of August 2009

The harmonic analysis graph of August shown in Figure 47 illustrates that the amplitude of the winds in August is smaller than the amplitude in July. In particular, we can see a sharp decrease in amplitude on August 10 and a sharp increase on August 13.

August 8, 9 and 10 are obvious sea breeze days, and the wind shift can be seen clearly on August 8 and 9. In our harmonic analysis, as mentioned before, 72-hour averaging is used. August 13 is the day when the strong synoptic winds are seen, and the wind shift in the afternoon cannot be seen. The wind profiler images of August 10 and 13 are shown in Figures 48 and 49, which prove that there is sea breeze on those days since wind speed increase can easily be seen in the afternoon.

In Figure 50, the isotach map shows that there is weak synoptic wind effect along the California coast on August 10; however, Figure 51 illustrates strong winds along the California coast on August 13. The 24-hour average map of surface current on August 10 in Figure 52 shows that there is no synoptic scale effect over the currents. The surface current map of 5 p.m. on August 10 in Figure 53 illustrates that surface currents are moving on shore at that time due to sea breeze influence. The 24-hour average map of surface current on August 13 in Figure 54 shows that there is clear synoptic scale effect over the currents. The surface current map of 5 p.m. on August 13, shown in Figure 55, illustrates that surface currents are moving on shore at that time due to sea breeze influence, but not as clearly as on August 10, due to synoptic effects.

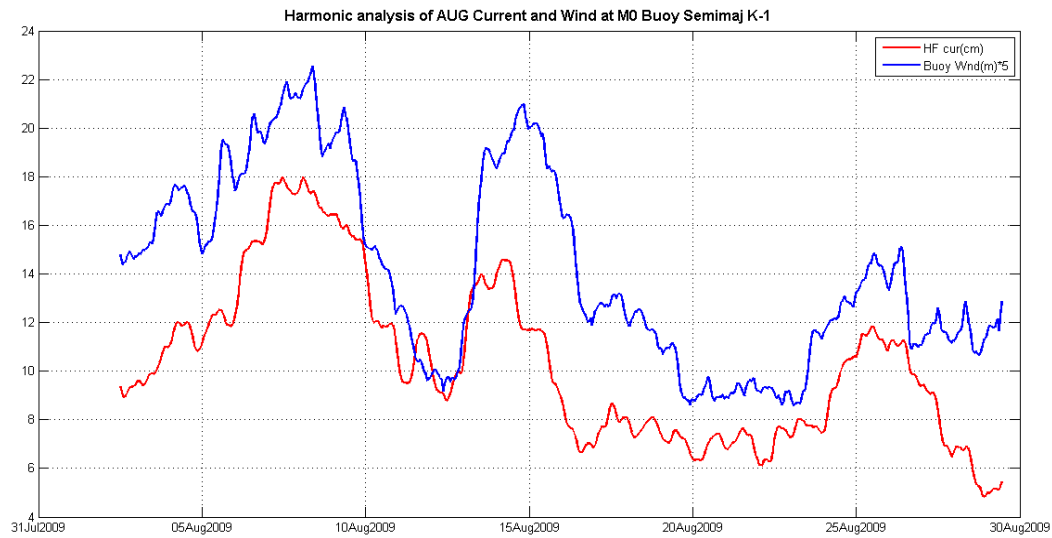


Figure 47. Harmonic Analysis of Buoy Wind and HF Radar-derived Surface Current at M0 Buoy Location (August 2009).

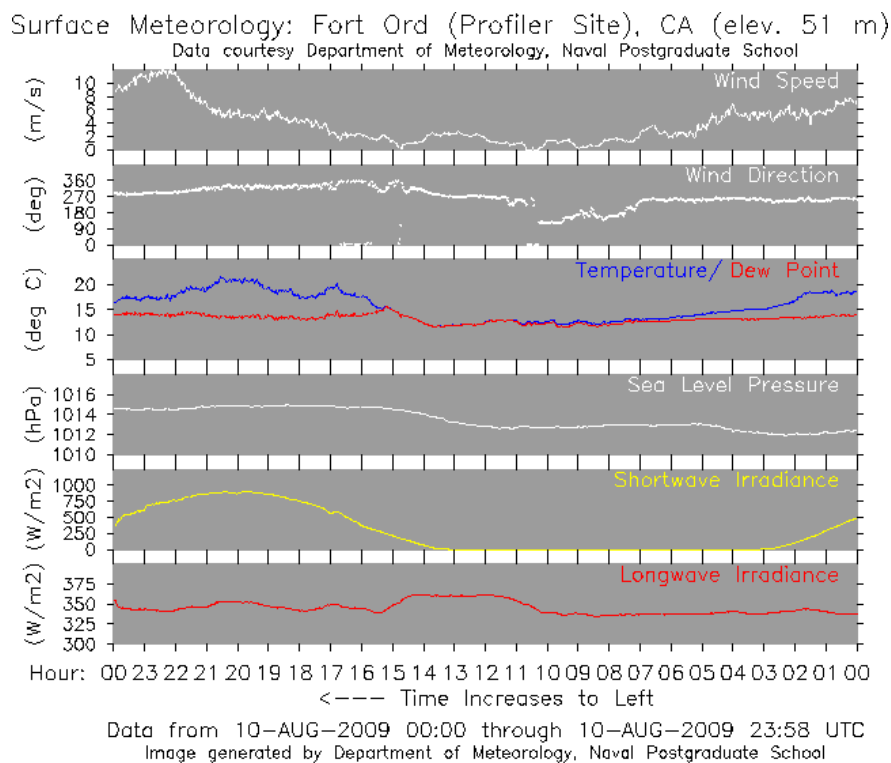


Figure 48. Wind Profiler Site Plot for Surface Meteorology Data (from <http://met.nps.edu/~lind/nps/archive/ARCHIVE.HTM>).

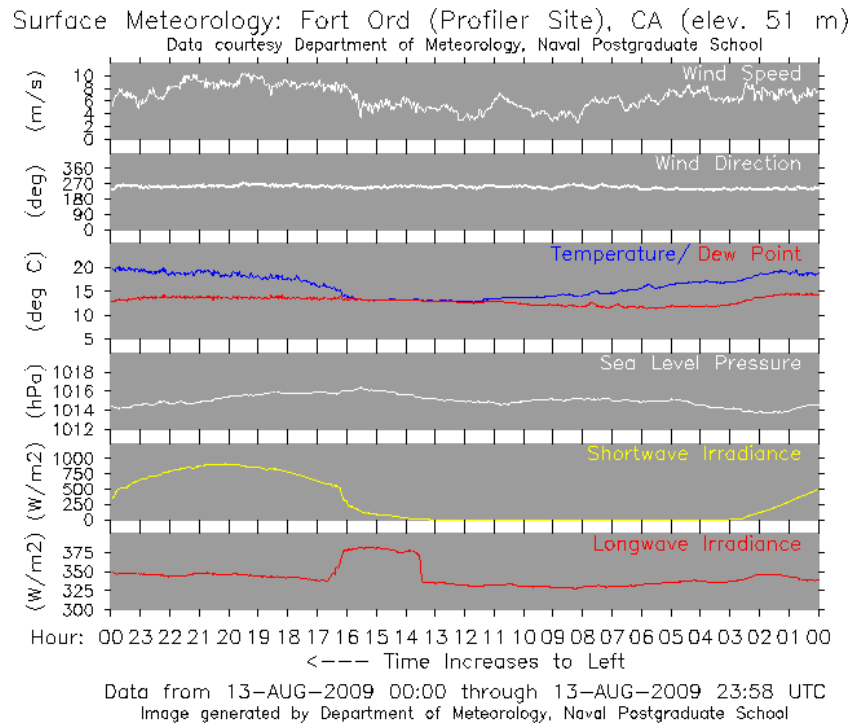


Figure 49. Wind Profiler Site Plot for Surface Meteorology Data (from <http://met.nps.edu/~lind/nps/archive/ARCHIVE.HTM>).

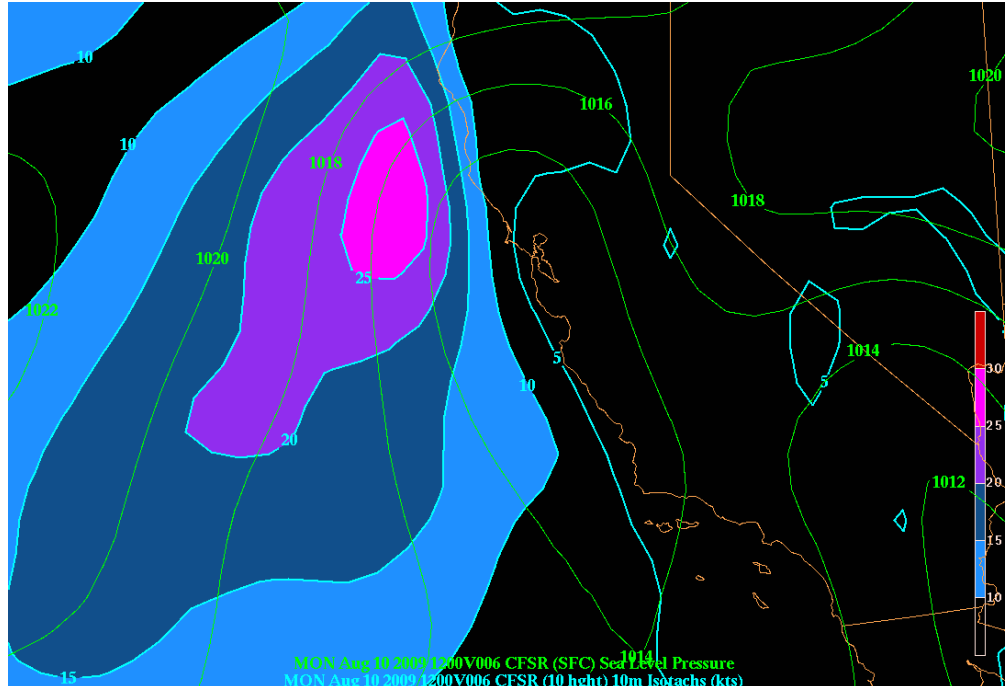


Figure 50. August 10, 2009 Sea Level Pressure and Horizontal Isotachs (obtained using GARP CFSR Model).

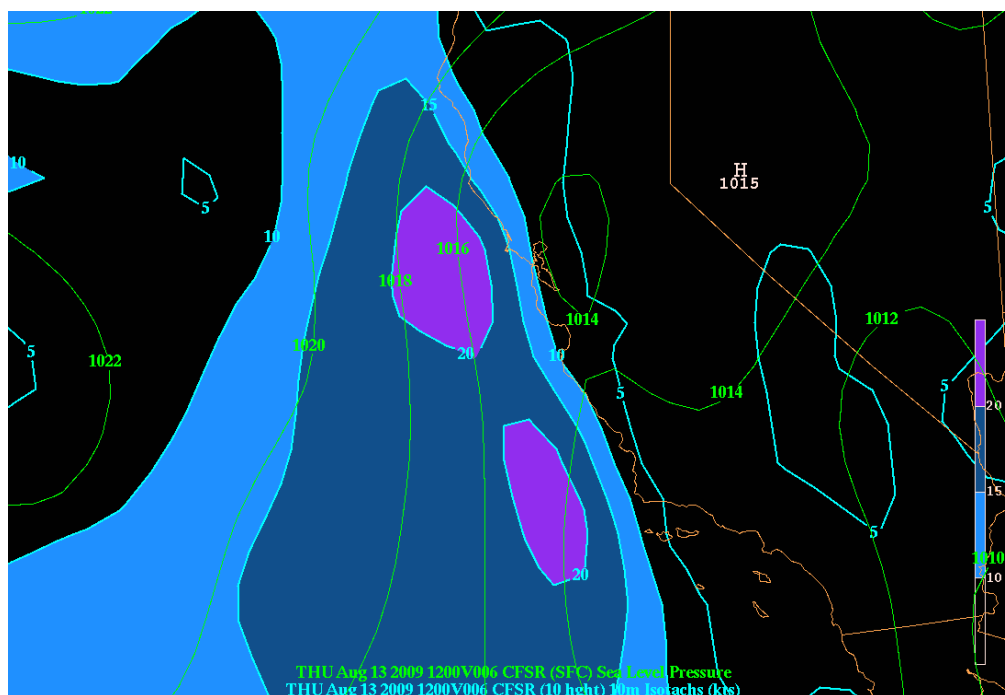


Figure 51. August 13, 2009 Sea Level Pressure and Horizontal Isotachs (obtained using GARP CFSR Model).

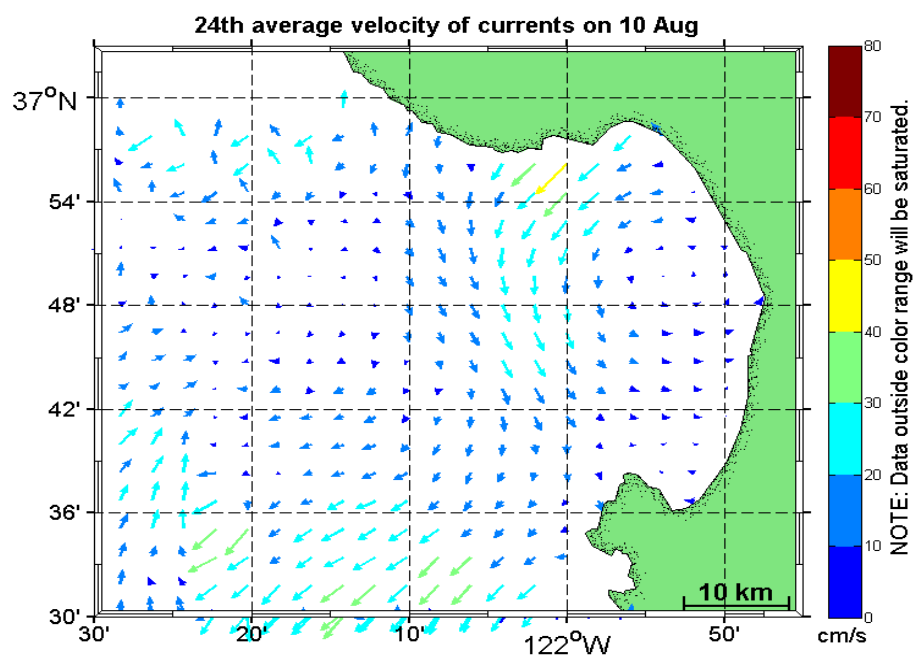


Figure 52. Average Velocity Map of Surface Current on August 10, 2009.

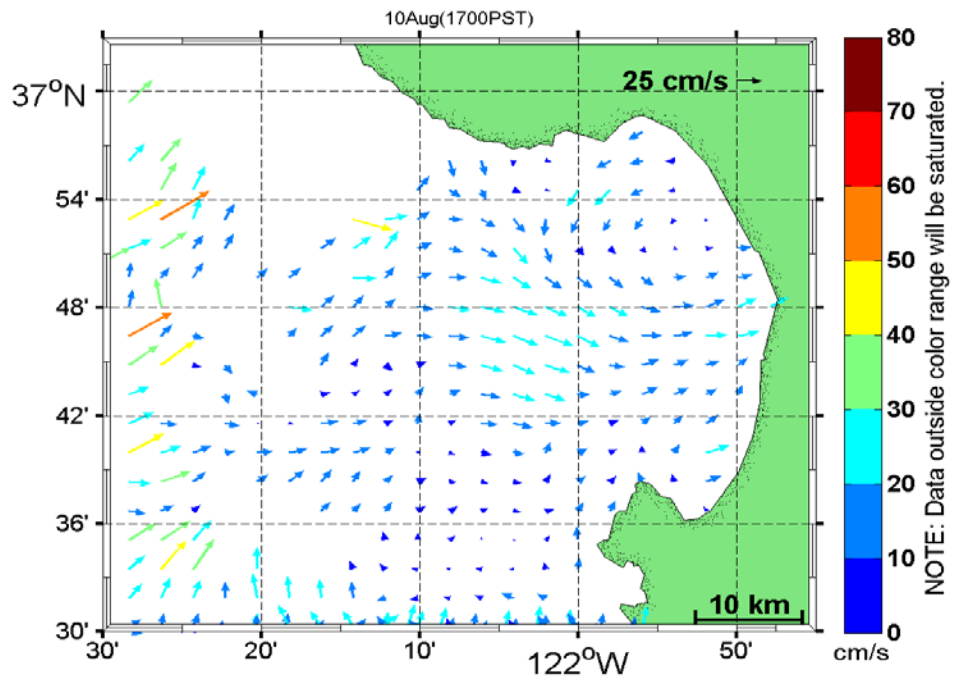


Figure 53. Surface Current Map at 5 p.m. on August 10, 2009.

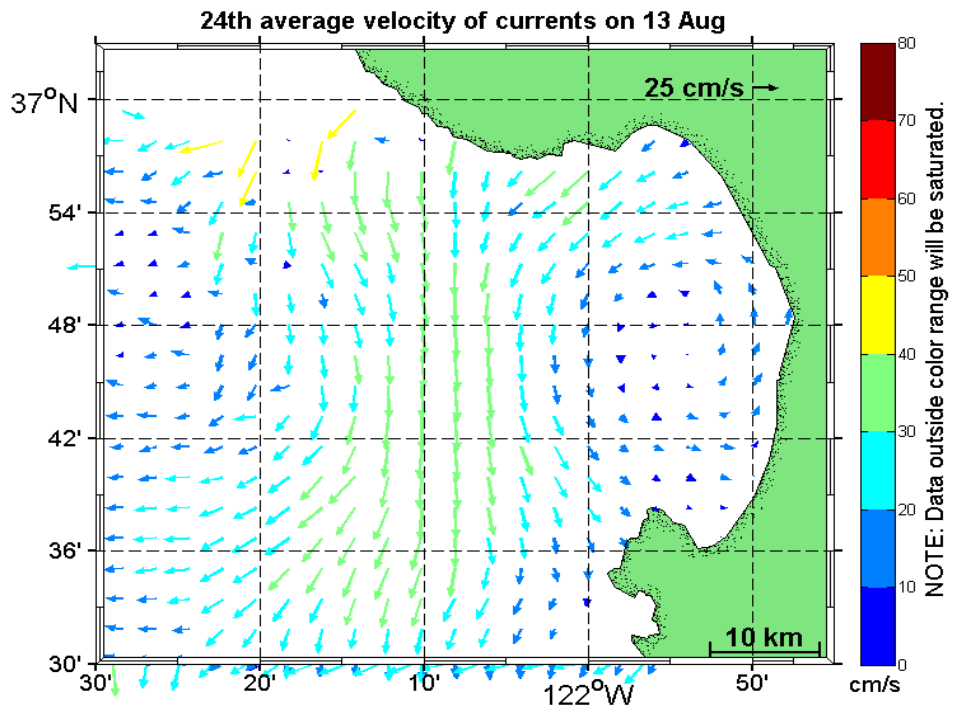


Figure 54. Average Velocity Map of Surface Current on August 13, 2009.

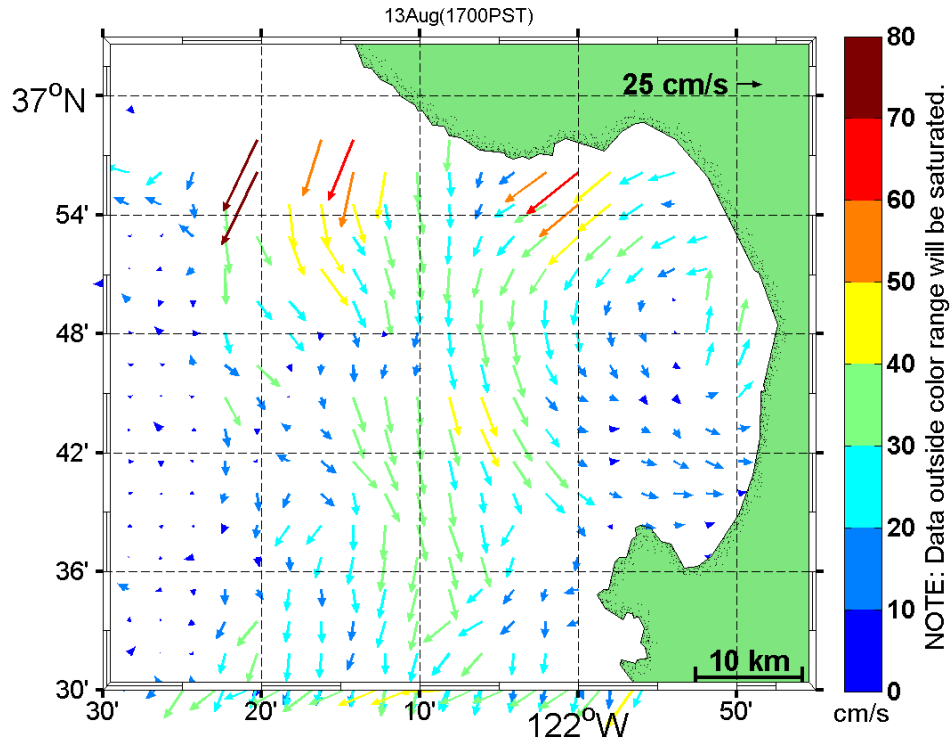


Figure 55. Surface Current Map at 5 p.m. on August 13, 2009.

3. Analysis of September 2009

The harmonic analysis graph of September 2009 shown in Figure 56 illustrates that the amplitude of winds is smaller than it was in July. There are two sharp decreases on September 9 and 18, which are the strong sea breeze days with clear wind shifting as shown in Figures 57 and 58. Figure 59 illustrates that on September 9 synoptic winds were weak. Also, the 24-hour average map of surface current on September 9, shown in Figure 61, is another good example of the absence of dominating synoptic winds in the region. Figure 61, which shows the surface currents at 4 p.m. on September 9, is a good illustration of the onshore flow due to sea breeze effect.

After we look thoroughly at the months of August and September 2009 we realize that the sharp decreases represent the evident sea breeze days with wind shifting, and the sharp increases represent the days with dominating synoptic effect in the region.

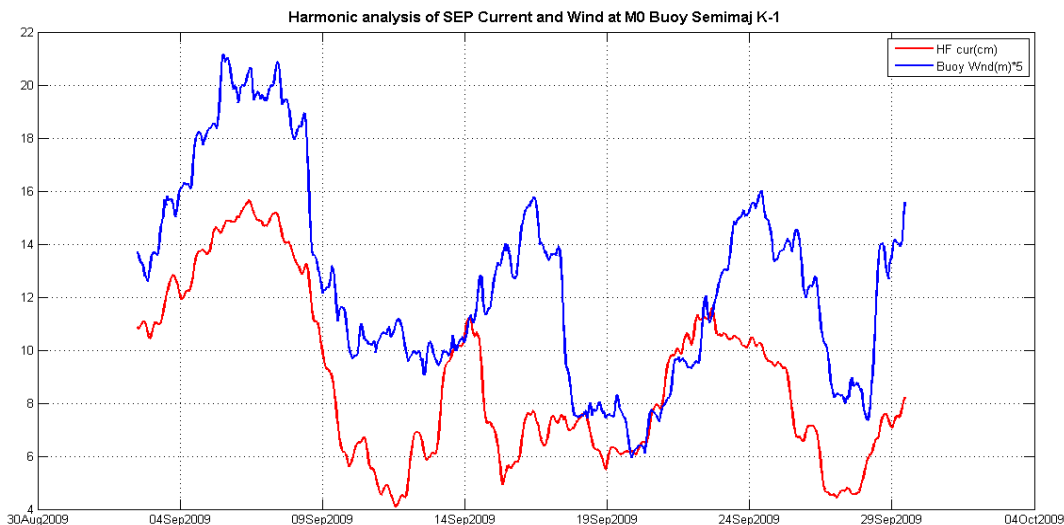


Figure 56. Harmonic Analysis of Buoy Wind and HF Radar-derived Surface Current at M0 Buoy Location (September 2009).

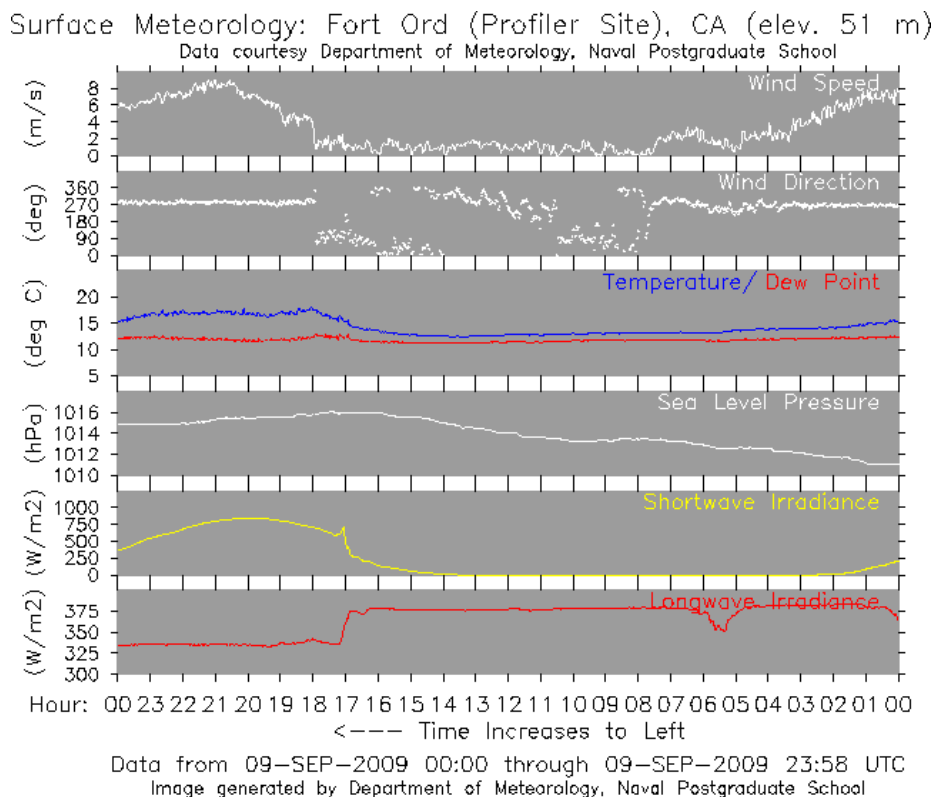


Figure 57. Wind Profiler Site Plot for Surface Meteorology Data (from <http://met.nps.edu/~lind/nps/archive/ARCHIVE.HTM>).

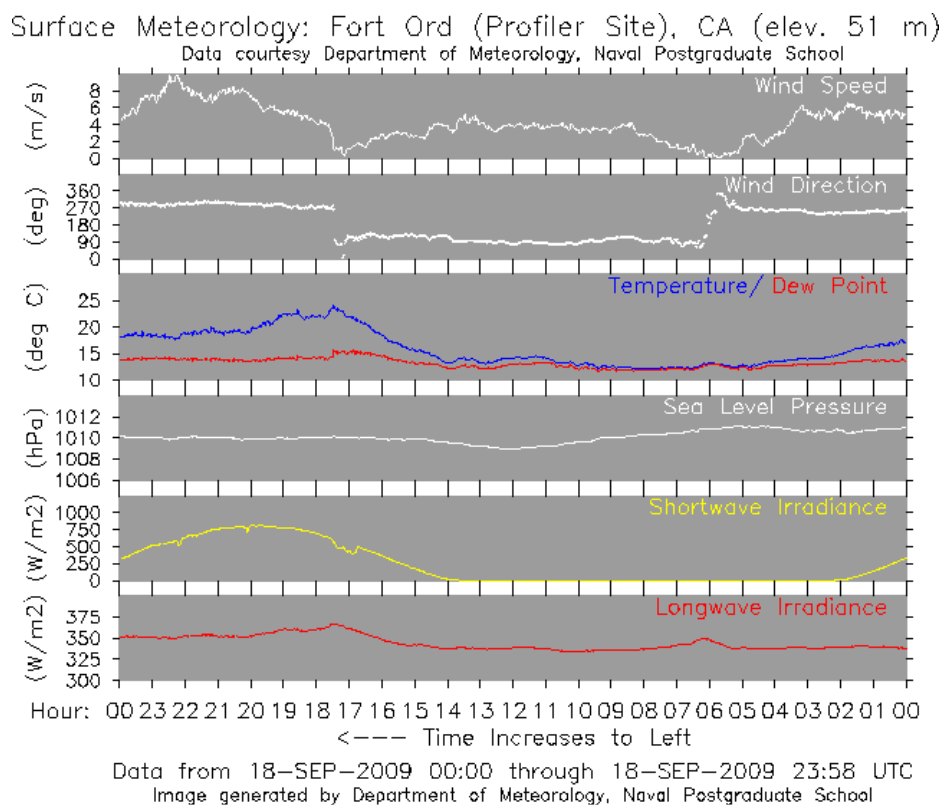


Figure 58. Wind Profiler Site Plot for Surface Meteorology Data (from <http://met.nps.edu/~lind/nps/archive/ARCHIVE.HTM>).

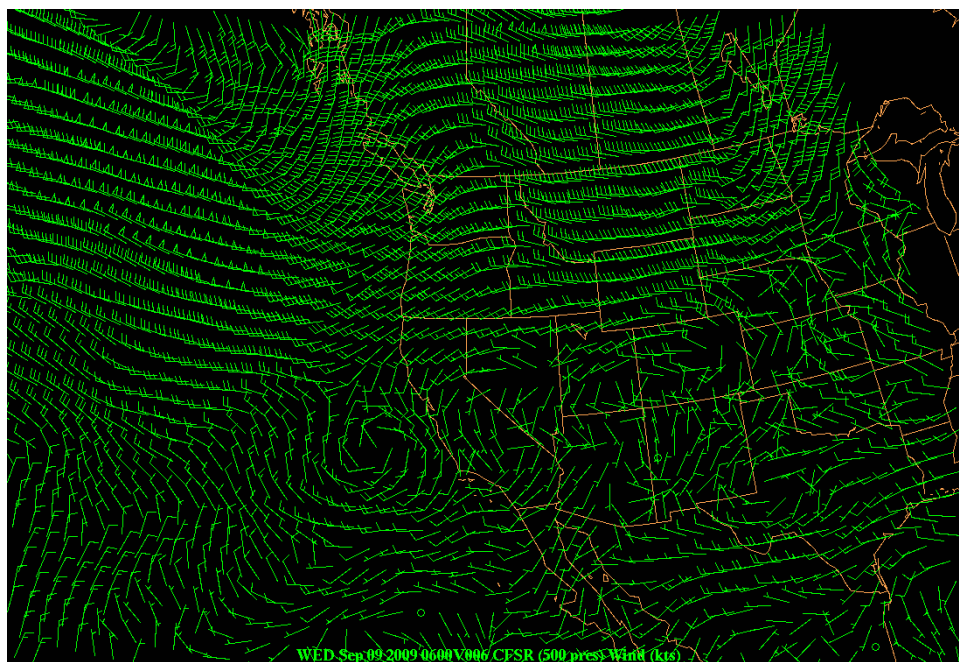


Figure 59. Synoptic Winds on September 9, 2009, along the California Coast (obtained from GARP, CFSR model).

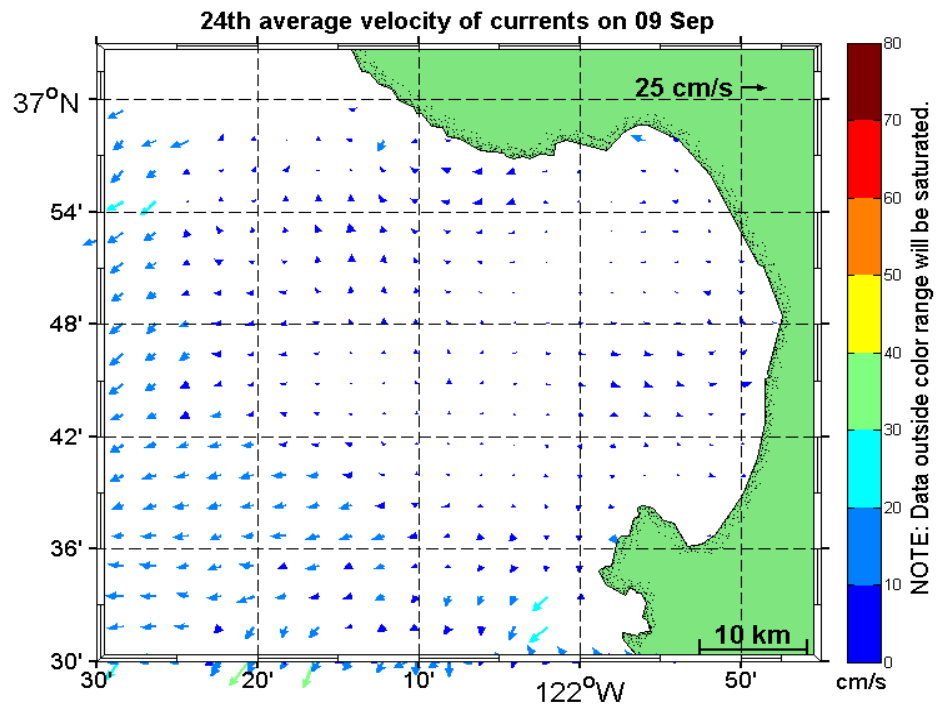


Figure 60. Average Velocity Map of Surface Current on September 9, 2009.

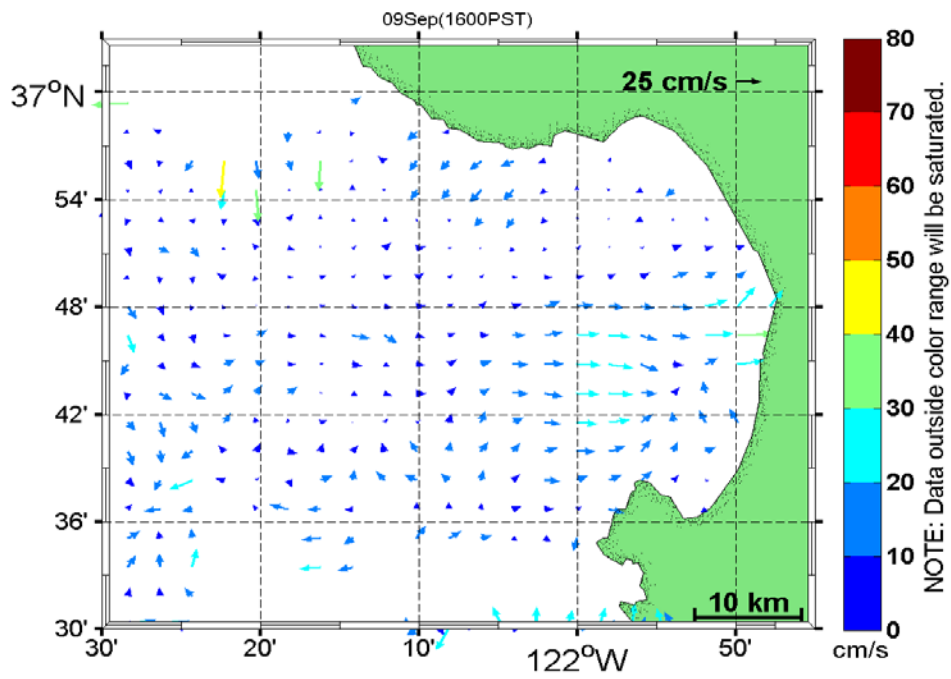


Figure 61. Surface Current Map at 4 p.m. on September 9, 2009.

G. SEA BREEZE STRENGTH

In this study to determine sea breeze we have needed to deal with many factors. Moreover, it is difficult to say which factor is the most important or how clearly the factors affect the sea breeze. MBL, synoptic winds, temperature, cloud coverage, topography, etc., are the factors known by many people to determine sea breeze effect. We create Table 6 to summarize how each of these factors affects the sea breeze strength.

The patterns shown in Figure 62 illustrate the power of the spatially distributed surface current observations provided by the HF radar network. Where one might have predicted that the primary spatial pattern to the sea breeze offshore would be largest close to shore and decaying with distance from shore, the observations show, in addition to that basic pattern, there is a strong asymmetry in the response north-to-south within Monterey Bay on the strong amplitude day. This asymmetry is repeated on other strong days when the daily maps of diurnal surface current amplitude (not shown) are investigated. Animations of those daily results for July, August and September 2009 can be viewed as a supplement to this thesis at <http://calhoun.nps.edu/public/handle/10945/41602>. With respect to these animations it can be said that wherever there are strong surface currents we can see strong winds due to the strong correlation between winds and surface currents as described in Chapter IV. This is an advantage of using HF radars since we cannot map the surface winds easily, but by looking at these harmonic analyzed K-1 component of amplitudes for surface currents we can tell where there are strong winds.

When we tried to think about all the factors at the same time or some of them together, we still could not come up with a definite answer regarding what influences sea breeze forcing and surface currents since it is a very complicated process. It is possible that if another type of analysis, such as complex demodulation, was used in conjunction with the harmonic analysis we employed, a firmer answer could be found. As will be discussed in Chapter V, this topic has room for further study.

	SEA BREEZE STRENGTH
Coastal Jet and Synoptic Winds	<ul style="list-style-type: none"> - It definitely increases the sea breeze strength and amplitude of the wind on shore. - Wind speed at 2 p.m. for the coastal jet days shows that wind speed on shore is greater than the onshore winds on no coastal jet days. - The direction/magnitude of synoptic winds is important since they have influence over the sea breeze strength. There is always background flow, so its direction and magnitude sometimes may increase or reduce the sea breeze strength.
Temperature Difference	<ul style="list-style-type: none"> - It is the main reason for all pressure difference and dynamics of the sea breeze. That is why we focus on summer instead of winter since there is the biggest temperature difference at those times. - However, the increase or decrease of in temperature difference in large scale between land and ocean is not causing any significant increase or decrease in the amplitude of sea breeze. Between M2 buoy and Los Banos, it does not make any significant difference. Temperature difference does have an indirect relation since it drives pressure difference, and pressure difference drives coastal jet and sea breeze. Results at local scales between the offshore mooring sites and the Fort Ord and Salinas onshore sites (not shown) also show no clear correlation with the variations in the diurnal amplitude of the winds at the M0 mooring site.
MBL	<ul style="list-style-type: none"> - If the MBL is shallow, then sea breeze is well formed. - Our analysis illustrates that there is definitely sea breeze on these days. Even though we have deep MBL on coastal jet days, sea breeze effect over surface currents could be strong if it is associated with coastal jets.
Cloud Coverage	<ul style="list-style-type: none"> - What we expect to see on cloud-free days is an increase in sea breeze strength due to more solar radiation reaching surface land, as shown in Figure 62. On cloudy days we also could see some strong sea breeze influence over the surface currents. We cannot say they are strongly related, but what we obtained in this study is evidence of a relationship between cloud and sea breeze. On cloudy days we notice that there is a decrease in the amplitudes of current and wind speed.

Table 6. Sea Breeze Strength with Respect to Standard Factors.

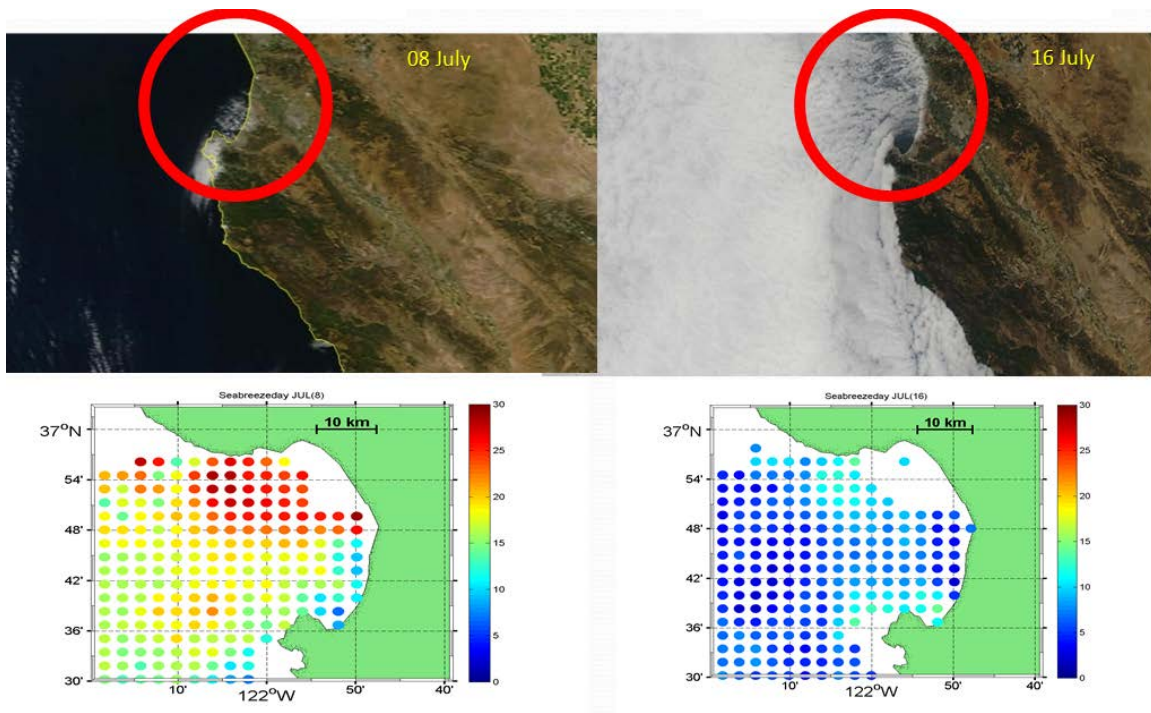


Figure 62. Cloud Coverage and Amplitudes of Surface Currents Map (from ge.ssec.wisc.edu/modis-today).

THIS PAGE INTENTIONALLY LEFT BLANK

V. CONCLUSION AND RECOMMENDATIONS FOR FUTURE RESEARCH

Studying sea breeze is a much more complicated process than people might think. We encountered some related factors that became more prominent than we had anticipated during this study. Understanding variations (in both time and space) of the sea breeze strength became the main focus of this study.

The tools we chose to illuminate the variable sea breeze patterns proved useful. Mapping the surface currents using HF radar was particularly useful, and it was made easy due to the existing MATLAB HFR_Progs toolbox. Using harmonic analysis for winds was not a common idea, but it provided meaningful results. We were concerned about the ocean tide effect in the harmonic analysis results for the ocean current data. When we compared results for the ~1m HF radar-derived currents against the 6m buoy-derived currents, we were able to discount the diurnal tide as a major factor in the variations we observed.

From our analysis of the relationship between sea breeze forcing and surface currents, we obtained several findings:

- There is an obvious relationship between winds and surface currents as described in the analysis of data section (Chapter IV). However, as Huyer and Pattullo (1969) and many others have pointed out, wind and surface currents are not necessarily parallel due to rotational effects. This is well known for sub-tidal-period surface currents, but it is much less well documented for diurnally fluctuating currents. Results here show clearly that the Ekman-like relationship with surface currents at about 45 degrees to the right of the wind forcing also holds for the diurnal currents.
- The sea breeze in Monterey is strongest during periods with a strong coastal jet in the atmosphere. This peak in diurnal response is present in both the winds and the surface currents. Furthermore, the diurnal current amplitudes are strongest in the northeast portion of Monterey Bay. They decay toward the southern portion of the bay and offshore. Given the very strong correlation between wind and surface current, including at the diurnal frequency band, it is safe to assume that the HF radar-derived diurnal current patterns offshore also reflect the patterns of the strength of the sea breeze itself.

- In power spectral analyses, it is seen that wind has a greater peak for diurnal cycles than for semi-diurnal cycles, as observed from the M0 mooring data close to the coast. On the other hand, surface currents have peaks for both diurnal and semidiurnal cycles that are more nearly equal. In this case, the semidiurnal peak is clearly associated with the tidal influence, including internal tidal currents (Petruncio et al. 1998). Tidal effect is obvious in the semidiurnal time scale. That result means surface winds, sea breeze and tides are definitely playing an important role over the surface currents.
- Wind speed differences between morning and afternoon at the places close to the coast, such as the M0 buoy, Fort Ord and Salinas, take greater values with respect to places that are far away from the coast. This difference is due to the sea breeze forcing mechanism and the spatial variations in sea breeze identified here.
- Diurnal surface currents are influenced by the diurnal winds, but the currents at the 6 meter depth are not affected by these atmosphere variations.
- Although sea breeze is predicted to occur preferentially in unstable and warm weather conditions at the small scales, we observe the strongest sea breeze amplitudes on the days with cool and stable conditions. The cool and stable days are associated with days when the coastal jet is present.
- In the results of harmonic analyses the days with sharp decreases in the amplitude of the diurnal winds represent the evident sea breeze days with wind shifting and the sharp increases represent the days with a dominating synoptic effect in the region. Also the peak amplitude times in harmonic analysis results represent the days with dominating coastal jets/synoptic winds, while low amplitude times represent the days without dominating synoptic scale events.
- Despite their relatively low diurnal fluctuation amplitudes, the days without coastal jet/synoptic winds behave the most classically with respect to the suite of sea breeze indices found in the literature and tested here.
- HF radar is useful and provides many advantages to the oceanographers with its coverage and resolution. It should be used all over the world to understand the behavior of surface currents.
- In the sea breeze algorithm, the filter for wind speed difference between afternoon and morning times is the most critical one to detect sea breeze days. Wind shifting cannot be applicable for all regions due to synoptic effects.

- If there is no coastal jet/synoptic wind then what we have is typical sea breeze day. Due to diurnal thermal heating on multiple scales we can see the effects of this daily heating over the region, but this time it is not a typical sea breeze.

Other researchers may find our approach useful. The conditions created in this study to determine sea breeze days are applicable to all the regions in the world with some small changes. They might change with respect to the topography and general characteristics of the region. Most of the conditions are helpful to make a prediction on sea breeze days when we compare with the results we got by using experience and knowledge. In Figure 63 it is seen that sea breeze algorithm works reasonably well for normal days; however, it does not do a good job for the days with coastal jets and synoptic winds. For coastal jet days, to determine sea breeze days we should have a different algorithm, and this algorithm should not have the conditions related to wind speed due to dominating synoptic scale effects.

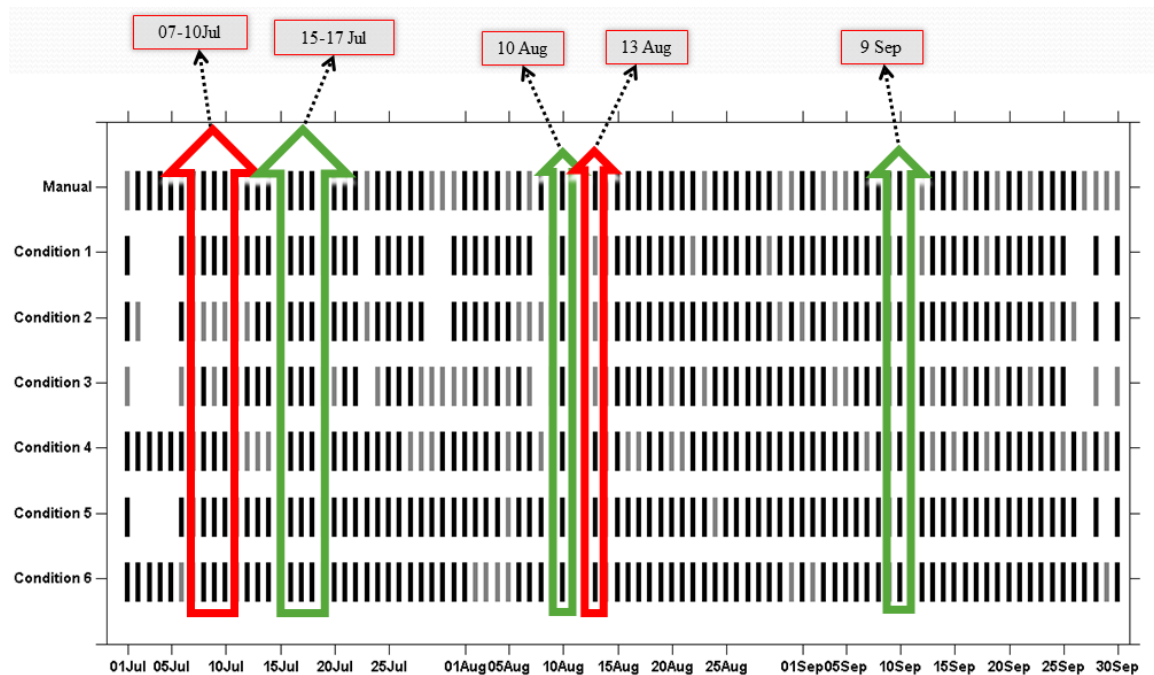


Figure 63. Sea Breeze Analysis for Specific Days.

Some other approaches might be used in future research. Instead of harmonic analysis if complex demodulation is used that might give us a chance to compare these two analyses to get better results. Also, it might be beneficial to perform analysis on a longer period of time. By getting the temperature and wind speed difference values for many years, we could choose the best time scale of any year to find the strongest sea breeze days without coastal jet influence. Then the sea breeze and surface current relationship could be examined more thoroughly. In this study data availability was the main reason for choosing summer 2009.

If the relationship between MBL and sea breeze forcing is defined better, that might help us to pick up sea breeze days correctly, and then we could add that kind of filter to our algorithm to determine sea breeze days. Understanding the relationship between MBL and sea breeze and how the coastal jet is affecting the sea breeze are complex questions to answer. To get a complete answer for this question coastal meteorology of the region should be understood and analyzed in depth.

Since the sea breeze is a complex phenomenon and there is sea breeze almost every day in Monterey Bay, it is good to focus—as we did in this study—on the days when synoptic scale winds, coastal jets, etc., do not dominate the region to see its significant effects over the currents or waves. We are hopeful that the sea breeze algorithm used for Monterey Bay in this study to determine sea breeze days could be used by other researchers on any coast in the world with some minor changes.

As we noticed in this study, the coastal jet and sea breeze correlation is complicated and not much research has been done on this topic. So we think that the relationship between the coastal jet and sea breeze will be good topic to explore in more detail.

LIST OF REFERENCES

- Ahrens, C. D., 1991: *Meteorology Today: Introduction to Weather, Climate & The Environment*. West, 576 pp.
- Anthes, R. A., 1978: The height of the planetary boundary layer and the production of circulation in a sea breeze model. *J. Atmos. Sci.*, **35**, 1232–1239.
- Barrick, D. E., 1968: A review of scattering from surfaces with different roughness scales. *Radio Sci.*, **3**, 865–68.
- Barrick, D. E., 1972: First order theory and analysis of MF/HF/VHF scatter from the sea. *IEEE Trans Antennas and Propag.* AP2-0(1), 10.doi:10.1109/TAP.1972.1140123.
- Beardsley, R. C., C. E. Dorman, C. A. Friehe, L. K. Rosenfeld, and C. D. Winant, 1987: Local atmospheric forcing during the Coastal Ocean Dynamics Experiment: A description of the marine boundary layer atmospheric conditions over a Northern California upwelling region. *J. Geophys. Res.*, 92(C2), 1467–1488.
- Borne, K., D. Chen, M. Numez, 1998: A method for finding sea breeze days under stable synoptic conditions and its application to the Swedish coast. *International J. of Climatology*, **18**, 901–914.
- Burk, S. D., and W. T. Thompson, 1996: The summertime low-level jet and marine boundary layer structure along the California coast. *Mon. Wea. Rev.*, **124**, 668–686.
- Crombie, D. D., 1955: Doppler spectrum of sea echo at 13.56 mc/s. *Nature*, **175**, 681–682.doi:10.1038/175681a0.
- Cross, P. S., 2003: The California coastal jet :Synoptic controls and topographically induced mesoscale structure. Ph.D. dissertation, NPS, Monterey, CA.
- Darby, L. S., R. M. Banta, R. A. Pielke, Sr., 2002: Comparisons between mesoscale model terrain sensitivity studies and Doppler lidar measurements of the sea breeze at Monterey Bay. *Mon. Wea. Rev.*, **130**, 2813–2837.
- Delgado, R., 1999: Mapping coastal surface winds in Monterey Bay using high frequency radar. M.S. thesis, NPS, Monterey, CA.
- Duvall, E., 2004: Factors influencing the structures of the Monterey Bay sea breeze. M.S. thesis, NPS, Monterey, CA.
- Emery, W. J., and R. E. Thomson, 2004: *Data Analysis Methods in Physical Oceanography*. Elsevier, 638 pp.

- Estoque, M. A., 1962: Sea breeze as a function of the prevailing synoptic situation. *J. Atmos. Sci.*, **19**, 244–250.
- Foster, M. D., 1996: California sea breeze structure and its relation to the synoptic scale. Ph.D. dissertation, NPS, Monterey, CA.
- Gonella J., 1972: A rotary component method for analyzing meteorological and oceanographic vector time series. *Deep-Sea Research*, **19**, 833–846.
- Harlan J., E. Terrill, L. Hazard, C. Keen, D. Barric, C. Whelan, S. Howden, J. Kohut, 2010: The integrated ocean observing system high frequency radar network: Status and local, regional and national applications. *Marine Soc. Paper J.*, 122–125.
- Haurwitz, B., 1947: Comments on the sea breeze circulation, *J. Met.*, **4**, 1–8.
- Hendrickson, J., J. MacMahan, 2009: Diurnal sea breeze effects on inner-shelf cross-shore exchange. *Continental Shelf Research*, **29**, 2195–2206.
- Holton, J.R., 1979: *An Introduction to Dynamic Meteorology*. Academic Press, 391 pp.
- Huyer, A., J. G. Pattull, 1969: A comparison between wind and current observations over the continental shelf off Oregon, Summer 1969. *J. of Geophys.*, 3215–3220.
- Kundu, P., 1975: Notes and correspondence Ekman Veering observed near the ocean bottom. *J. of Phys. Oceanogr.*, **6**, 238–242.
- Long, R., N. Grafield, D. E. Barrick, 2006: The effect of salinity on monitoring San Francisco Bay surface currents using surface current monitoring instruments. Presentation at the *California and the World Ocean '06 Conference*, September 17–20, Long Beach, CA.
- Militello, A., N. K. Kraus, 2001: Generation of harmonics by sea breeze in nontidal water bodies. *J. of Phys. Oceanogr.*, **31** (6), 1639–1647.
- Neal, T. C., 1992: Analysis of Monterey Bay CODAR-derived surface currents. M.S. thesis, NPS, Monterey, CA.
- Nuss, W., 2003: Coastal Meteorology and Forecasting, course notes for MR 4240: Coastal Meteorology, NPS, Monterey, CA.
- Paduan J., L. Washburn, 2013: High frequency radar observations of ocean surface currents. *Annu. Rev. Marine. Sci.*, **5**, 115–118.
- Paduan J., K. Rosenfeld, 1996: Remotely sensed surface currents Monterey Bay from shore-based HF radar (Coastal Ocean Dynamics Application Radar). *J. Geophys. Res.*, **101** (C9), 20669–20686.

- Paduan, J., H. Graber, 1997: Introduction to high frequency radar: Reality and myth. *Oceanogr.*, **10**, 36–39.
- Petruncio, E. T., L. K. Rosenfeld, and J. D. Paduan, 1998: Observations of the internal tide in Monterey Submarine Canyon. *J. Phys. Oceanogr.*, **28**, 1873–1903.
- Samelson, R. M., 1992: Supercritical marine-layer flow along a smoothly varying coastline. *J. Atmos. Sci.*, **49**, 1571–1584.
- Shearman, E. D. R., 1981: Remote sensing of ocean waves, currents and surface winds by deka metric radar. *Remote Sensing Meteorology, Oceanography and Hydrology*. A. P. Cracknell, Ed., Ellis Horwood, 312–335.
- Stec, J. D., 1996: Wind profiler study of the central California sea/land breeze. M.S. thesis, NPS, Monterey, CA.
- Stevens, R. S., 1997: The sensitivity of the coastal jet to the synoptic scale. M.S. thesis, NPS, Monterey, CA.
- Vesecky J. F., C. C. Teague, R. G. Onstott, J. M. Daida, P. Hansen, D. Fernandez, N. Schnepf and K. Fischer, 1997: Surface current response to land-sea breeze circulation in Monterey Bay, California as observed by a new multifrequency HF radar. *Oceans' 97.MTS/IEEE Conference Proceedings*, **2**, 1019–1023.
- Watts, A. 1955: Sea breeze at Thorney Island. *Meteorol. Mag.*, **84**, 42–48.
- Wexter, R., 1946: Theory and observations of land and sea breezes. *B. Am. Met. Soc.*, **27**, 272–287.
- Winant, C. D., C. E. Dorman, C. A. Friehe and R. C. Beardsley, 1988: The marine layer off northern California: An example of supercritical channel flow. *J. Atmos. Sci.*, **45**, 3588–3605.
- Zemba, J., and C. A. Friehe, 1987: The marine atmospheric boundary layer jet in the Coastal Ocean Dynamics Experiment. *J. Geophys. Res.*, **92**, 1489–1496.

THIS PAGE INTENTIONALLY LEFT BLANK

INITIAL DISTRIBUTION LIST

1. Defense Technical Information Center
Ft. Belvoir, Virginia
2. Dudley Knox Library
Naval Postgraduate School
Monterey, California